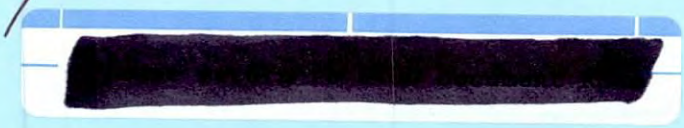

NUREG/CR–5363
BNL–NUREG–52196

A Study of the Use of Crosslinked High–Density Polyethylene for Low–Level Radioactive Waste Containers

Prepared by P. Soo, C. I. Anderson, J. H. Clinton

Brookhaven National Laboratory

Prepared for
U.S. Nuclear Regulatory
Commission

AVAILABILITY NOTICE

Availability of Reference Materials Cited in NRC Publications

Most documents cited in NRC publications will be available from one of the following sources:

1. The NRC Public Document Room, 2120 L Street, NW, Lower Level, Washington, DC 20555

2. The Superintendent of Documents, U.S. Government Printing Office, P.O. Box 37082, Washington, DC 20013-7082

3. The National Technical Information Service, Springfield, VA 22161

Although the listing that follows represents the majority of documents cited in NRC publications, it is not intended to be exhaustive.

Referenced documents available for inspection and copying for a fee from the NRC Public Document Room include NRC correspondence and internal NRC memoranda; NRC Office of Inspection and Enforcement bulletins, circulars, information notices, inspection and investigation notices; Licensee Event Reports; vendor reports and correspondence; Commission papers; and applicant and licensee documents and correspondence.

The following documents in the NUREG series are available for purchase from the GPO Sales Program: formal NRC staff and contractor reports, NRC-sponsored conference proceedings, and NRC booklets and brochures. Also available are Regulatory Guides, NRC regulations in the *Code of Federal Regulations*, and *Nuclear Regulatory Commission Issuances*.

Documents available from the National Technical Information Service include NUREG series reports and technical reports prepared by other federal agencies and reports prepared by the Atomic Energy Commission, forerunner agency to the Nuclear Regulatory Commission.

Documents available from public and special technical libraries include all open literature items, such as books, journal and periodical articles, and transactions. *Federal Register* notices, federal and state legislation, and congressional reports can usually be obtained from these libraries.

Documents such as theses, dissertations, foreign reports and translations, and non-NRC conference proceedings are available for purchase from the organization sponsoring the publication cited.

Single copies of NRC draft reports are available free, to the extent of supply, upon written request to the Office of Information Resources Management, Distribution Section, U.S. Nuclear Regulatory Commission, Washington, DC 20555.

Copies of industry codes and standards used in a substantive manner in the NRC regulatory process are maintained at the NRC Library, 7920 Norfolk Avenue, Bethesda, Maryland, and are available there for reference use by the public. Codes and standards are usually copyrighted and may be purchased from the originating organization or, if they are American National Standards, from the American National Standards Institute, 1430 Broadway, New York, NY 10018.

NUREG/CR–5363
BNL–NUREG–52196
RW

A Study of the Use of Crosslinked High–Density Polyethylene for Low–Level Radioactive Waste Containers

Manuscript Completed: March 1989
Date Published: June 1989

Prepared by
P. Soo, C. I. Anderson, J. H. Clinton

Brookhaven National Laboratory
Upton, NY 11973

Prepared for
Division of Engineering
Office of Nuclear Regulatory Research
U.S. Nuclear Regulatory Commission
Washington, DC 20555
NRC FIN A3291

ABSTRACT

A comprehensive research program has been completed to evaluate the effects of chemical and gamma-irradiation environments on the mechanical properties of crosslinked high-density polyethylene. The studies included uniaxial creep tests and crack initiation and crack propagation studies in statically-stressed U-bend samples. From the results obtained standard testing protocols were recommended for quantifying the various failure modes which could be present in this material during service as a low-level waste container.

EXECUTIVE SUMMARY

Crosslinked high-density polyethylene (HDPE) is a plastic that is being used as a high-integrity container material for certain types of low-level radioactive waste. Among the reasons for its selection are its relatively low cost compared to metallic materials and its excellent resistance to many corrosive environments. The current research effort was designed to quantify the mechanical behavior of such a material (Marlex CL-100, marketed by the Phillips Petroleum Co.) in chemical and irradiation environments that could be present in a waste container. The ultimate objective of the study is to first identify and quantify those failure and degradation modes that could lead to failure of the container before and after disposal in a shallow-land burial trench and then to specify a testing protocol for HDPE that could eventually lead to its qualification as a high-integrity container material.

Based on an earlier preliminary study (Soo and others, 1986), it was decided that the effort should concentrate in two areas:

a) Semi-quantitative U-bend tests to determine the effects of selected chemical, irradiation, and material variables on the rates of crack initiation and propagation, and

b) Quantitative uniaxial creep tests in chemical and irradiation environments to determine how they influence the creep rate, elongation-at-failure (ductility), and the failure time at a given stress level.

The test results are discussed below and are then followed by a description of the rationale that was used to specify a material testing protocol.

U-Bend Tests in Chemical Environments

The U-bend samples were prepared by cutting strips from the 3.2 mm (0.125 in.) wall of a Marlex CL-100 HDPE rotationally-molded drum. During the high-temperature molding process the internal surface of the drum becomes oxidized by the surrounding air causing the surface ductility to decrease. The outer surface of the drum, on the other hand, remains in a non-oxidized, higher ductility condition since it remains in intimate contact with the steel mold. The U-bends prepared for the chemical-interaction studies all had oxidized material on the outer bend surface since it represents a conservative case where the bending of the material causes surface cracking. It is the growth of these cracks, and the nucleation of new ones, which was investigated.

Since oxygen is generally known to be detrimental to HDPE properties, batches of eight U-bend specimens were placed in four test environments at room temperature. Each environment was selected because of the different quantities of oxygen that would be present. They included air, deionized water (DIW), nitrogen, and a vacuum obtained by a rotary pump.

It was found that air, water, and nitrogen give larger crack growth rates than those for the vacuum. Both water and the nitrogen environment are known to contain dissolved oxygen and oxygen contamination, respectively. These observations are consistent with many other studies which show that oxygen is detrimental to the mechanical properties of plastics. The fastest rate of increase in large cracks is seen to be obtained for water, and this is in accord with the theory that surface wetting at the tips of growing cracks leads to accelerated growth (Shanahan and Shultz; 1979, 1980).

U-Bend Tests in Gamma Radiation Environments

Batches of U-bend specimens, similar to those used for the chemical environment tests described above, were also used to determine crack propagation effects for three gamma dose rates, viz. 1.4×10^3, 8.4×10^4, and 4.4×10^5 rad/h in air. The study showed that irradiation leads to rapid growth in both small and large crack densities. However, a very important point is that the low and intermediate dose rates give the larger cracking effects. This proves that accelerated irradiation tests must be used with caution, since they do not always give conservative results.

Other tests in this series show that if the oxidized surface layer is removed prior to bending the specimens into the U-bend configuration, or if the HDPE is bent so that the non-oxidized surface resides at the apex of the bend, then crack initiation is very greatly delayed. Clearly, oxygen already present in the HDPE encourages cracking in the irradiation field but non-oxidized material will eventually crack because of interaction with atmospheric oxygen.

Uniaxial Creep in Chemical Environments

Chemical environments used in the creep evaluation included scintillation fluid, turbine oil, and Igepal CO-630. Scintillation fluid contains xylene and toluene which are representative of a class of detrimental organic solvents that could initiate a particular type of failure for HDPE. Turbine oil was selected since it could be a contaminant in low-level waste, and Igepal is a standard ASTM-recommended surfactant, used for detecting susceptibility of HDPE to environmental stress-cracking. Air and deionized water were also used as control test environments.

The specimens studied were made from as-received material with one surface in the oxidized condition, and also from material which had the oxidized surface removed by abrasive paper. It was found that removal of the layer often results in faster initial creep rates but it usually leads to higher ductility and longer failure times for a given stress level. Close examination of the creep curves for as-received and non-oxidized HDPE shows that the differences appear after about 20 percent elongation. This is almost certainly associated with the first appearance of cracks in the oxidized layer. When cracks appear, localized deformation occurs in the cracked regions because of stress concentration effects. Until the cracks are nucleated, deformation in both types of specimen occurs uniformly throughout the gagelength in a similar fashion. Several types of failure may then occur in as-received HDPE depending on the environment:

a) "Environmental stress-cracking" in which the cracks grow quickly in a "brittle" manner causing early failure. Igepal and turbine oil cause such failure over a range of low stresses.

b) "Ductile failure" which is common for environments such as air, water, turbine oil and Igepal at intermediate and high stresses

c) "Superplastic failure" in which the cracks formed in the oxidized layer become blunted by easy plastic deformation so that they grow very slowly, if at all. Deformation then occurs more evenly throughout the gagelength giving higher ductility (>200 percent) and failure times compared to those for stress-cracking conditions. Such failure is promoted by high stress levels and, more importantly, by the removal of oxidized surface material.

d) "Low stress creep embrittlement" which occurs when the stress level is too low to give large scale plasticity. Failure, if it occurs, takes a long time and results from "brittle" crack growth.

Uniaxial Creep During Gamma Irradiation

Gamma irradiation during test is shown to strengthen crosslinked HDPE during the early stages of creep (Stages I and II). It is postulated that the slower creep rates during this time are caused by additional crosslinking of the polymer structure. It should be appreciated that the effects of gamma irradiation become important very early in irradiation-creep. For example, at a stress of 12.58 MPa (1825 psi) the greatly reduced creep rate caused by irradiation at 5×10^3 and 2×10^4 rad/h is noticeable after about 1 h, or less. The accumulated doses would be 5×10^4 and 2×10^5 rad, respectively, which are quite low dose levels. Obviously, stress and irradiation together provide a strong interactive effect.

The greatly enhanced rupture times and ductilities of in-test irradiated HDPE are interesting observations since it has been shown previously that prior irradiation causes a decrease in failure time and ductility upon subsequent testing (Soo, and others, 1986). Quite likely, the enhanced plasticity is associated with chain scission which could become important in the later stages of creep.

Testing Protocol

In order to specify a testing proposal to insure that HDPE is suitable as a high-integrity container material it is first necessary to identify all possible failure or degradation modes that a container could experience during service. Review of the literature and laboratory testing should be used to accomplish this goal. From the current study the following failure modes have been identified:

a) Environmental stress-cracking
b) Ductile failure
c) Superplastic failure
d) Low-stress embrittlement
e) Impact embrittlement
f) Irradiation embrittlement
g) Buckling (this is a composite failure mode involving early creep followed by fast plastic deformation.)

Standard ASTM tests and other tests are available to quantify the above failure modes. However, a comprehensive knowledge of the failure modes will not alone demonstrate that a container will meet NRC or State performance criteria. This must be accomplished by first specifying container design criteria that guarantee compliance and then demonstrating that these criteria are met. In many cases, these criteria are of an arbitrary nature and reflect the degree of conservatism the designer chooses. For example, a design criterion to prevent failure by tensile creep could be one of the following:

a) Specification of a design stress limit for the container which would insure that creep never enters the Stage III creep region where failure begins.

b) Specification of a maximum allowable design strain (elongation) so that failure could not occur.

Alternate design criteria could also be defined but once one has been selected it could be used to demonstrate compliance with an NRC (or State) requirement. Below is summarized a sequence of events which would lead to demonstration of compliance.

Step 1

Identify from literature surveys and preliminary testing all possible failure/degradation modes for HDPE containers. Rank them in order of importance with respect to early failure.

Step 2

Initiate comprehensive testing to quantify the failure modes concentrating, first, on the most important ones.

Step 3

Try to specify container service conditions which would render the container immune to as many failure modes as possible. These modes could then be removed from further consideration.

Step 4

Specify container design criteria which, if met, will prevent failure during service.

Step 5

Use materials test data to show that the design criteria are likely to be met and, therefore, that regulatory requirements are similarly met.

Recommended test protocols to quantify the various failure modes include the following standard ASTM tests:

ASTM D-1693:	for environmental stress-cracking
ASTM D-638:	for tensile testing
ASTM D-2990:	for creep testing
ASTM D-3029:	for impact embrittlement

These should be supplemented by the BNL U-bend test and any standard fracture mechanics protocol to quantify crack initiation and propagation in chemical and gamma-radiation environments. By establishing the extent to which the failure modes become important under expected service conditions, it should be possible to incorporate design features in the containers that will assure that they meet their design life of 300 years. Full details of the overall testing protocol are given in Section 6 of this report.

CONTENTS

CONTENTS (continued)

LIST OF FIGURES

LIST OF FIGURES (continued)

LIST OF TABLES

LIST OF TABLES (continued)

ACKNOWLEDGEMENTS

The authors gratefully acknowledge K. Bothe, E. Karlund and A. Lopez for their patience and skills in the preparation of this report. Mr. E. Sweeney helped with some of the creep tests and photography.

1. INTRODUCTION

Disposal of Class B and Class C low-level radioactive wastes in a high integrity container is listed in the NRC Technical Position on Waste Form as an option for meeting waste stability requirements under the Rule 10 CFR Part 61, "Licensing Requirements for Land Disposal of Radioactive Waste." High integrity containers are currently employed for the disposal of dewatered demineralizer resin waste and high density crosslinked polyethylene (HDPE), a thermoplastic polymer, is one of the materials used in their fabrication. This choice is based on low cost, ease of fabrication by high-temperature molding, and its excellent resistance to attack by a very wide range of chemical environments. A shortcoming, however, is its tendency to deform (creep) under the action of low applied stresses. This could lead to buckling of a HDPE container from soil overburden loads in a shallow-land burial trench. In addition, very little information is available on the mechanical behavior of crosslinked HDPE. Much more data is available for the non crosslinked polymer, but these are not representative. The rate of deformation is dependent on the service environment that the container encounters. In particular, the contents of the container may cause loss of mechanical integrity of the plastic through chemical interactions or gamma radiation damage mechanisms. External conditions around buried containers may also influence long term behavior but preliminary short-term test results in an earlier study indicate that HDPE gamma irradiated while in contact with Hanford (Washington) and Barnwell (South Carolina) soils show similar tensile properties to material irradiated in air (Dougherty and others, 1984).

In order to qualify a container for a particular design lifetime it is first necessary to define through testing, or from reviewing the open literature, all viable failure/degradation modes and then to carry out research to quantify failure times under prototypic environments. However, for crosslinked HDPE there is little information available on mechanical behavior as a function of chemical and radiation environments. Some preliminary data were obtained in an earlier study at Brookhaven National Laboratory (BNL) but the tests were of short duration and did not address all potential failure modes (Soo, and others, 1986). Because of this lack of information it is very difficult for the Nuclear Regulatory Commission (NRC) to reach findings on the licensability of high-integrity containers fabricated from crosslinked HDPE.

The objective of the current effort, therefore, is to determine and quantify the failure/degradation mechanisms for HDPE which are critical to container life. Furthermore, a testing protocol will be specified so that these mechanisms can be adequately assessed with respect to their potential to cause early container failure. Where possible, existing standard tests will be recommended. In situations where a new or modified procedure is desirable these will be added to the recommended testing protocol.

Testing environments used include air and deionized water, the control environments, and various classes of chemical environments which would scope potential types of failure mechanism. In addition, in-test gamma irradiation will be utilized to check synergistic effects between applied stress and irradiation-induced structural changes in the HDPE.

2. EXPERIMENTAL

2.1 Material Selection

Marlex CL-100 (a highly crosslinked HDPE, produced by the Phillips Chemical Company) was selected for the study because containers fabricated from this material have been licensed by South Carolina for the disposal of dewatered resin wastes at the Barnwell site. Test coupons were stamped from the side walls of two rotationally molded 5000-L capacity drum type containers manufactured by Poly-Processing, Inc., Monroe, LA. Although the 5000-L container does not conform to the design specifications of a high integrity container in terms of its size or wall thickness, the same basic feed material was used and Poly-Processing employed a similar process to that used in fabricating currently-licensed high integrity containers. The majority of the tests were conducted on a Marlex CL-100 container purchased in 1985. However, for the creep tests carried out in the presence of gamma radiation, specimens were prepared from a similar but older container purchased in 1983. This was planned because of the availability of prior data on irradiation-creep for this "old" batch of HDPE (Dougherty and others, 1984; Soo, and others, 1986).

Usually, tests were performed on material in the as-received condition. During molding, the Marlex resin is heated in a metal mold to about 300° C, often by high-temperature forced air (Phillips). By rotating the mold about two independent orthogonal axes, a uniform wall thickness is achieved. The molding process is completed by cooling the mold by water. As a result of this procedure, the internal surfaces of the container have a thin oxidized layer of about 5 microns, whereas the opposite surfaces in contact with the mold are not significantly affected. Studies have shown that the oxidized material is less ductile and will crack more quickly during deformation (Soo, and others, 1986).

2.2 Sample Preparation and Pretreatment

2.2.1 U-Bend Test Specimens

In addition to the more sophisticated creep tests, several series of statically-stressed "U-bend" specimens were prepared. They were made from flat strips of HDPE which were carefully bent into a U shape and the two ends were held together using a nut and bolt. Such tests proved to be extremely useful for metallic and plastic materials because of their simplicity, ease of preparation, inexpensiveness, and their ability to simulate situations in which a buried container may be subjected to a static stress caused by in-situ deformation. Note that the tensile stress will usually be greatest at the apex of the bend but it will decrease continuously with distance from the apex, eventually becoming zero. Any local cracking of the HDPE during bending will cause some stress reduction, as will inelastic (creep) deformation in the specimen after the bending has been completed.

Two different sizes of U-bend specimen were evaluated in the current work. Initially, eight large specimens were prepared for scoping tests on irradiation embrittlement. They were made from strips measuring 25cm x 2.5cm x 0.32cm (10" x 1" x 0.125"). The strips were bent into a U shape with the oxidized surface of the plastic on the outer surface of the bend. The bending

process caused cracks to form in the oxidized layer. The free ends of the specimens were held together with stainless steel nuts and bolts, passing through holes located 7.6cm (3") from the ends of the strips. The propagation of the cracks under the conjoint action of irradiation and tensile stresses was monitored visually.

Based on the success of the U-bend configuration, additional samples of U-bend specimens were prepared for both irradiation and chemical environment studies. These newer samples were made from smaller HDPE strips measuring 10.2cm x 1.27 cm x 0.32cm ((4" x 0.5" x 0.125"). Holes for the nuts and bolts were drilled at a distance of 1.27cm (0.5") from the ends of the strips. These U-bends were prepared with the outer surfaces in three different conditions:

Type I - the as-received oxidized condition, which will have "natural" cracks present, as a result of bending,

Type II - as above, but with 0.25 mm (0.010") of the oxidized surface removed with fine abrasive paper prior to bending. (No cracks were seen after bending),

Type III - the as-received "non-oxidized" surface which does not crack during the bending process.

The smaller U-bend specimens were more practical because they required smaller test facilities and allowed more replicate tests to be conducted.

2.2.2 Creep Test Specimens

Test specimens were stamped to specifications given in ASTM Standard D-638 (Tensile Properties of Plastics). Various specimen dimensions were used depending on the thickness of the test material (Table 2.1). Since the containers used in this work had wall thicknesses of 3.2 mm (0.125 in) a Type IV specimen was selected, as shown in Figure 2.1. All specimens were stamped using Die C described in ASTM D-412 (Rubber Properties in Tension).

2.3 Test Environments

The HDPE tests were carried out for a range of chemical and irradiation environments. Table 2.2 lists them and gives the rationale for selection.

The range of test environments used in the study allows potentially different failure mechanisms to be identified. Although some are unlikely to be present in burial trenches, the knowledge gained from the severe test environments may allow conservative estimates to be made on the long term behavior of HDPE under actual service conditions.

Table 2.1 Dimensions of ASTM specimens of different thicknesses, T.[a]

Parameter	Type II (T≤ 7 mm)	Type III (T=7-14 mm)	Type IV (T≤ 4 mm)
Width of narrow section, W	6	19	6
Length of narrow section, L	57	57	33
Width overall, min. WO	19	29	19
Length overall, min. LO	183	246	115
Gage length, G	50	50	25
Distance between grips, D	135	115	64
Radius of fillet, R	76	76	14
Outer radius, RO	-	-	25
a) All dimensions in mm.			

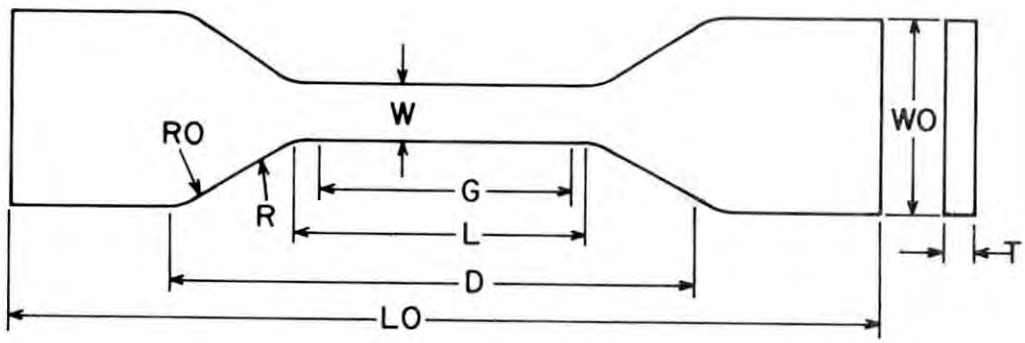

Figure 2.1 Schematic of a typical Type IV specimen (see Table 2.1 for corresponding dimensions).

Table 2.2 Environments used for HDPE testing

Test	Environment	Temperature (°C)	Basis For Selection
Creep	Scintillation fluid (INSTA-GEL)	20	Typical aromatic solvent representing severe scoping test.
	Turbine oil (Mobil OTE 797/Mobil DTE Medium)	20	Simulant of turbine pump oil contaminant.
	Igepal {Nonylphenoxy poly (ethyleneoxy) ethanol}	20	Surfactant employed in environmental stress cracking resistance test for HDPE (ASTM D-2552)
	Air	20	Control environment
	Deionized water	20	Control envoronment
	Gamma radiation (Cs-137 Source)	20	Gamma radiation present in low-level waste
U-bend	Air	20	Control environment
	Deionized water	20	Control environment
	N_2	20	Inert gas
	Vacuum	20	Oxygen-free environment
	Gamma radiation (Co-60 source)	10	Gamma radiation present in low-level waste

3. CRACK INITIATION AND GROWTH IN U-BEND SPECIMENS

Three series of U-bend tests were completed in the current program. The first involved small Type I specimens exposed to air, water, nitrogen, and a vacuum; the second involved large Type I specimens irradiated in air at three separate gamma dose rates; and the third comprised small Types I, II and III specimens irradiated at three separate gamma dose rates. Each series is discussed separately below.

3.1 Crack Initiation and Growth in Chemical Environments

In the preparation of the Type I specimens (oxidized surface on the outer bend), it was decided to standardize the bend procedure to ensure that excessive bending did not occur during sample preparation. The strips of HDPE were gently bent around a 1.27 cm (0.5" rod) and a bolt threaded through the holes in the end sections. After tightening the nut and bolt so that the ends of the strip were pulled together, the rod was removed and final tightening carried out so that the ends of the strip were held flatly against each other.

Bending of the Type I specimens caused cracking to occur in the apex region because of the lower ductility of oxidized material. Some cracks were large, spanning the width of the sample, whereas others were much smaller. Since oxidation is known to be detrimental to many plastics it was decided to study how the existing cracks in the Type I specimens grew in air, nitrogen, deionized water, and a vacuum.

The test equipment consisted of glass desiccators (without desiccant) with the lids sealed with stopcock grease. The air, nitrogen and water environments were maintained at atmospheric pressure at room temperature. The low pressure achieved for the vacuum environment was assumed to be typical of that for a rotary mechanical pump (about 10^{-2} mm mercury).

For each test environment, eight replicate U-bend specimens were studied. The propagation of existing cracks and the initiation of new ones was followed by sketching the initial crack patterns at the apex of each specimen and then resketching the patterns after accumulated test periods of 227 days and 437. It was discovered, however, that the vacuum environment was not maintained throughout the first test cycle of 227 days. Thus, some oxidation effects may have been present for part of this test cycle. A good vacuum was maintained during the second 210 day cycle.

Figures 3.1 through 3.12 show the crack patterns in each batch of eight U-bend specimens tested in the various environments. The first figure in each series was sketched 24 hours after specimen bending, the second after 227 days of exposure to the test environment, and the third after an additional 210 days of testing. Cracks are categorized as being large or small depending on their length. The width or depth of the cracks were not quantified. Thus, a large crack had a length measuring more than one-half of the width of the strip the U-bend was made from, i.e. greater than 0.64 cm(0.25") A small crack is one measuring less than this size. Tables 3.1 and 3.2 show the numbers of large and small cracks immediately prior to test and after each of the two test cycles. It was noted that despite care in bending the specimens,

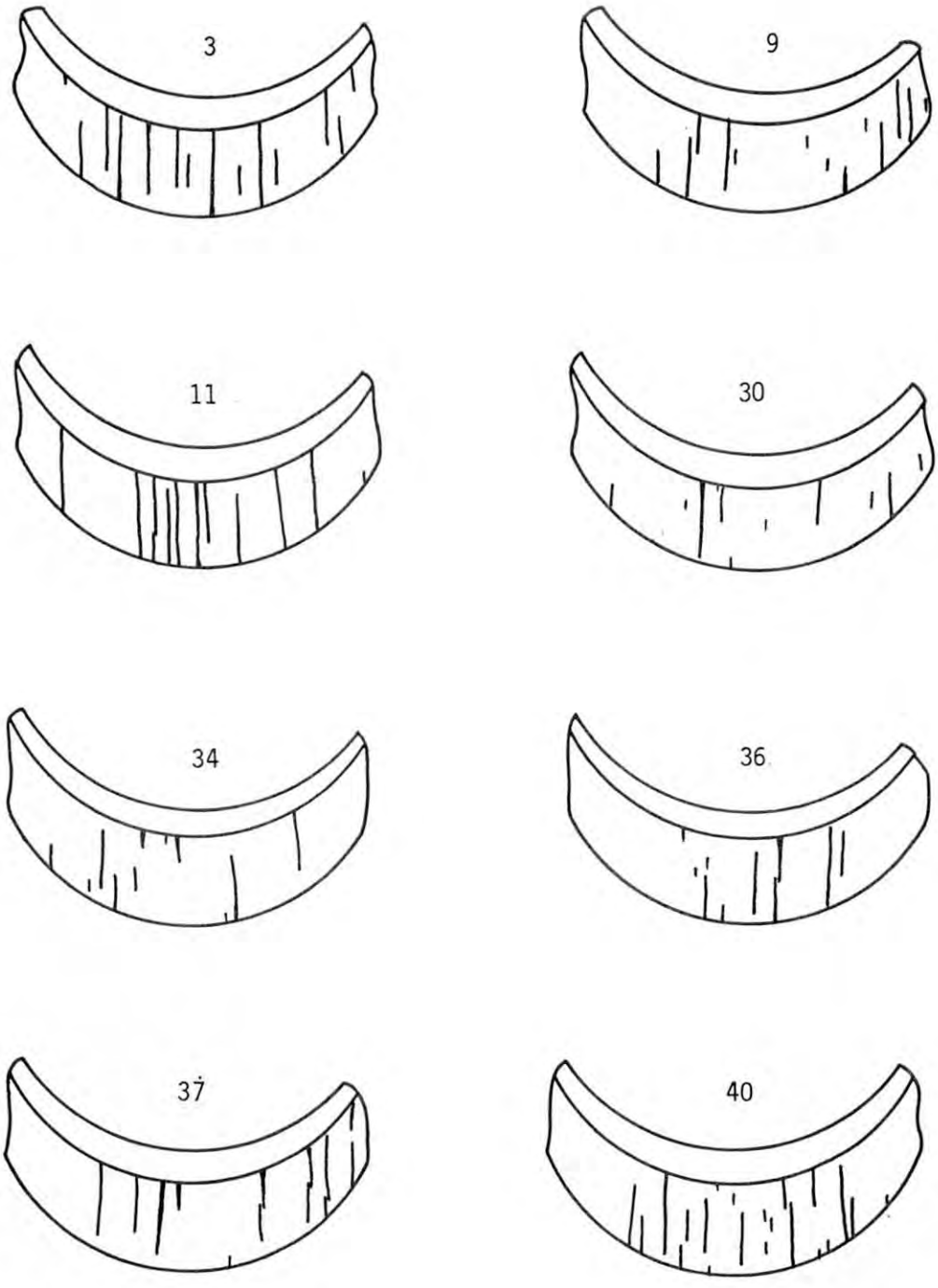

Figure 3.1 Crack patterns formed in the apex regions of Marlex CL-100 HDPE U-bend specimens prior to long-term exposure to air. Specimen numbers given above sketches.

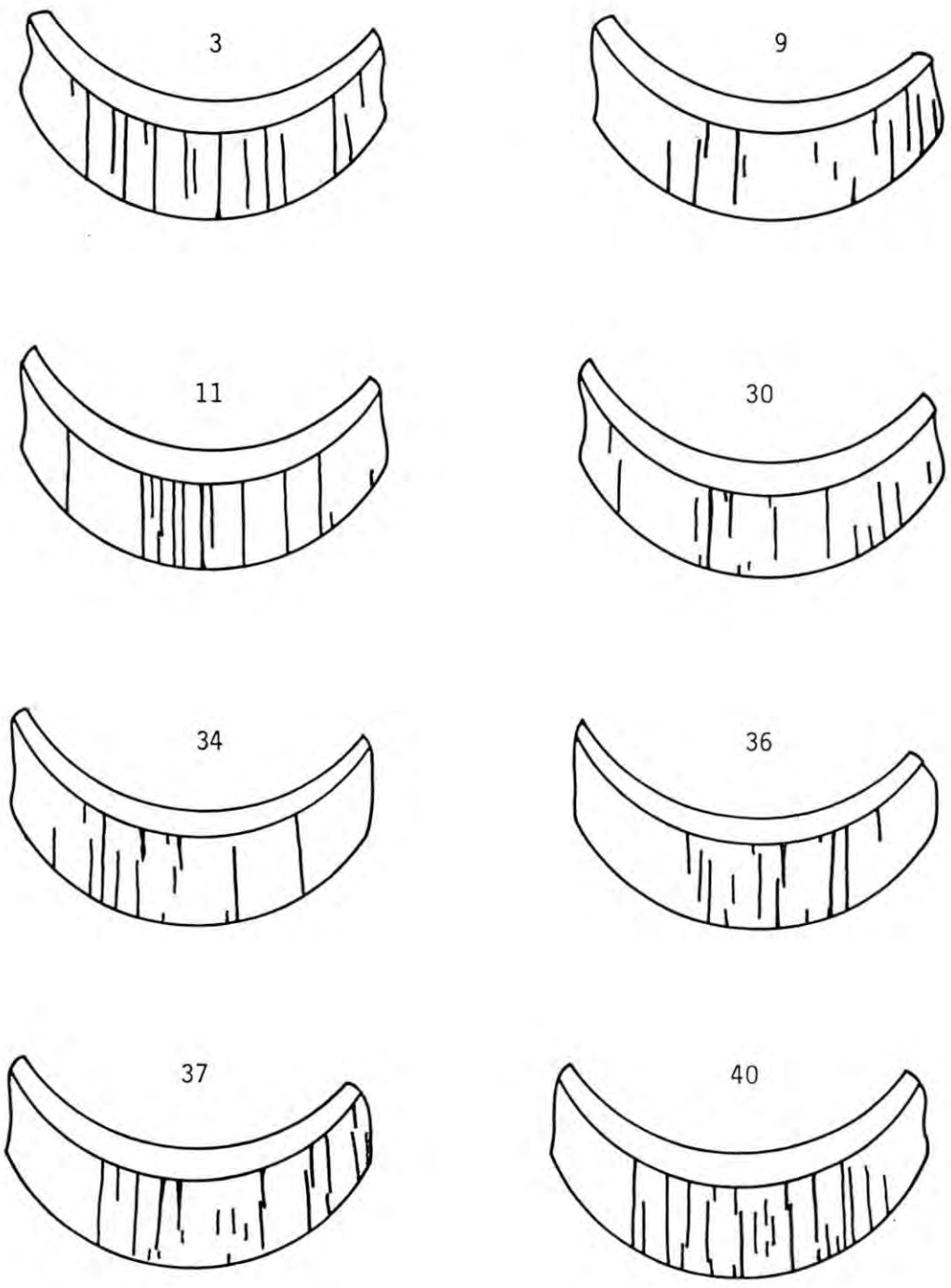

Figure 3.2 Crack patterns in the HDPE U-bend specimens shown in Figure 3.1 after 227 d exposure to air at 20°C. Specimen numbers given above sketches.

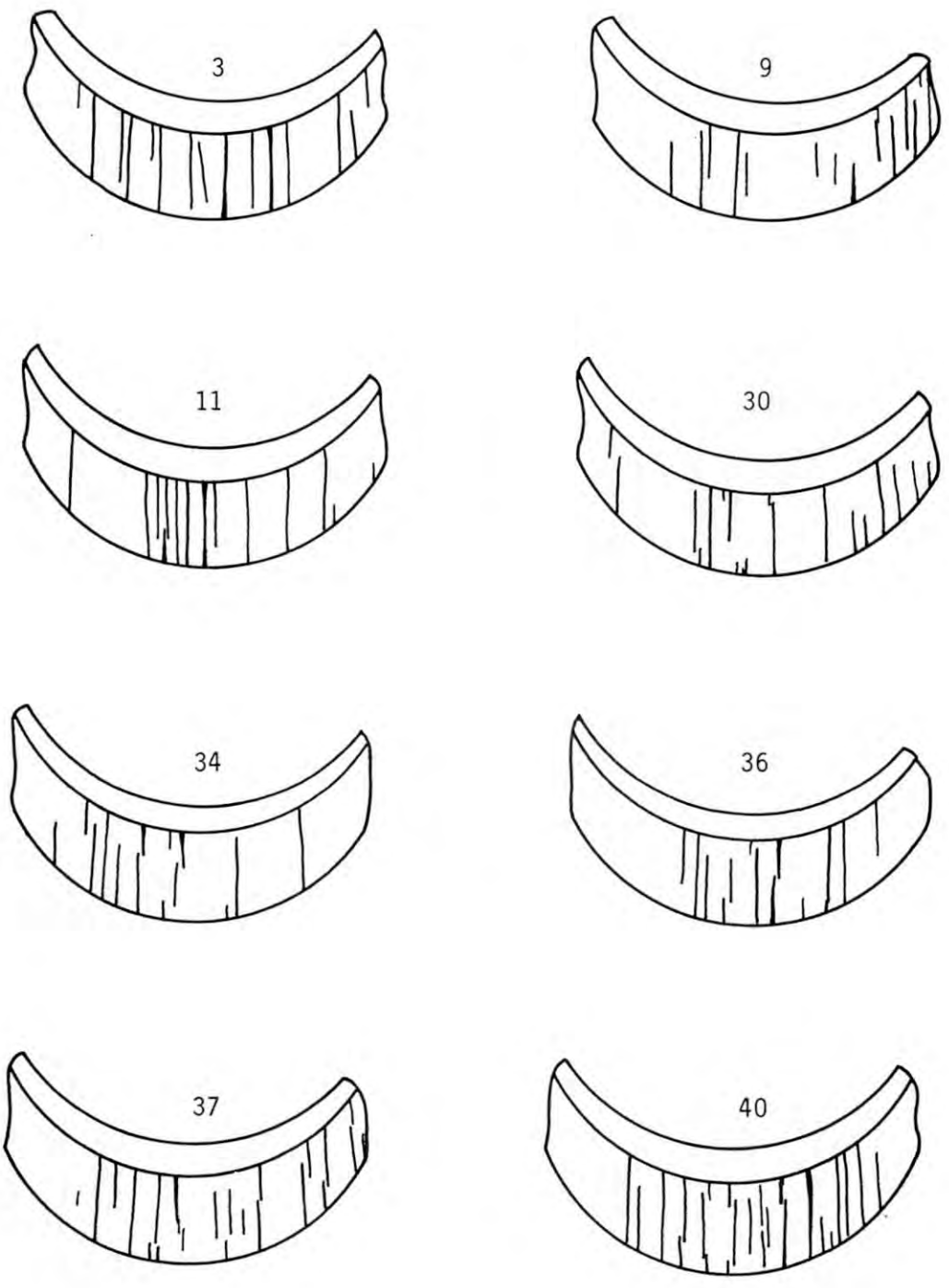

Figure 3.3 Crack patterns in the HDPE U-bend specimens shown in Figure 3.1 after 437 d exposure to air at 20°C. Specimen numbers given above sketches.

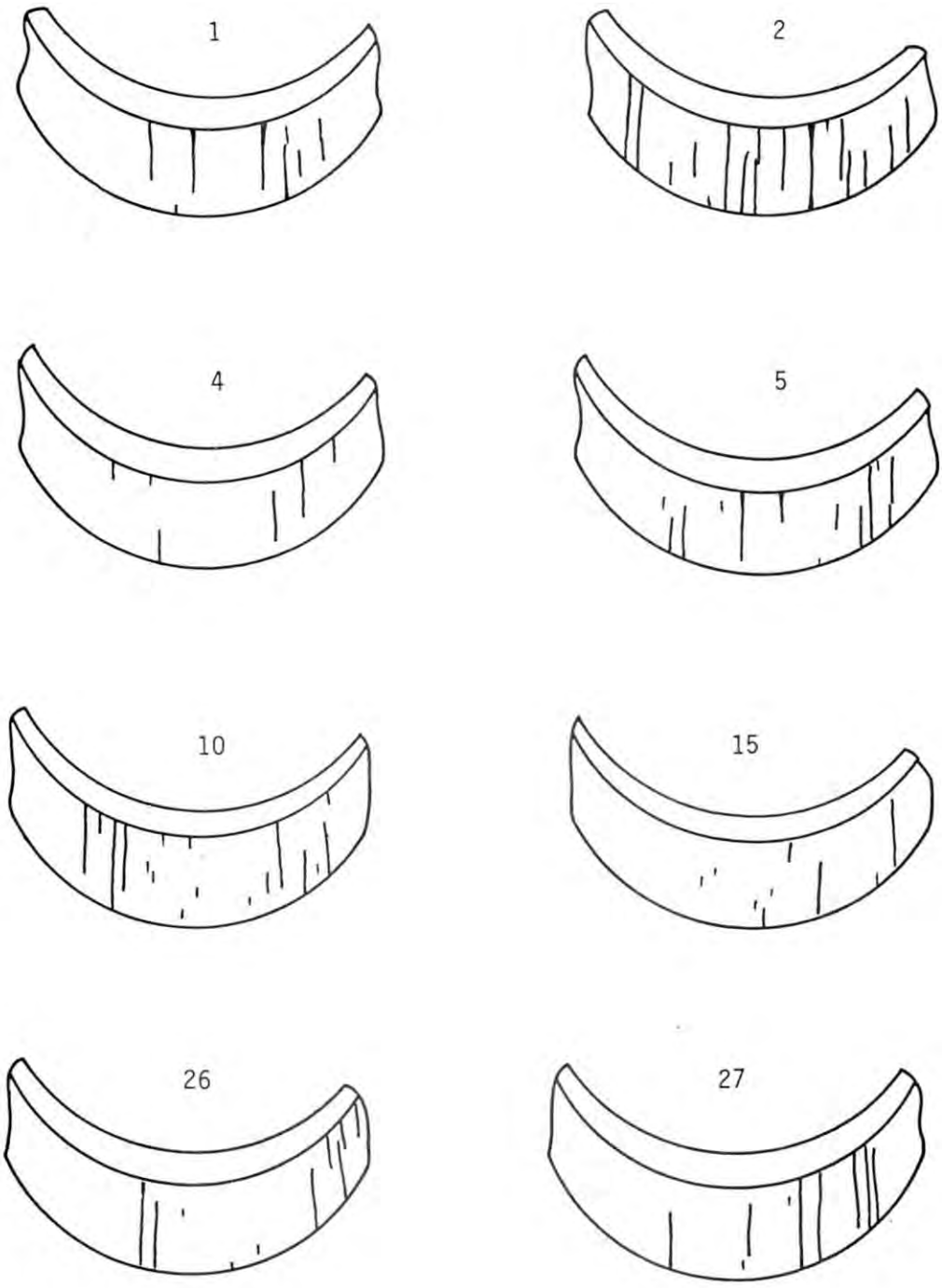

Figure 3.4 Crack patterns formed in the apex regions of Marlex CL-100 HDPE U-bend specimens prior to long-term exposure to deionized water. Specimen numbers given above sketches.

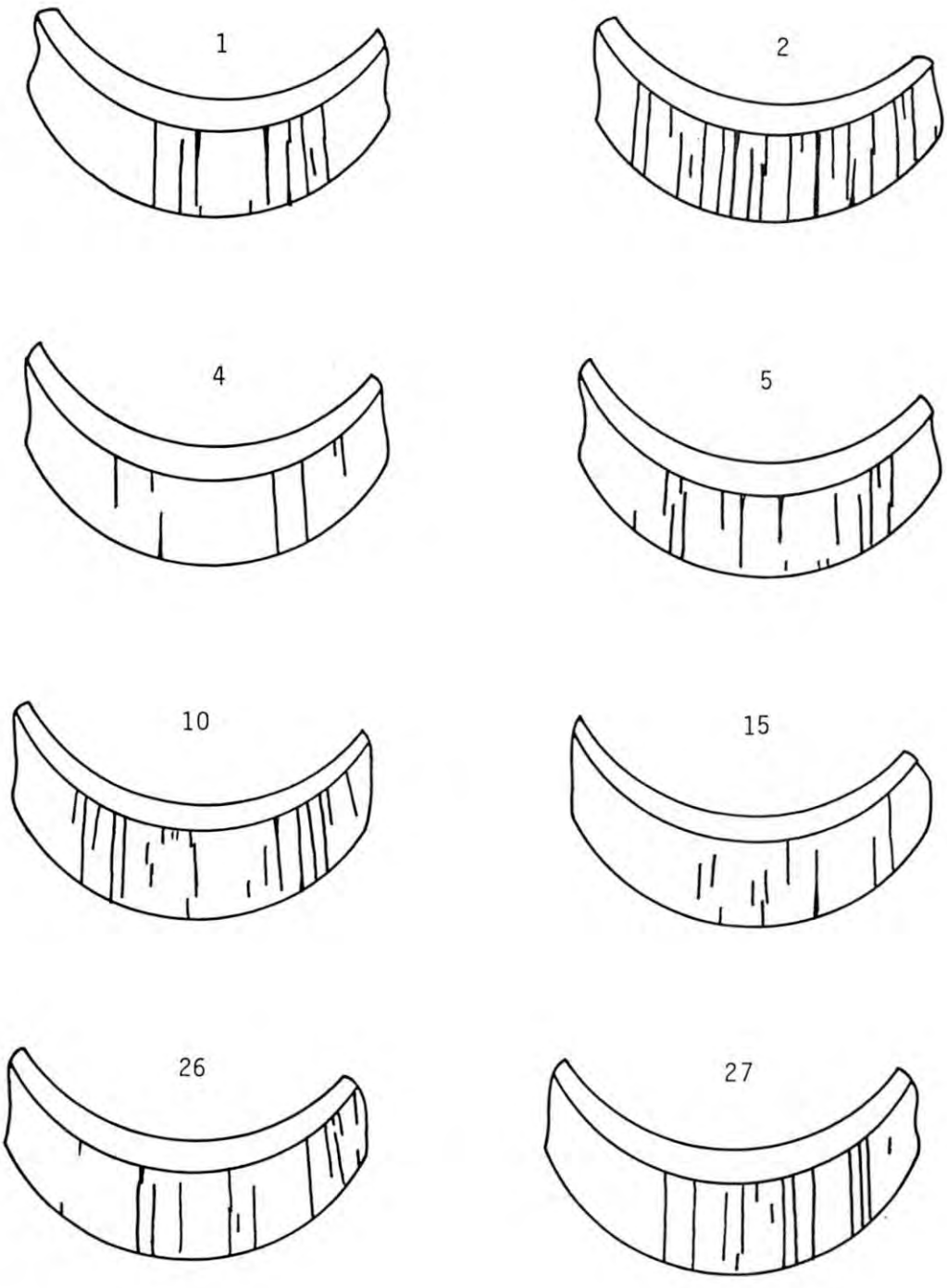

Figure 3.5 Crack patterns in the HDPE U-bend specimens shown in Figure 3.4 after 227 d exposure to deionized water at 20°C. Specimen number given above sketches.

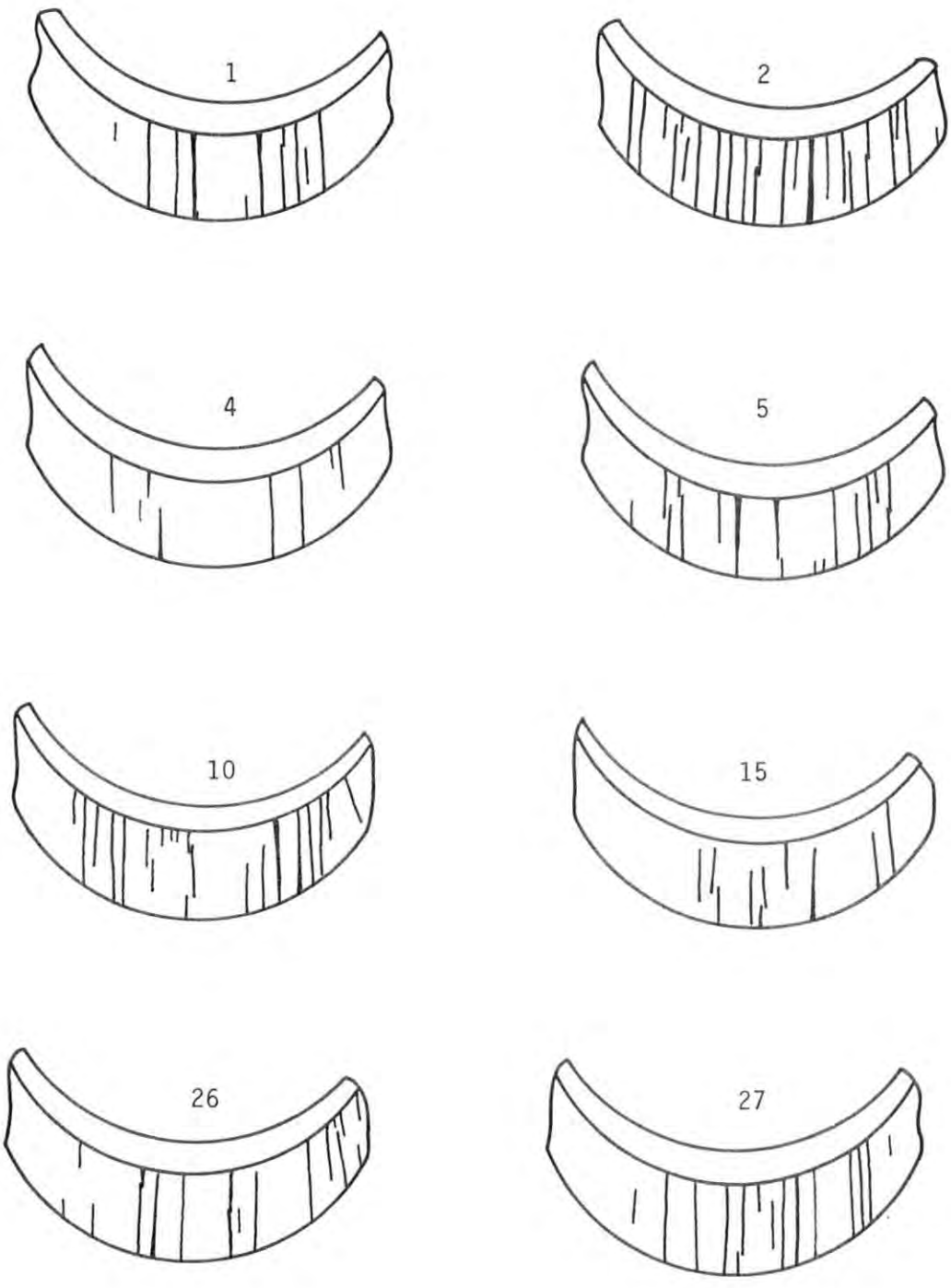

Figure 3.6 Crack patterns in the HDPE U-bend specimens shown in Figure 3.4 after 437 d exposure to deionized water at 20°C. Specimen numbers given above sketches.

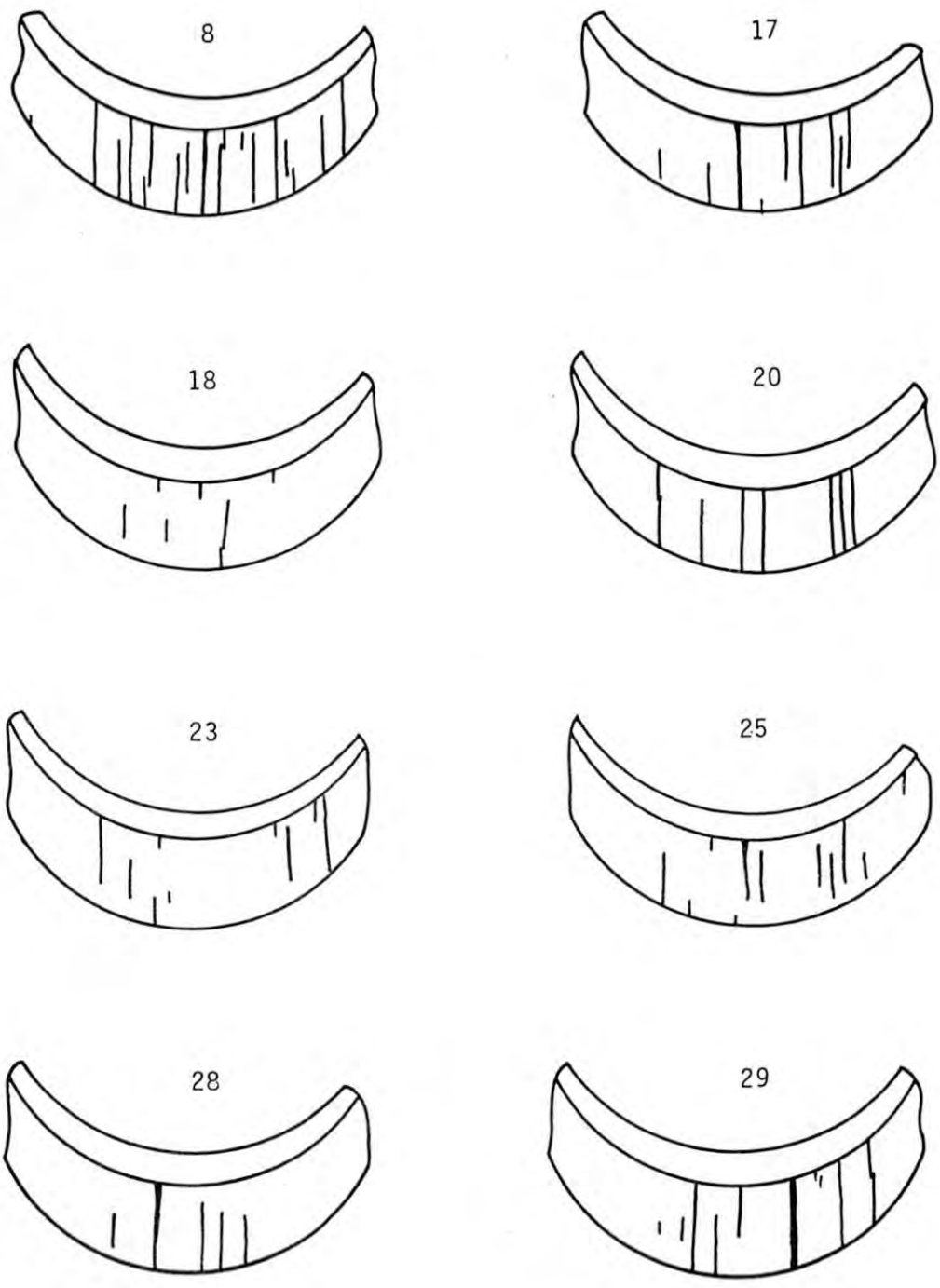

Figure 3.7 Crack patterns formed in the apex regions of Marlex CL-100 HDPE U-bend specimens prior to long-term exposure to nitrogen. Specimen numbers given above sketches.

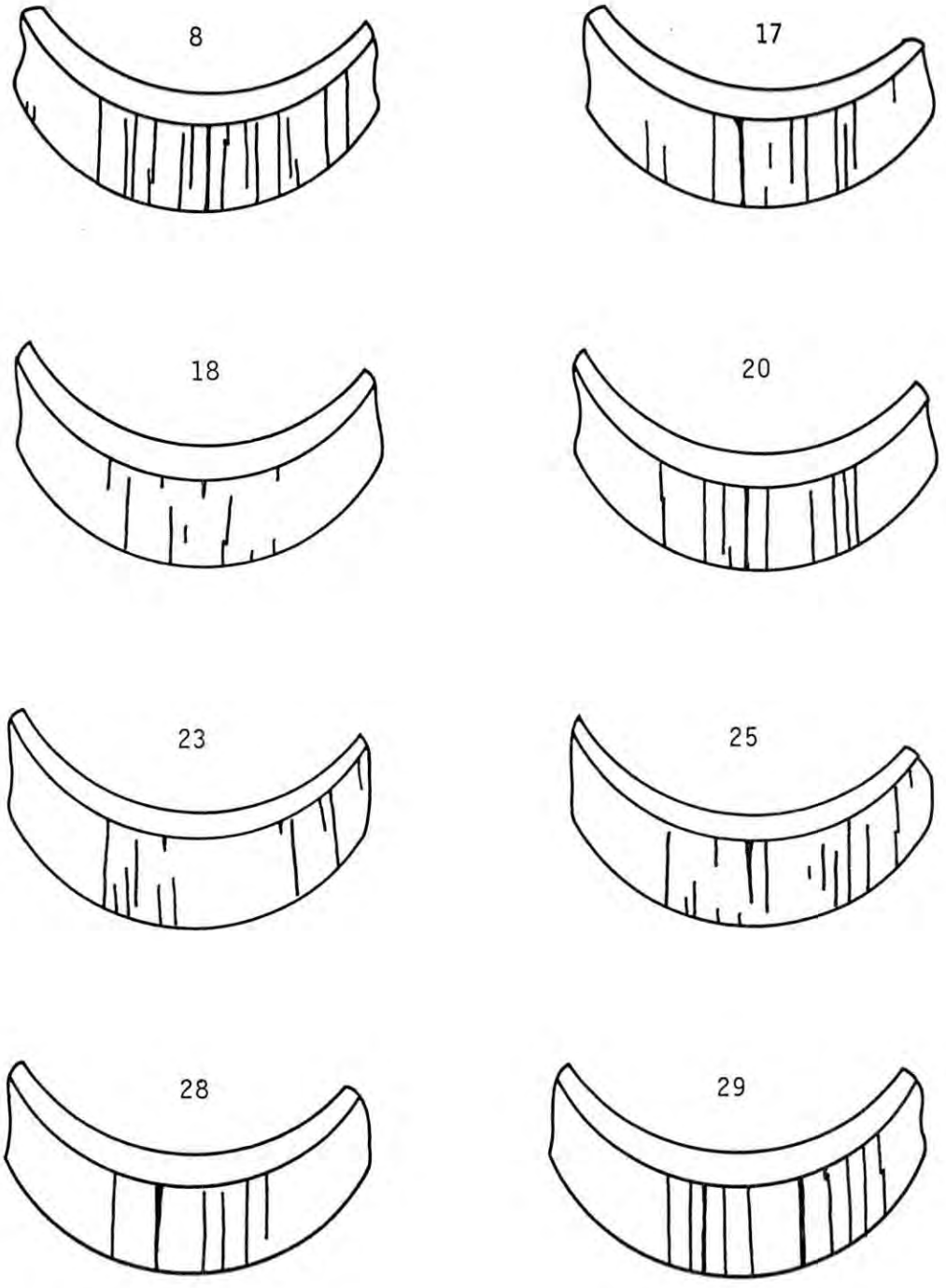

Figure 3.8 Crack patterns in the U-bend specimens shown in Figure 3.7 after 227 d exposure to nitrogen at 20°C. Specimen numbers given above sketches.

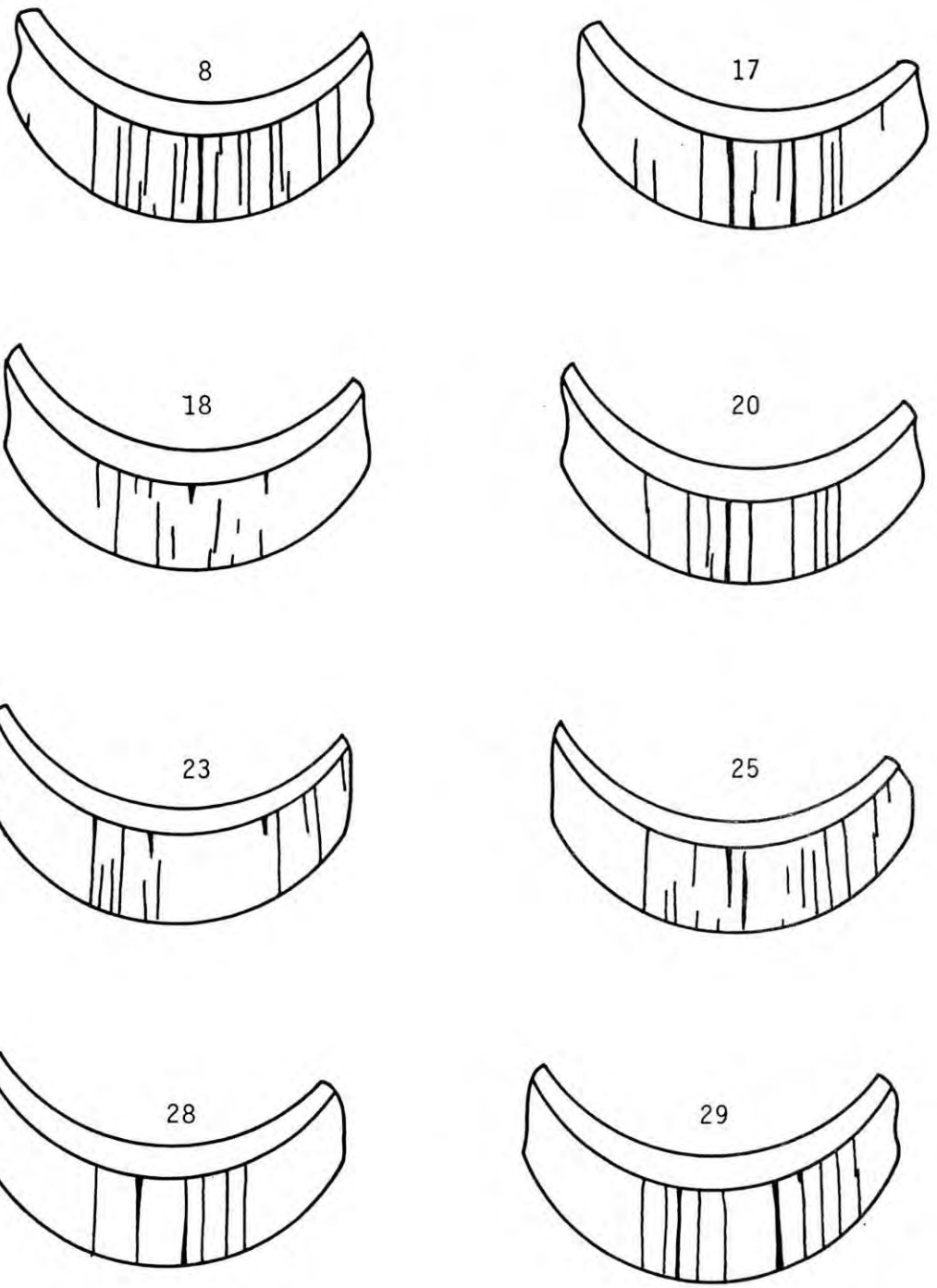

Figure 3.9 Crack patterns in the HDPE U-bend specimens shown in Figure 3.7 after 437 d exposure to nitrogen at 20°C. Specimen numbers given above sketches.

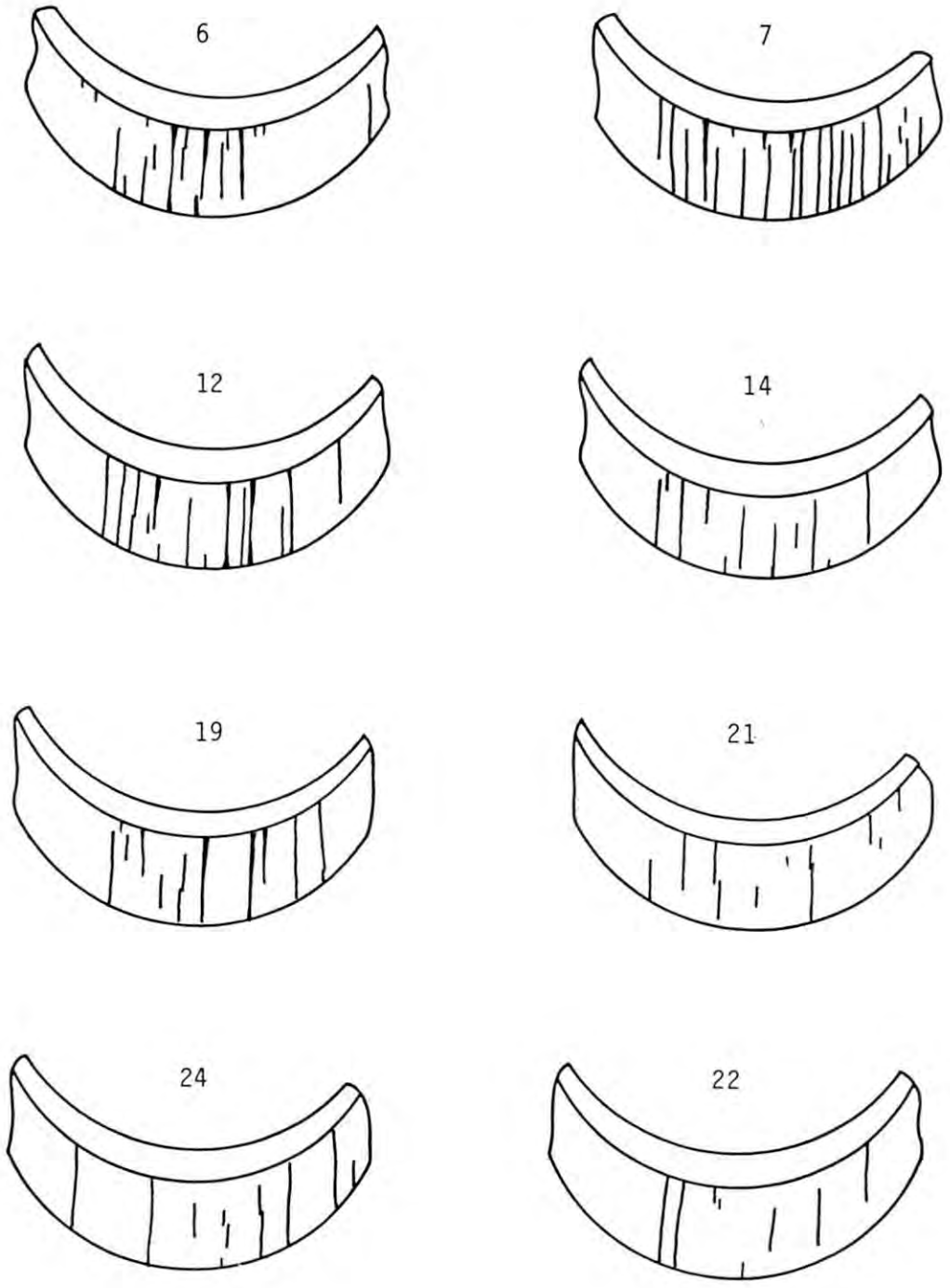

Figure 3.10 Crack patterns formed in the apex regions of Marlex CL-100 HDPE U-bend specimen prior to long-term exposure to a vacuum. Specimen numbers given above sketches.

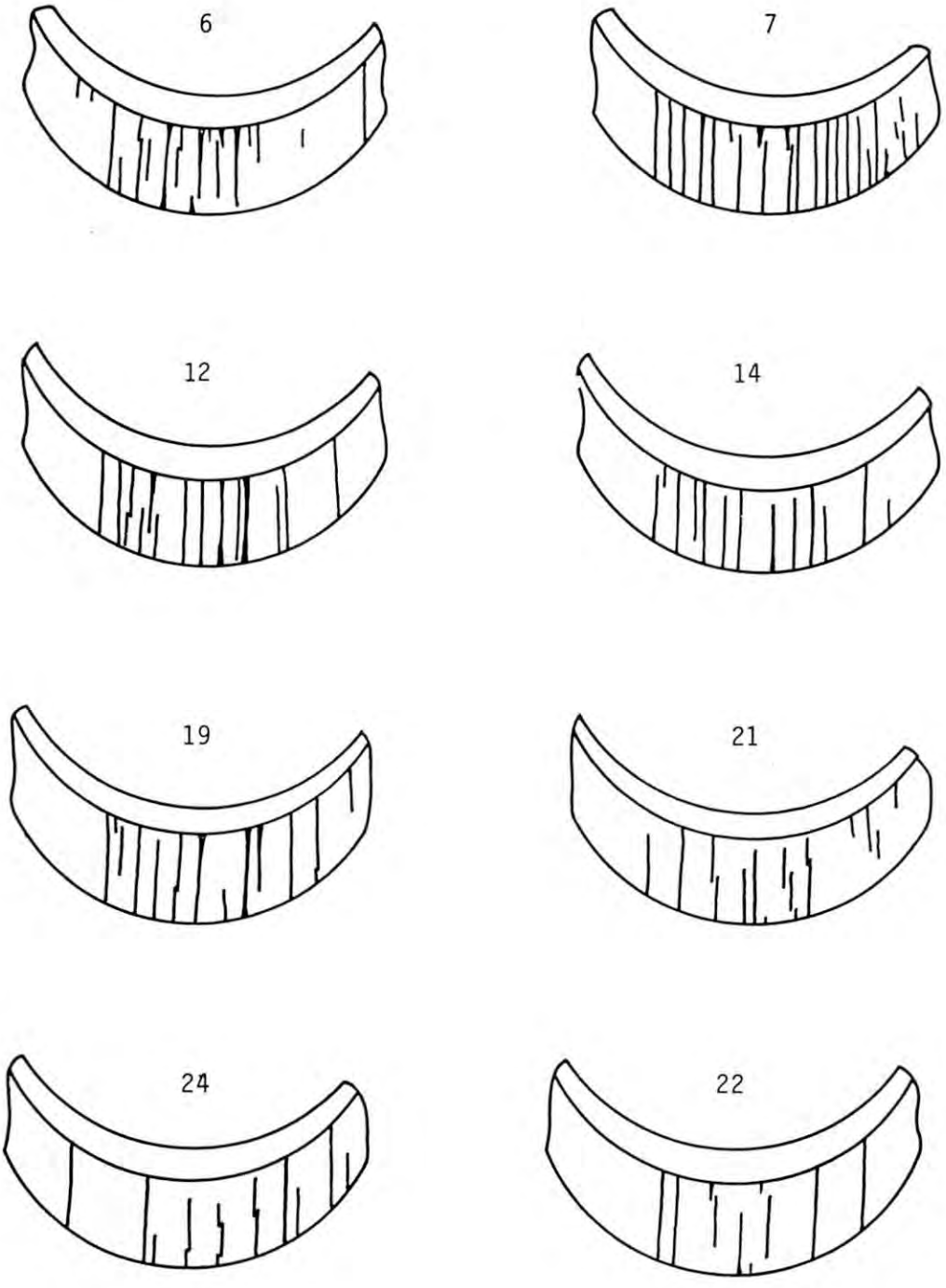

Figure 3.11 Crack patterns in the U-bend specimens shown in Figure 3.10 after 227 d exposure to initial vacuum conditions at 20°C. Vacuum was lost through a slow leak during the test period. Specimen numbers given above sketches.

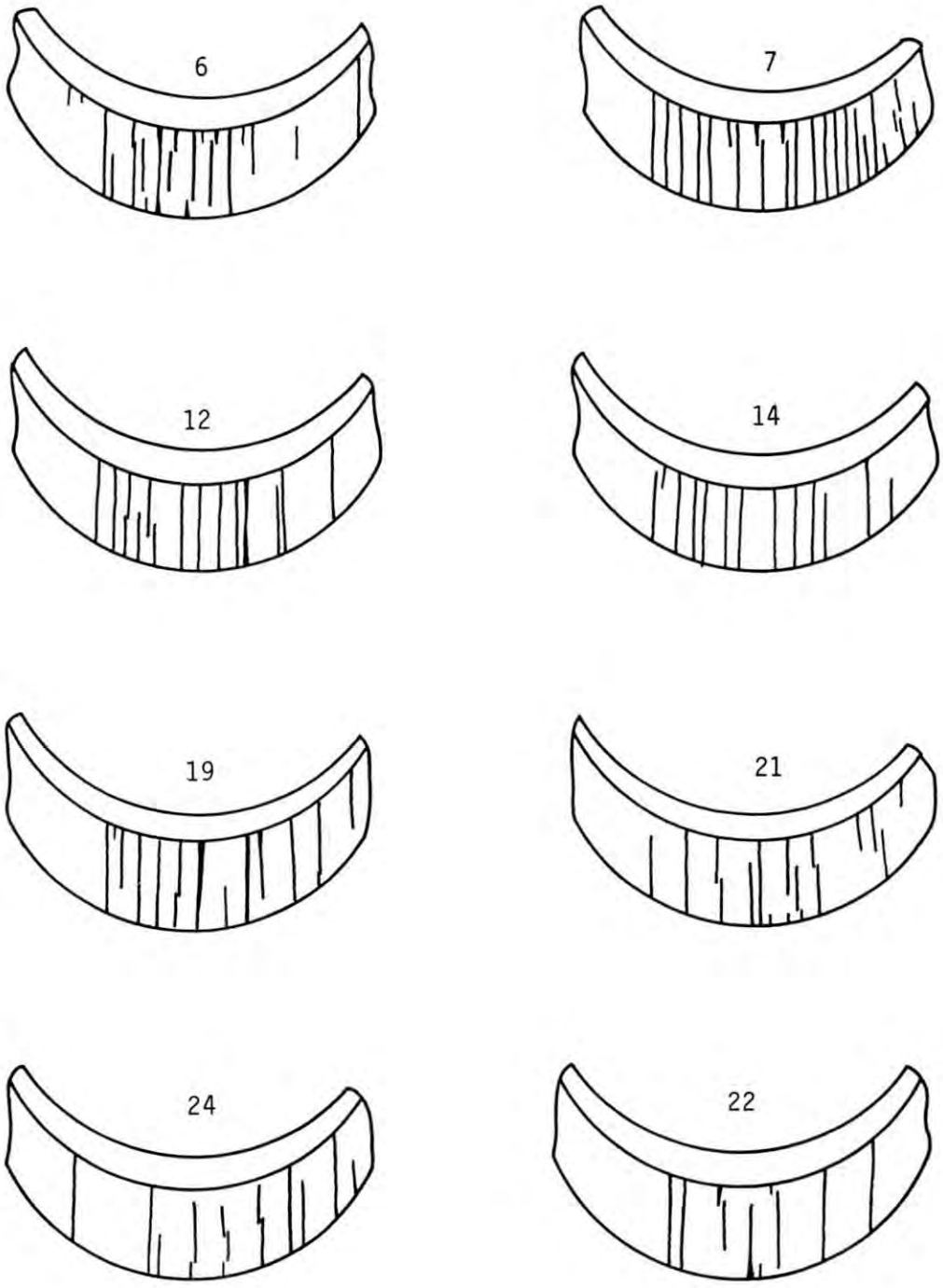

Figure 3.12 Crack patterns in the U-bend specimens shown in Figure 3.10 after 437 d exposure to vacuum conditions at 20°C. Vacuum was lost through a slow leak during part of the previous test cycle period. Specimen numbers given above sketches.

Table 3.1 Cracking in Type I HDPE U-bend specimens exposed for 227 d to various test environments at room temperature.[1]

Environment	Cracks Before Exposure			Cracks After Exposure			Percent Change in Numbers of Cracks		
	Large	Small	Total	Large	Small	Total	Large	Small	Total
Air	48	58	106	70	63	133	45.8	8.6	25.5
DIW	41	48	89	69	50	119	68.3	4.2	33.7
N_2	44	34	78	63	36	99	43.2	5.9	26.9
Vacuum[2]	58	52	110	80	46	126	37.9	-11.5	14.6

Notes:

1. The numbers of cracks are the totals counted for each batch of 8 replicate specimens.
2. Vacuum not maintained throughout test period.

Table 3.2 Cracking in Type I HDPE U-bend specimens exposed for 437 d to various test environments at room temperature.(1)

Environment	Cracks Before Exposure			Cracks After Exposure			Percent Change in Numbers of Cracks		
	Large	Small	Total	Large	Small	Total	Large	Small	Total
Air	48	58	106	85	51	136	77.1	-12.1	28.3
DIW	41	48	89	79	45	124	92.7	-6.3	39.3
N_2	44	34	78	67	36	103	52.3	+5.9	32.1
Vacuum(2)	58	52	110	87	42	129	50.0	-19.2	17.3

Notes:

1. The numbers of cracks are the totals counted for each batch of 8 replicate specimens.
2. Vacuum maintained throughout the second test period of 210 d.

and their random allocations to batches of eight replicate samples, the numbers of starting cracks were not always similar for each batch. For example, the batch to be tested in nitrogen contained a total of 78 cracks whereas those exposed to a vacuum had 110 cracks. Since a large crack density would tend to give lower tensile stresses at the U-bend surface, care must be taken to ensure that erroneous conclusions are not made regarding the roles of the test environment and the magnitude of the stress with respect to crack initiation and propogation.

Consider first the data in Table 3.1 showing crack distributions after 227 days of exposure. A comparison between the air and vacuum test data is most appropriate since the initial numbers of cracks are about the same in each case (106 vs. 110). If one assumes that the stress levels in each batch of eight specimens are similar then it maybe inferred that higher oxygen levels encourage crack initiation and propagation. During this period the air-test specimens show a 25.5 percent increase in small cracks versus 14.6 percent to the vacuum-tested samples. During the second test period (Table 3.2) the rate of crack initiation slowed considerably and only three new cracks were nucleated in each batch of specimens. Overall, it is seen that the air-tested specimens started with fewer cracks and ended with significantly more than those tested in a vacuum.

U-bend specimens tested in deionized water and nitrogen contained far fewer cracks at test initiation compared to air and vacuum tested samples. Therefore, on average, they should be more highly stressed. The data on crack initiation and growth Tables 3.1 and 3.2 are basically consistent with this assumption since the rates of increase in total cracks are highest for water and nitrogen.

Another way of analyzing the effects of environment on the cracking of the U-bend specimens is to consider the total numbers of new cracks initiated during the test rather than the percent increases, as described above. It will be seen from Table 3.2 that 35 new cracks were nucleated in the water environment, 30 in the air, 25 in nitrogen, and only 19 in vacuum. Although the results may not be fully significant from a statistical standpoint, they indicate that specimens tested in air, and which were probably stressed to a relatively low value because of the larger number of starting cracks, were still very susceptible to crack nucleation. The abundance of oxygen is the most likely reason for this enhanced cracking.

Of the four test environments, the water medium probably contains the least oxygen. At room temperature it is well known that the dissolved oxygen level is only 8 ppm. Impurities in the nitrogen gas used, small vacuum leaks, and the general difficulty in maintaining gaseous test environments over long periods of time would certainly give oxygen levels in the nitrogen and vacuum systems much higher than the 8 ppm known to be dissolved in the water. Nevertheless, cracking in water occurred most easily both in terms of percent increase and the total number of new cracks. Abundance of oxygen cannot be invoked to explain this observation. A possible explanation lies in the wetting of material at the tips of cracks. Work by Shanahan and Shultz (1979, 1980) explored the effects of wetting agents on creep and environmental stress cracking in polyethylene in terms of the ability of liquids to flow into the tips of moving cracks thereby enhancing their growth. They postulated that at

high stresses non-active liquids (such as water) give behavior similar to that for air. The current data for water show, in fact, that water is just as aggressive as air in crack initiation and propagation.

3.2 Crack Initiation and Growth in a Gamma Field (Large Prototype U-Bends)

To check the usefulness of U-bend specimens for monitoring cracking in stressed HDPE in the presence of a gamma field, eight large U-bends were initially made for scoping tests. The Marlex CL-100 Type I specimens were cut from the sidewall of the "old" HDPE batch. Sample preparation is described in Section 2.2.1. Bending introduced surface cracking, as described previously.

One pair of specimens was maintained at room temperature to serve as unirradiated controls whereas three other pairs were irradiated at three separate Co-60 gamma dose rates, viz. 3.4×10^3, 5.6×10^4, and 2.1×10^6 rad/h. The irradiations were conducted in air at a temperature of about 10°C in the Brookhaven High Intensity Radiation Development Laboratory (HIRDL).

The specimens were periodically removed from the irradiation facility and checked for physical and chemical change and general cracking effects. Figure 3.13 shows a general view of a single unirradiated U-bend specimen, and three pairs of samples irradiated at the different dose rates. The specimens irradiated to 3.6×10^7 rad were tan in color and had a slight odor. One crack had nearly penetrated through the thickness of the specimen and at least one other deep crack was present. Figure 3.14 shows a magnified view of the crack. Note, also, the presence of a fine network of parallel cracks in the oxidized surface of the specimen which are perpendicular to the larger cracks in the apex region.

The specimens irradiated to 5.9×10^8 rad were a dark brown in color and had several cracks which had penetrated through about a half of the specimen thickness. An important observation is that the deepest cracks in the specimens irradiated at the two lower dose rates were nearly always located away from the apex of the U-bend even though one might expect the highest tensile stresses to be located at the apex. This will be discussed in detail later.

For the highest dose achieved (1.7×10^{10} rad) the specimens were embrittled and both fractured into pieces when they were gently squeezed to check their elasticity. Prior to achieving the 1.7×10^{10} rad dose, the samples had become black in color and gas generation in the form of small bubbles at the surface of the plastic were noticed. (Figure 3.15). It was found that once the specimens had achieved a 10^{10} rad dose they were no longer sticky, indicating that a new stage of the gamma-induced degradation process had been reached.

Table 3.3 summarizes observations made on the large prototype U-bend specimens. In comparison, there was no obvious change in the appearance of the unirradiated controls. However, it must be stated that close examination of crack propagation rates was not carried out because of the scoping value of the tests.

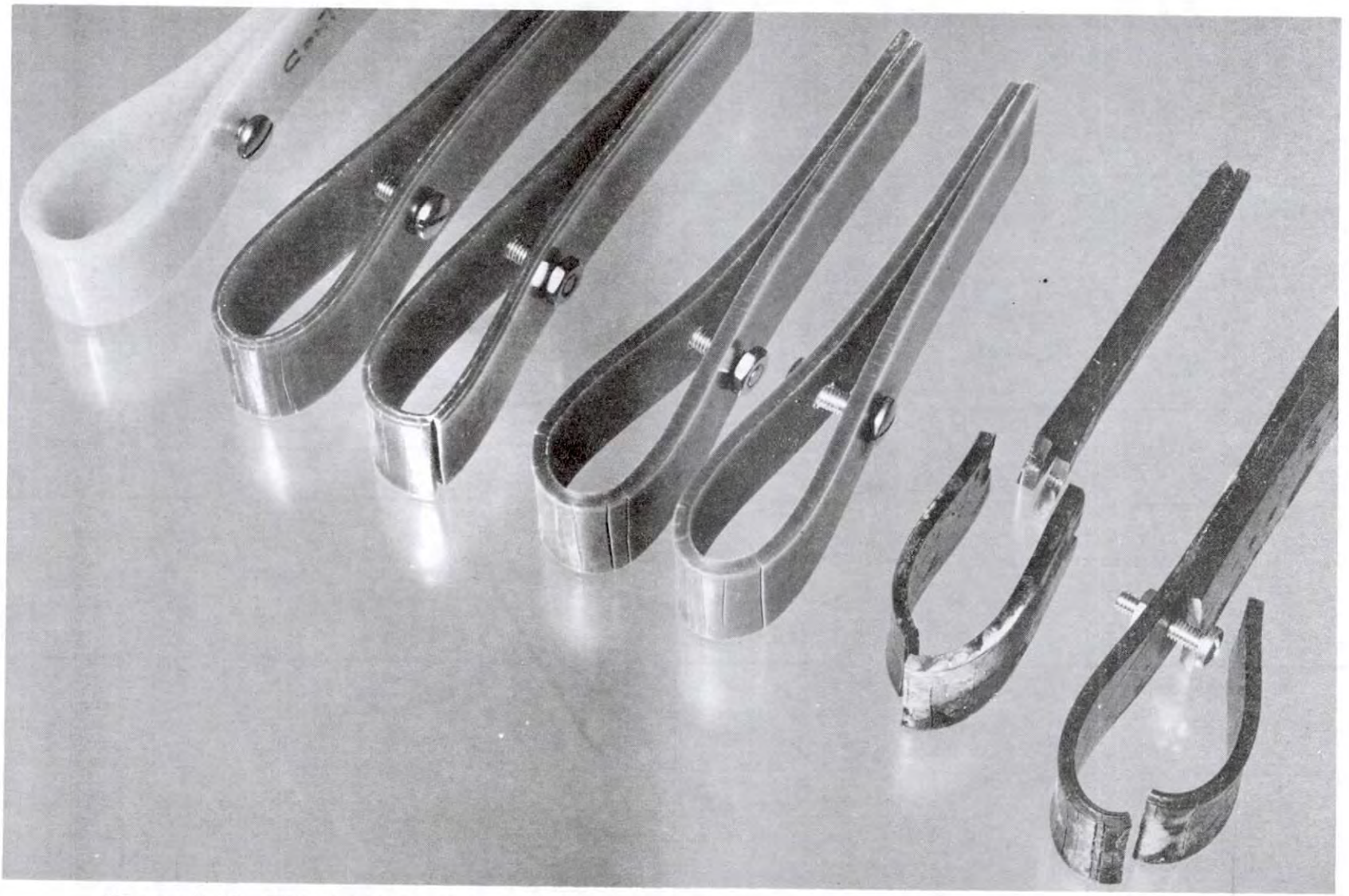

Figure 3.13 Effect of gamma irradiation on crack propagation in bent Marlex CL-100 HDPE specimens. Sample on left is an unirradiated control; others from left to right were irradiated at 10°C to 3.6×10^7 rad (at 3.4×10^3 rad/h), 5.9×10^8 rad (at 5.6×10^4 rad/h), and 1.7×10^{10} rad (at 2.1×10^6 rad/h). Magnification 0.75 X.

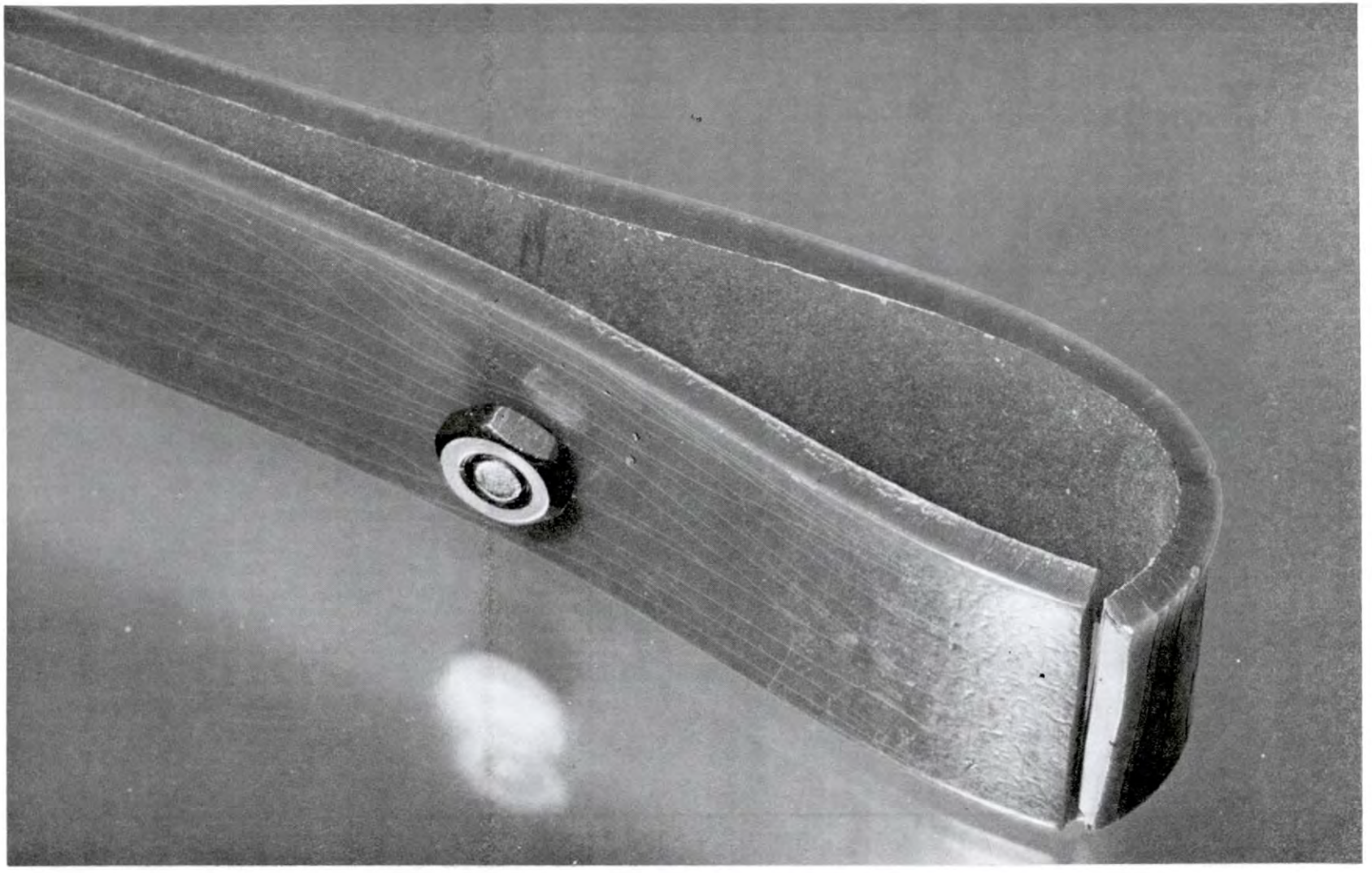

Figure 3.14 Full-penetration crack in a Marlex CL-100 HDPE U-bend specimen gamma irradiated to 3.6×10^7 rad (at 3.4×10^3 rad/h) at 10°C. Note the fine network of cracks in the oxidized surface layer lying along the length of the specimen. Magnification 1.4 X.

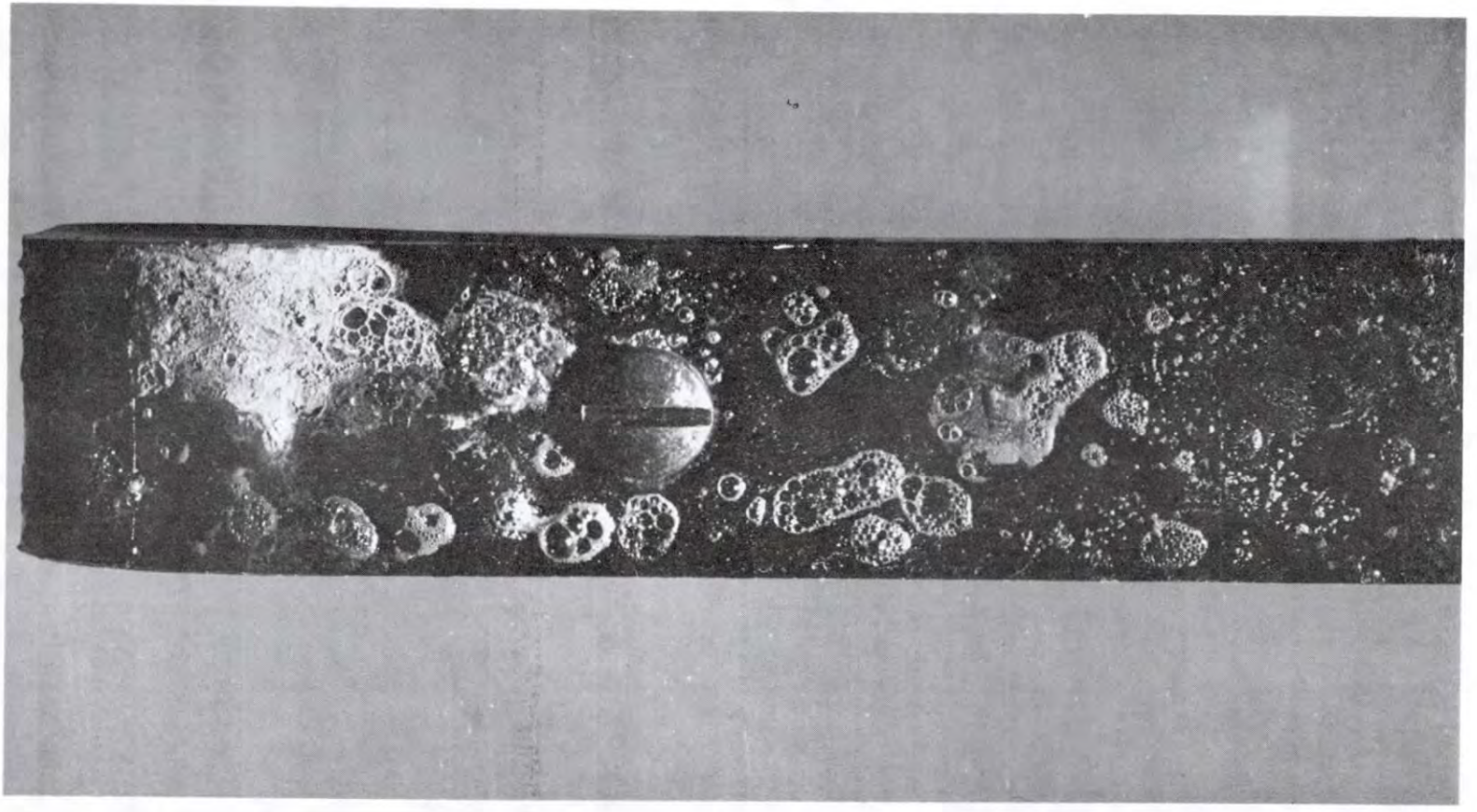

Figure 3.15 Gas Bubble generation in Marlex CL-100 HDPE gamma irradiated at 10°C to 1.7 x 10^{10} rad/h). Magnification 1.9 X.

Table 3.3 Observations on Marlex CL-100 HDPE U-bend specimens exposed to gamma radiation.

Dose (rad)	Dose Rate (rad/h)		
	3.4×10^3	5.6×10^4	2.1×10^6
4.9×10^6	Cracks appear to grow.	Specimen color is light brown.	-
1.6×10^7	Cracks definitely growing. Specimen color is tan.	-	-
2.0×10^7	One crack propagated through specimen.	-	-
2.9×10^7	Little additional crack propagation. Specimens still flexible.	-	-
3.6×10^7	Large crack at apex still propagating. Another crack also growing rapidly. Both cracks almost full penetration. Specimens have slight odor.	-	-
9.9×10^7	(a)	-	Specimen color dark brown.
1.6×10^8	(a)	Specimen color medium brown. One crack growing.	-
3.2×10^8	(a)	Several cracks growing in size.	-
5.9×10^8	(a)	Noticeable crack growth in both specimens. Cracks about 50% through thickness of specimen.	-
1.2×10^9	(a)	(a)	Specimen becoming sticky. Small shiny areas developing.
2.9×10^9	(a)	(a)	Specimen very sticky, brown/black color. Strong aroma noticed.
5.8×10^9	(a)	(a)	Small surface bubbles form on original shiny areas.
8.8×10^9	(a)	(a)	Many bubbles now seen on surface. Specimen black.
1.7×10^{10}	(a)	(a)	Tests terminated. Specimens completely brittle, no longer sticky.

(a) Dose not yet reached.

3.3 Crack Initiation and Growth in a Gamma Field (Small U-bend Specimens)

The success of the large prototype U-bend samples for characterizing cracking in irradiated HDPE, prompted the fabrication of smaller specimens to more quantitatively assess irradiation-induced crack propagation effects. As mentioned in Section 2.2.1 batches of eight replicated U-bend specimens were made using Type I, Type II, and Type III specifications. Table 3.4 shows the test matrix for the small U-bend irradiation tests. Eight replicate specimens were tested for each irradiation condition and for the unirradiated controls. The irradiations were also carried out in air in the HIRDL facility at 10°C. Control samples were maintained in a refrigerator at the same temperature.

Table 3.4 Test matrix for crack-propagation studies on irradiated Marlex CL-100 HDPE small U-bend specimens

Gamma Dose Rate (rad/h)	Outer Surface Condition of U-Bend		
	Oxidized Surf. Present (Type I)	Oxidized Surf. Removed (Type II)	Non-Oxidized Surf. Present (Type III)
0	8(1)	8	8
1.4×10^3	8	8	8
8.4×10^3	8	8	8
4.4×10^5	8	8	8

(1) Number of specimens per batch.

Figure 3.16 shows the physical arrangement of samples that were irradiated in the program. The A, B, and C samples were irradiated at successively higher dose rates. Each of these batches comprises Type I, Type II, and Type III specimens designated as "a", "b", and "c", respectively. The samples are attached to angled aluminum alloy bar used nuts and bolts. Figure 3.16 shows, again, the coloration imparted to HDPE during gamma irradiation. Figure 3.17 is a magnified view of Type I (foreground) and Type III U-bend specimens after an accumulated gamma dose of 6.0×10^7 rads (at a dose rate of 8.4×10^3 rad/h. Note the deep cracks in the Type I specimens and the very fine cracks in Type III specimens. The fine cracks are, of course, related to the fact that upon preparing the Type III U-bend specimens, no cracks were formed. Therefore, the cracks are relatively "young" compared to the cracks in Type I samples. Cracks are also formed during the irradiation of Type II specimens (Figure 3.18). They are also very fine and much less numerous than those in Type III specimens. Note that the cracks in the Type II and III specimens are never formed at the apex of the samples. They are present in areas which would appear to be at a lower stress. This observation is in accord with the results for the Type I U-bend samples in which most of the very deep cracks which cause fracture were remote from the apex.

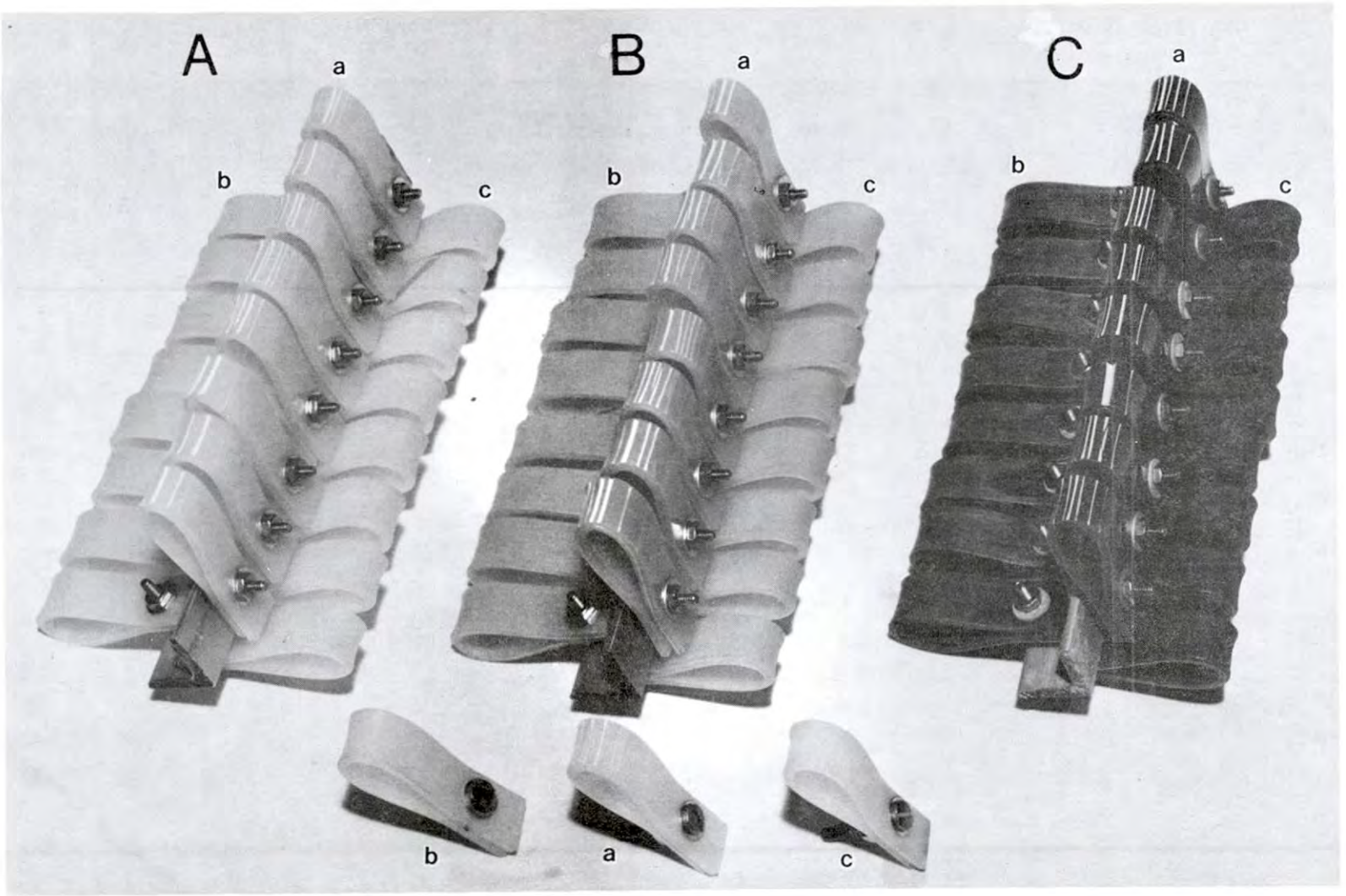

Figure 3.16 Appearance of Type I (a), Type II (b) and Type III (c) Marlex CL-100 HDPE U-bend specimens gamma irradiated to 2.1 x 10^6 rad (A), 1.3 10^7 rad (B), and 6.7 x 10^8 rad (C). Individual unirradiated Type I, Type II and Type III control specimens are shown at the bottom of the figure. Magnification 0.8 X.

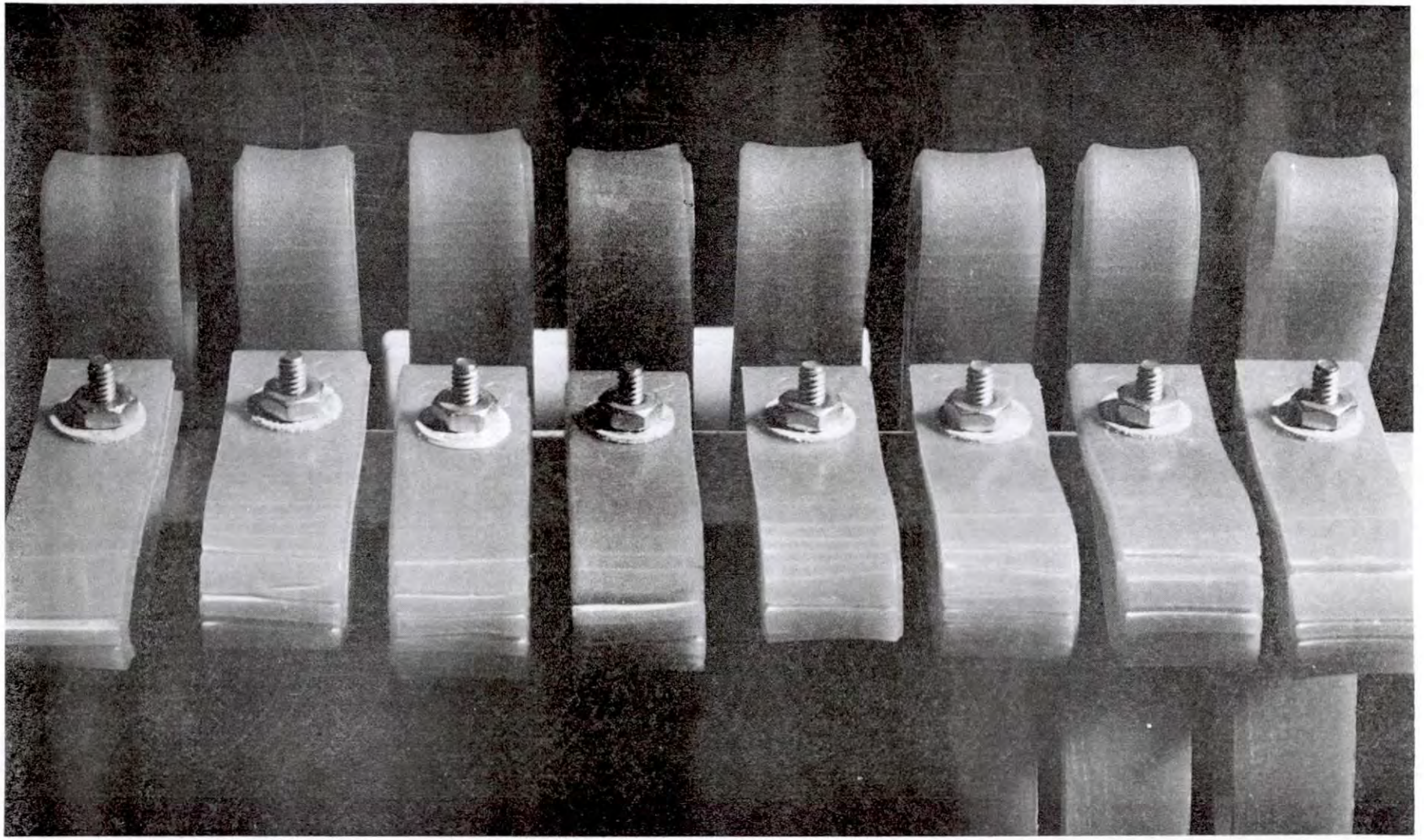

Figure 3.17 Cracking in Type I (bottom row) and Type III (top row) Marlex CL-100 HDPE U-bend specimens irradiated to 6.0×10^7 rad (at 8.4×10^3 rad/h). Note that the cracks in the Type III specimens are not in the apex region. Magnification 1.7 X.

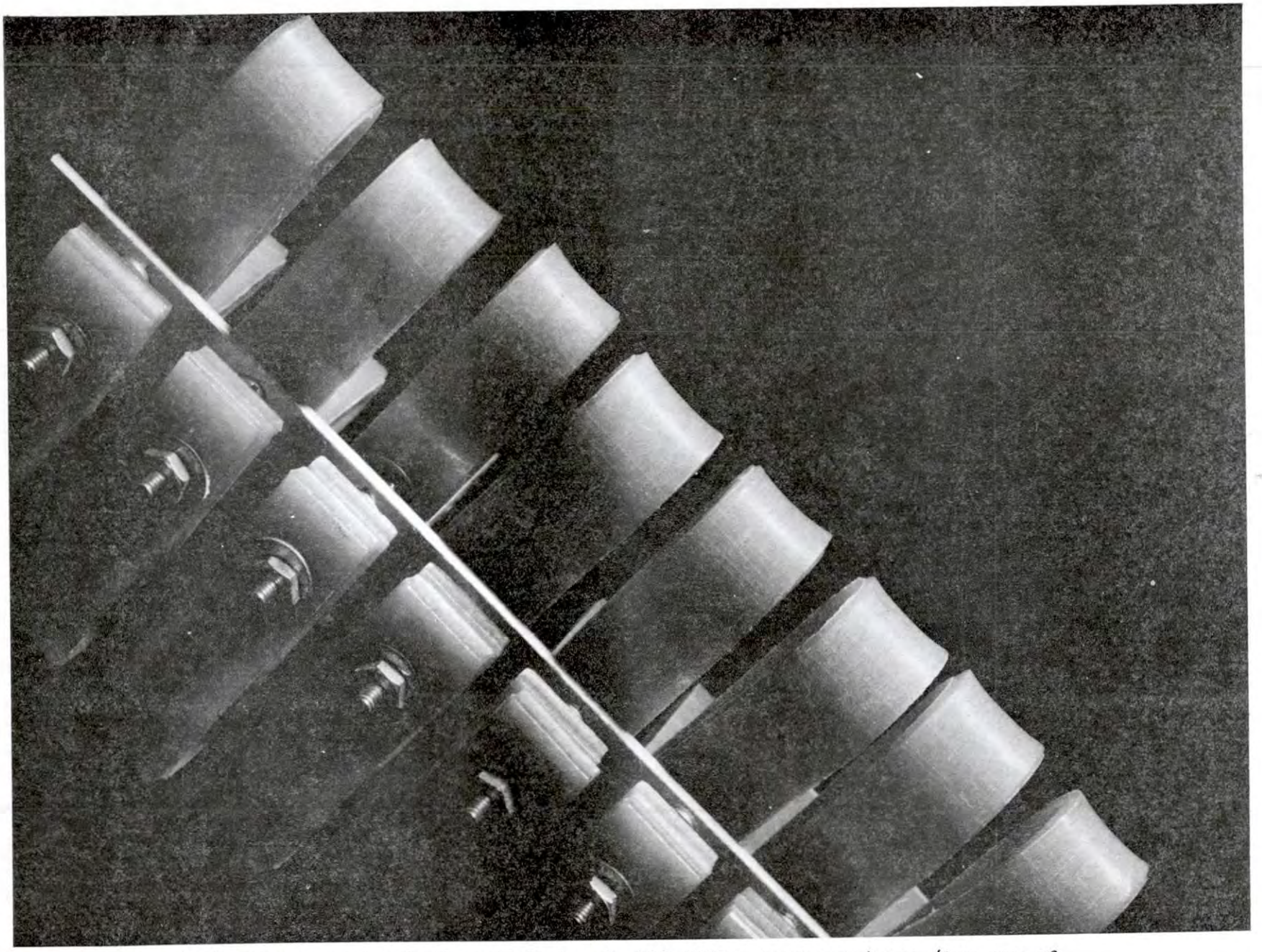

Figure 3.18 Fine cracking in Type II Marlex CL-100 HDPE U-bend specimens (top row of 8) irradiated to 6.0×10^7 rad (at 8.4×10^3 rad/h). Note that the cracks are not in the apex region. Magnification 1.7 X.

Figures 3.19 through 3.30 show sketches of cracks in Type I U-bend specimens prior to and after irradiation to two different dose levels. Data for non-irradiated controls are also shown. Crack distributions were counted and are given in Tables 3.5 and 3.6 for the two successive irradiations. For the first irradiation cycle (Table 3.5) which lasted 350 days, all irradiated specimens showed a larger increase in the numbers of cracks compared to unirradiated specimens. No accelerated crack initiation rate was noted for the highest dose rate condition, even though embrittlement was a more serious problem. This is an important finding since the lower dose rates, which are more typical of actual container irradiation conditions, are more prone to cause failure by radiation-induced crack growth mechanisms. This is concluded on the basis of the numbers of full-penetration, or close-to-full penetration, cracks (see Table 3.5).

After the second irradiation cycle (Table 3.6) the largest numbers of new cracks were found in unirradiated material. Usually, the irradiated samples showed no new crack initiations. This may be a result of stress relaxation in the irradiated U-bend samples caused by polymer chain scission mechanisms or by the rapid growth of cracks to full-penetration size which would lead to a major stress relaxation increment. From Table 3.6 there are 8 very large cracks in the U-bend specimens irradiated at the two lower dose rates. Possibly, the most highly irradiated specimens suffered the greatest amount of radiation-induced stress relaxation and were, therefore, unable to cause very fast crack growth. Chemical changes in the HDPE at high doses may be an important factor, also.

3.4 Discussion of Crack Propagation in Statically-Stressed HDPE

The results for the chemical environment tests indicate that oxygen is important in the initiation and growth of cracks in crosslinked HDPE under static loads. Air is probably the most deleterious environment but low-oxygen environments such as water are also capable of causing crack growth aided by liquid wetting effects at the tips of cracks under tensile stresses. Large amounts of oxygen in air do not greatly enhance the rate of cracking compared to those for oxygen-contaminated systems such as the nitrogen and vacuum environments used in this study. Faster cracking will undoubtedly occur if liquids which can promote environmental stress-cracking are present. This would be especially true if the HDPE was not molded and cured to produce optimum properties (Phillips).

Gamma irradiation has been shown, above, to cause embrittlement of HDPE and, under certain irradiation conditions, sharp "brittle" cracks are able to cause fracture in U-bend samples. Many prior studies of thermoplastic materials show that radiation-induced crosslinking stiffens the material, increases the molecular weight, and lowers the ductility. This mechanism is probably responsible for the embrittlement observed in the current U-bend tests, even through the Marlex CL-100 used in this study is already highly crosslinked.

Another factor that could help a crack to grow quickly in irradiated material is the occurrence of main-chain scission (Clough and Gillen, 1981; Gillen and Clough, 1981). During this process, polymer chains in the crack tip region which are subjected to large tensile stresses as well as gamma radiation, should experience a locally-enhanced rate of chain scission which

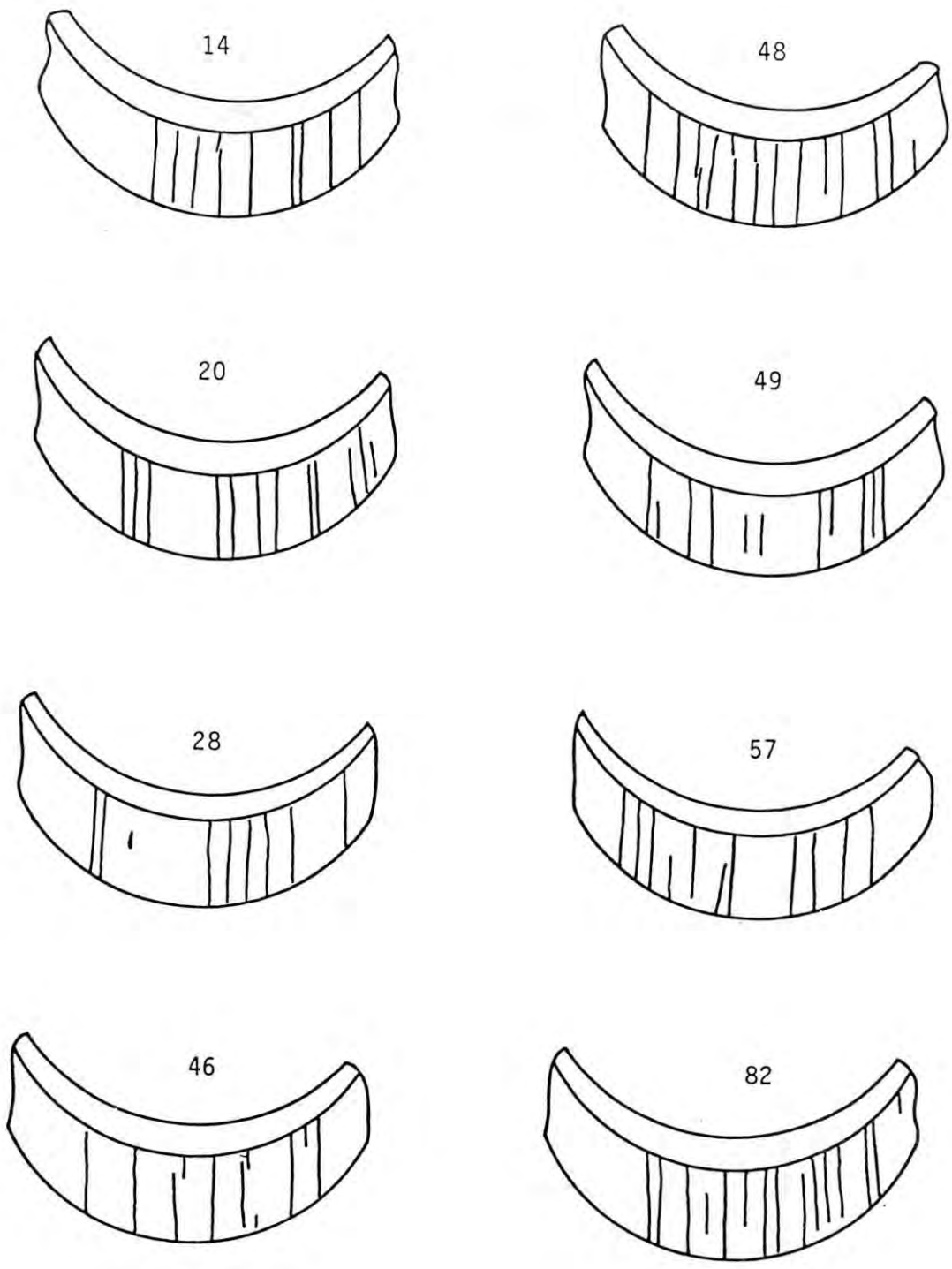

Figure 3.19 Crack patterns in as-prepared Type I Marlex CL-100 HDPE U-bend samples. Specimens are unirradiated controls. Specimen numbers given above each sketch.

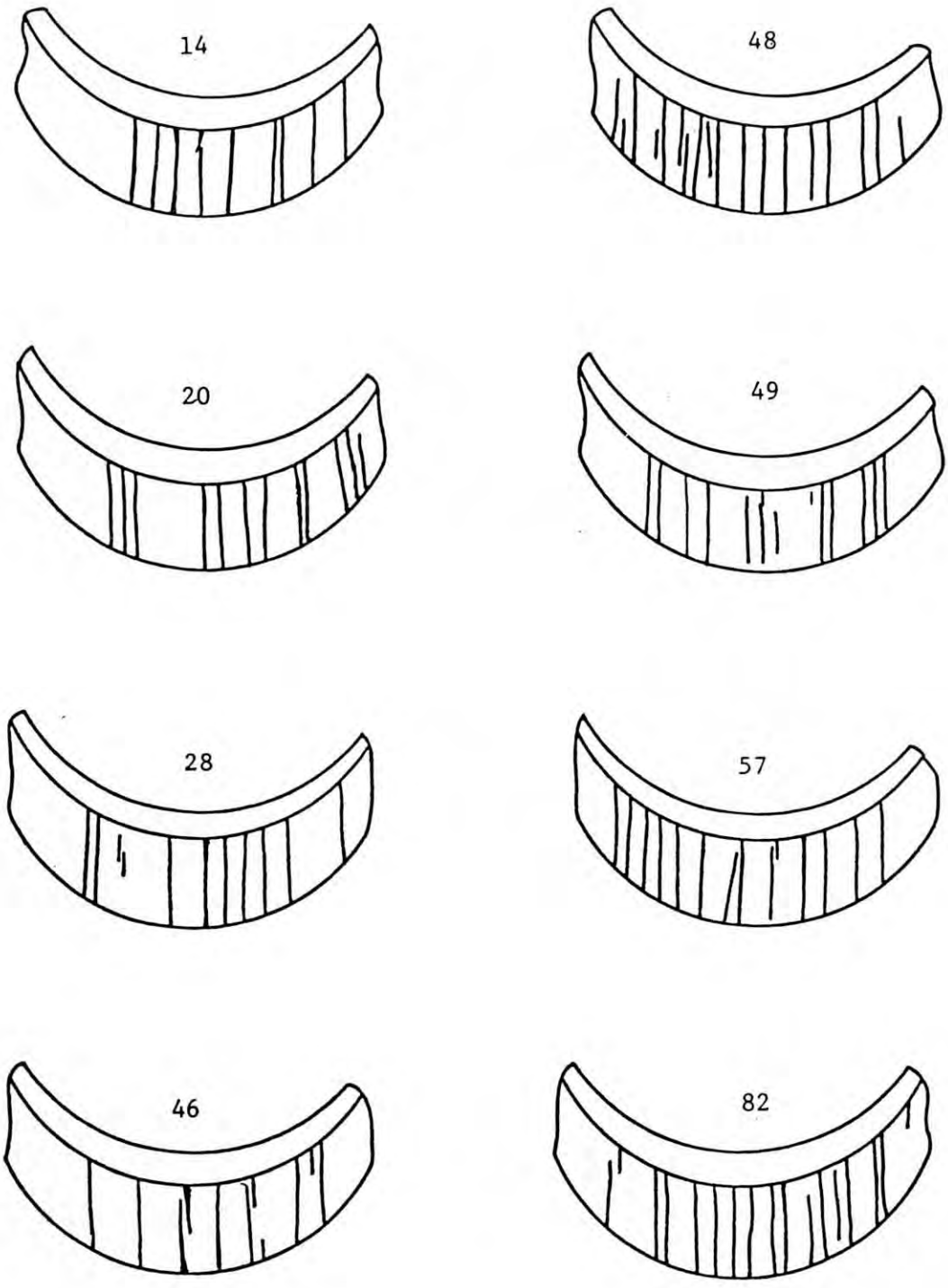

Figure 3.20 Crack patterns in unirradiated Type I Marlex CL-100 HDPE U-bend samples held at 10°C for 350 d. Specimen numbers given above each sketch.

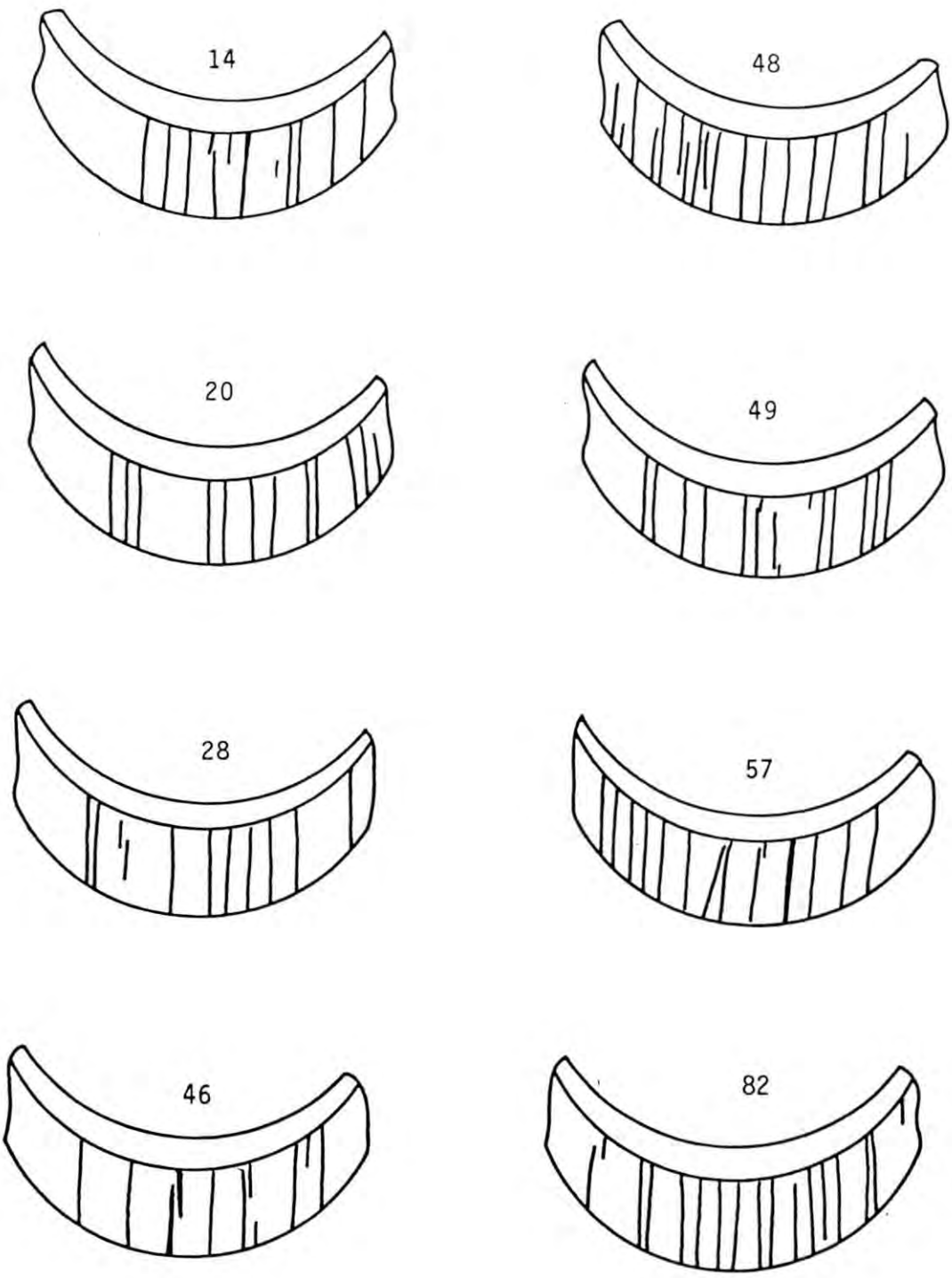

Figure 3.21 Crack patterns in unirradiated Type I Marlex CL-100 HDPE U-bend samples held at 10°C for 530 d in air. Specimen numbers given above each sketch.

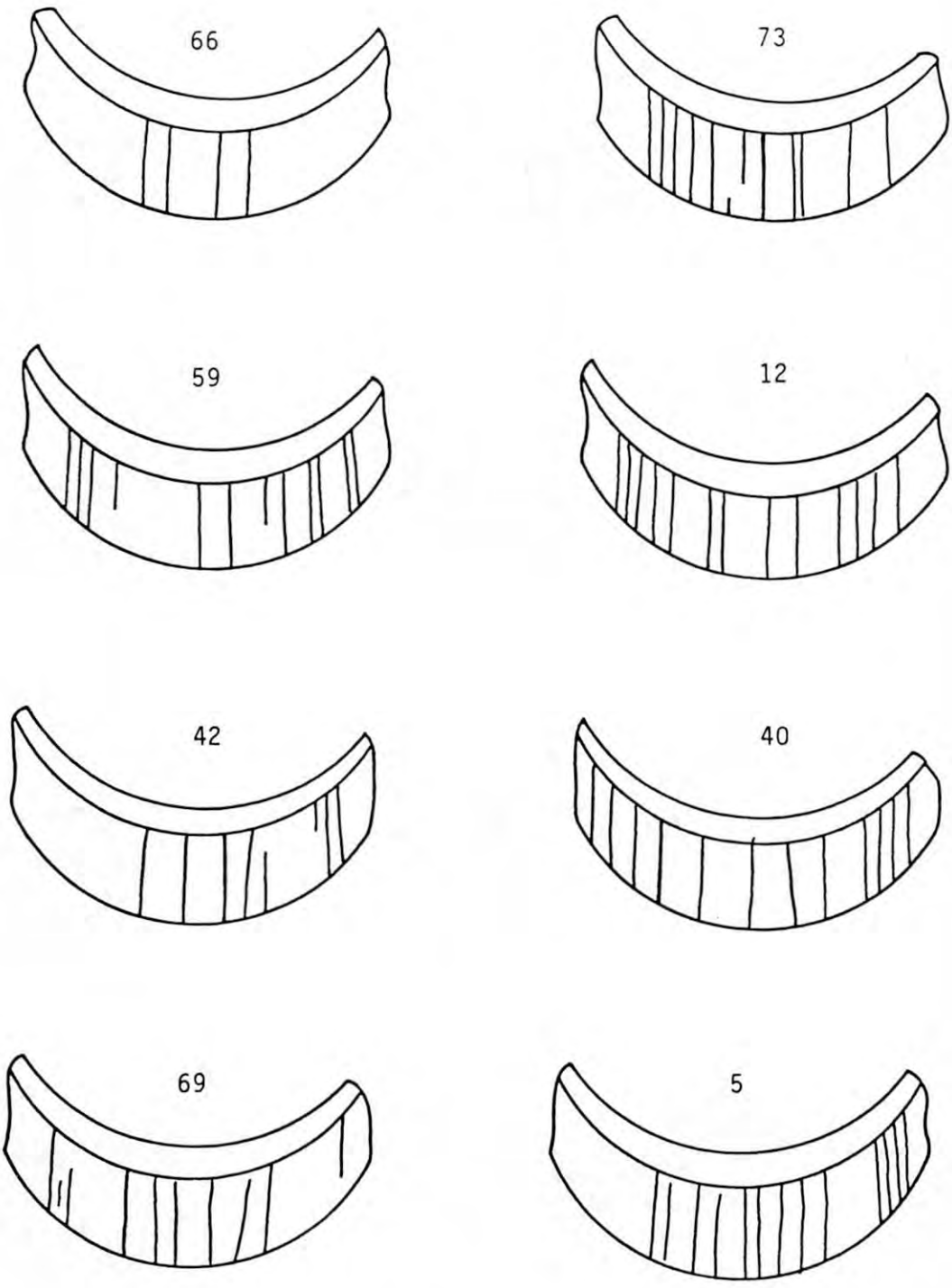

Figure 3.22 Crack patterns in as-prepared Type I Marlex CL-100 HDPE U-bend samples prior to gamma irradiation at 1.4×10^3 rad/h. Specimen numbers given above each sketch.

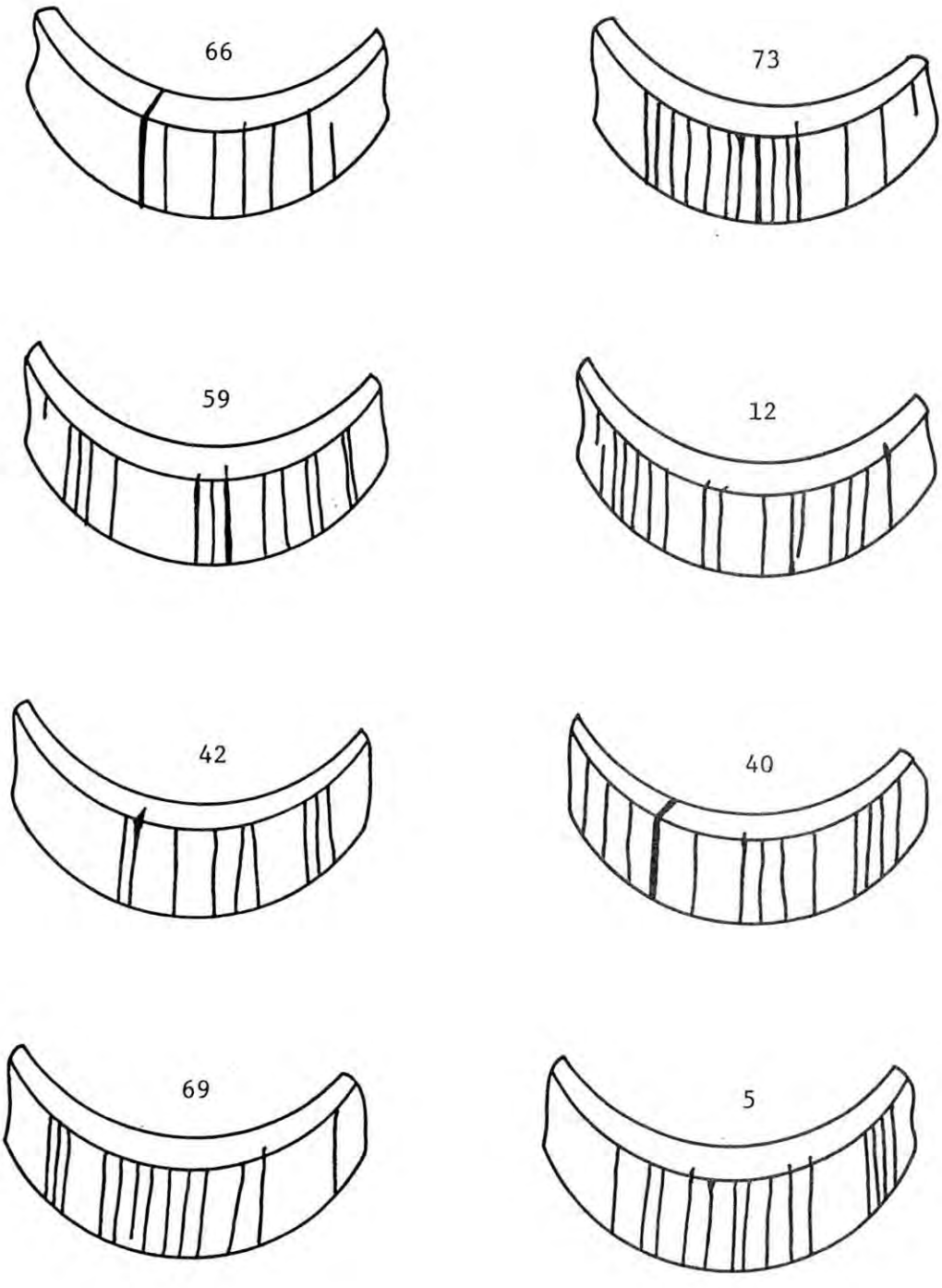

Figure 3.23 Crack patterns in Type I Marlex CL-100 HDPE U-bend samples after gamma irradiation to 7.5×10^6 rad at a dose rate of 1.4×10^3 rad/h. Specimen numbers given above each sketch.

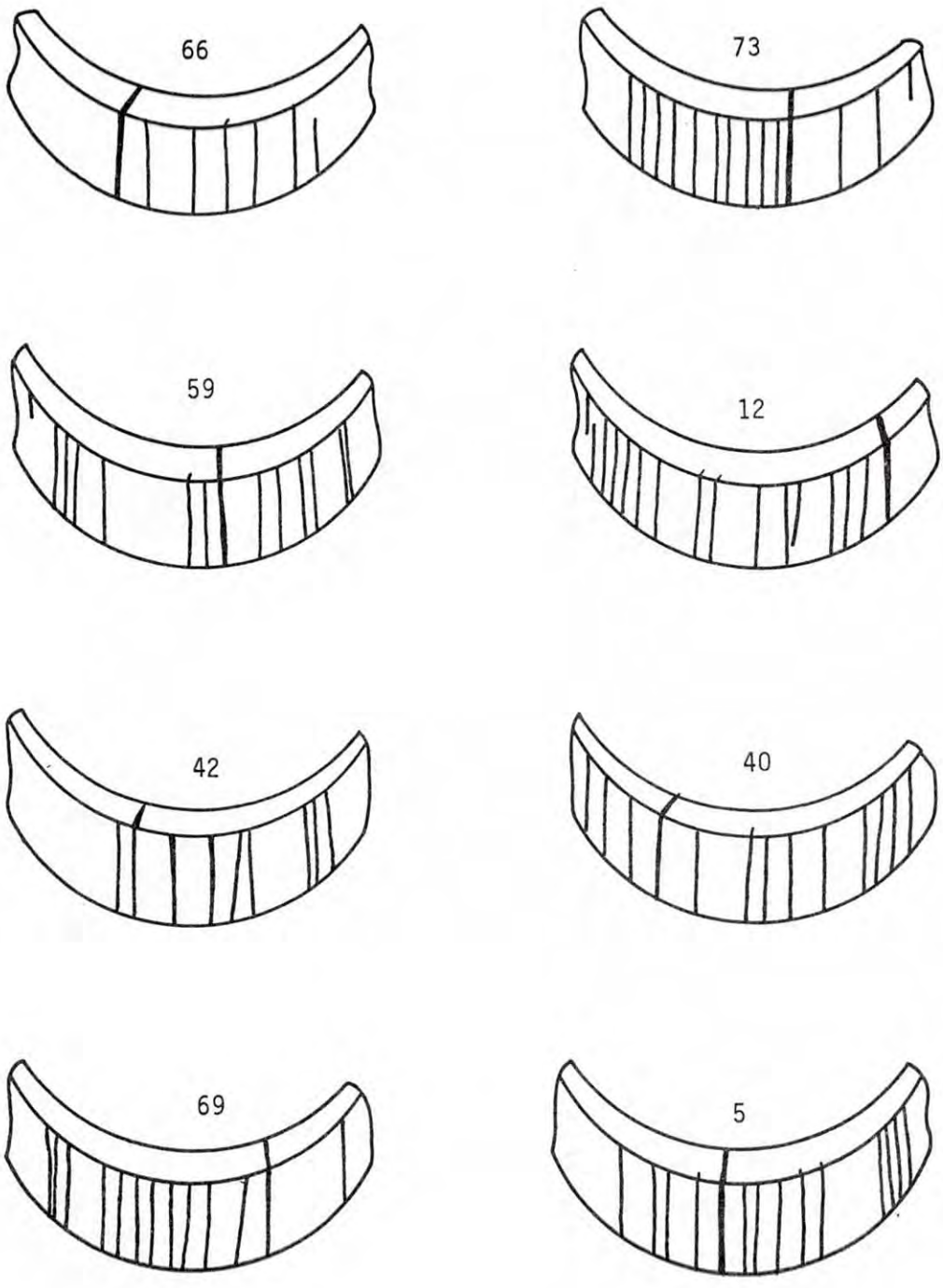

Figure 3.24 Crack patterns in Type I Marlex CL-100 HDPE U-bend samples after gamma irradiation to 1.3×10^7 rad at a dose rate of 1.4×10^3 rad/h. Specimen numbers given above each sketch.

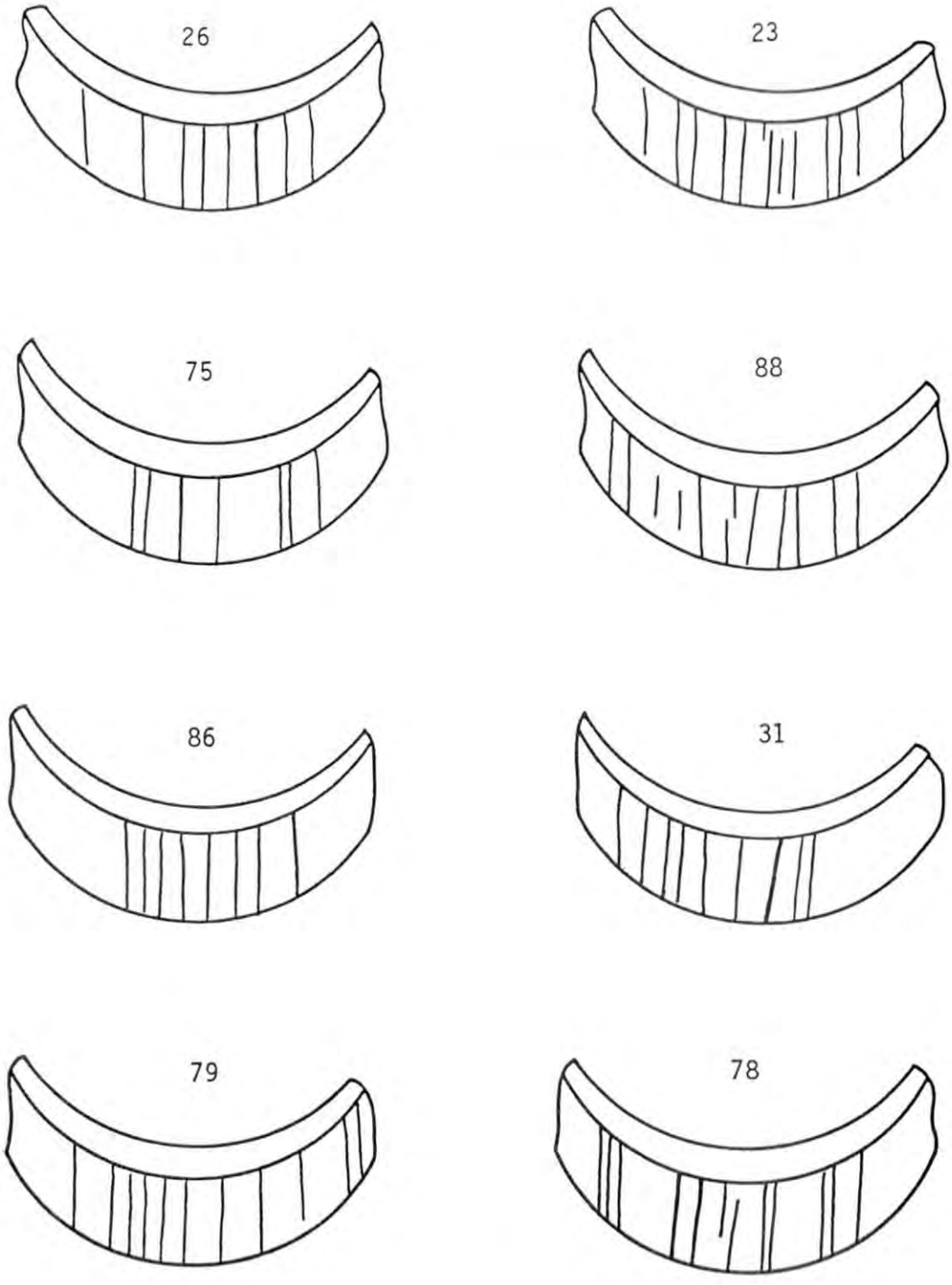

Figure 3.25 Crack patterns in as-prepared Type I Marlex CL-100 HDPE U-bend samples prior to gamma irradiation at 8.4×10^3 rad/h. Specimen numbers given above each sketch.

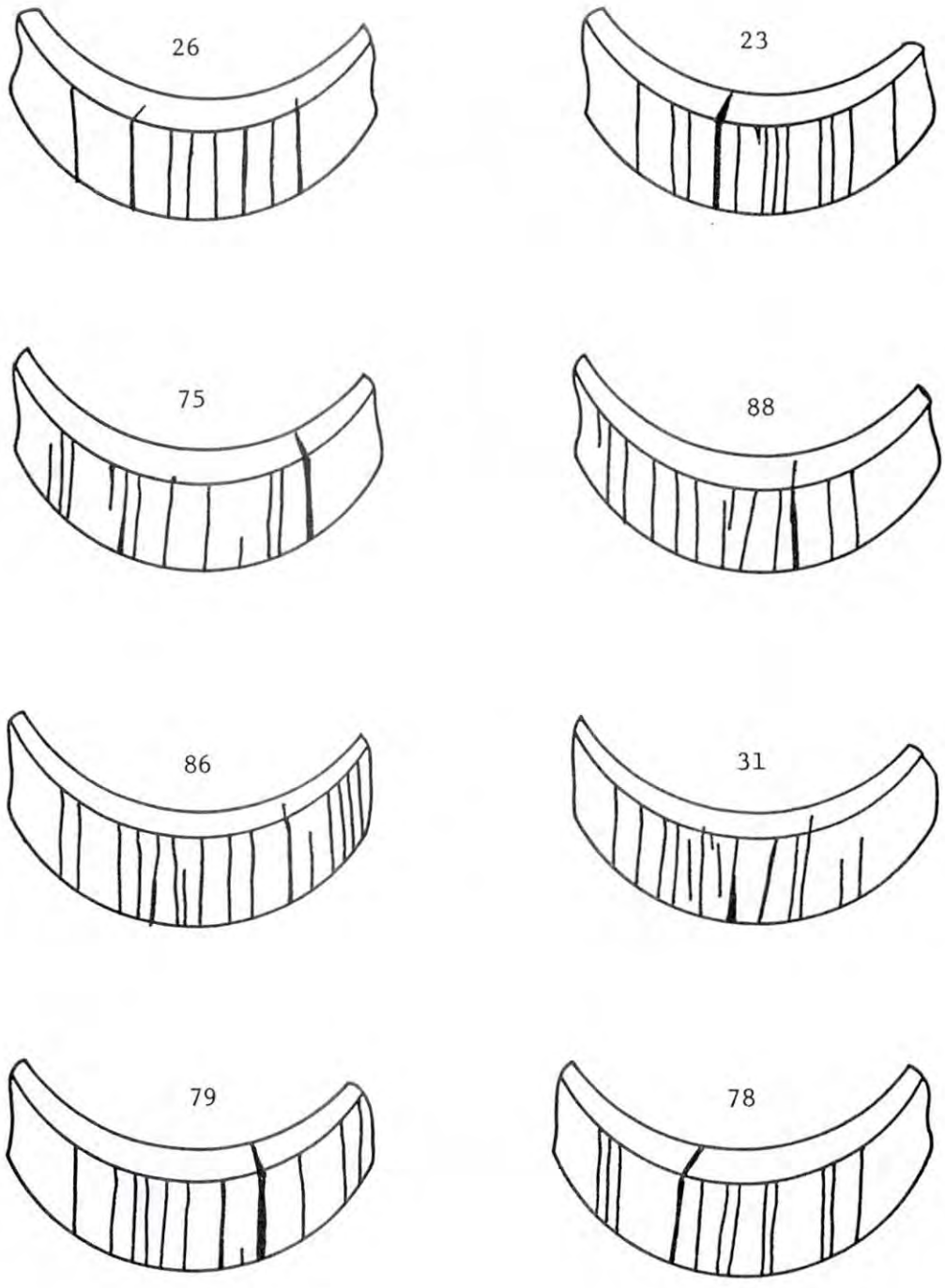

Figure 3.26 Crack patterns in Type I Marlex CL-100 HDPE U-bend samples after gamma irradiation to 6.0×10^7 rad at a dose rate of 8.4×10^3 rad/h. Specimen numbers given above each sketch.

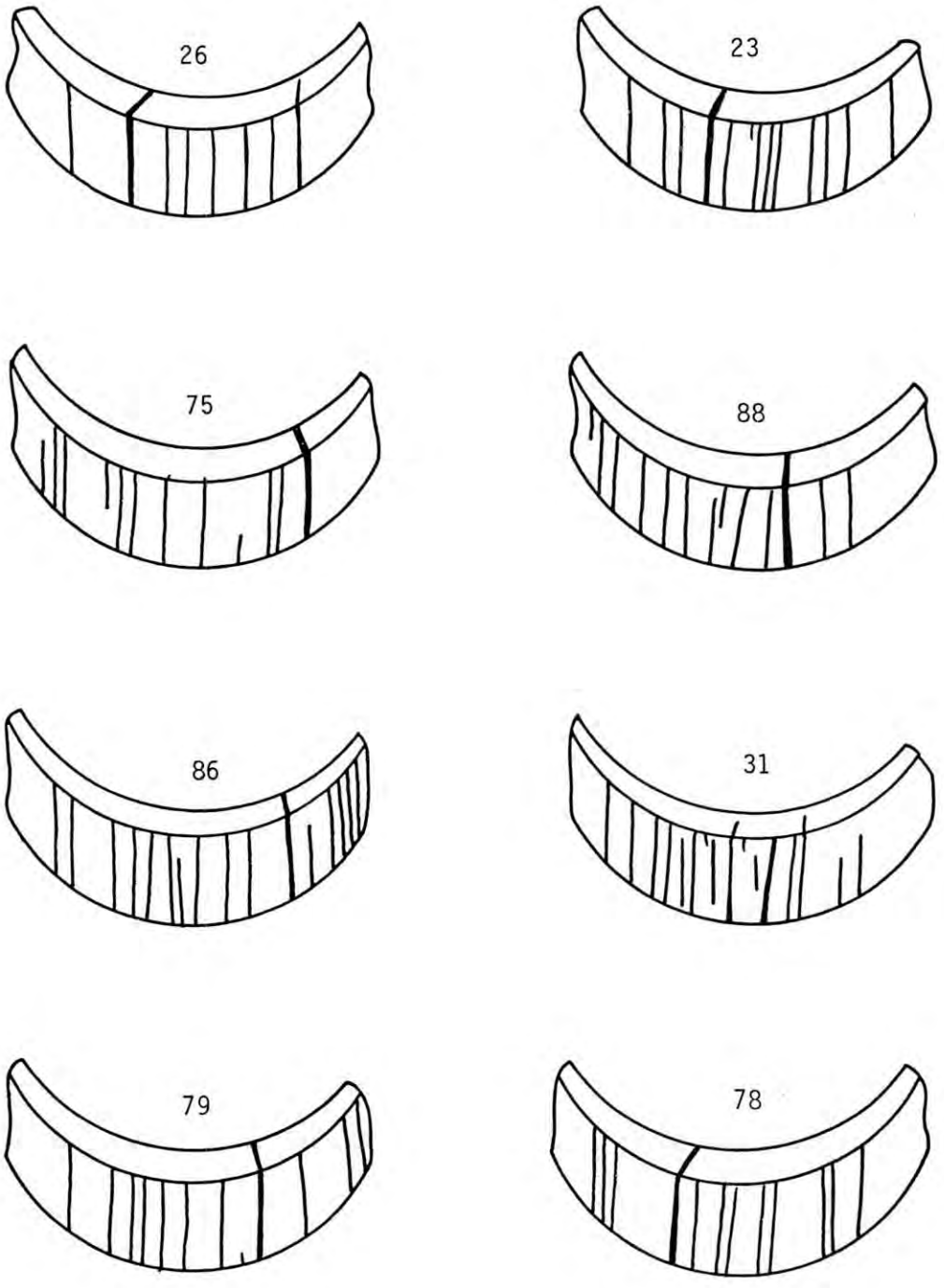

Figure 3.27 Crack patterns in Type I Marlex CL-100 HDPE U-bend samples after gamma irradiation to 9.5×10^7 rad at a dose rate of 8.4×10^3 rad/h. Specimen numbers given above each sketch.

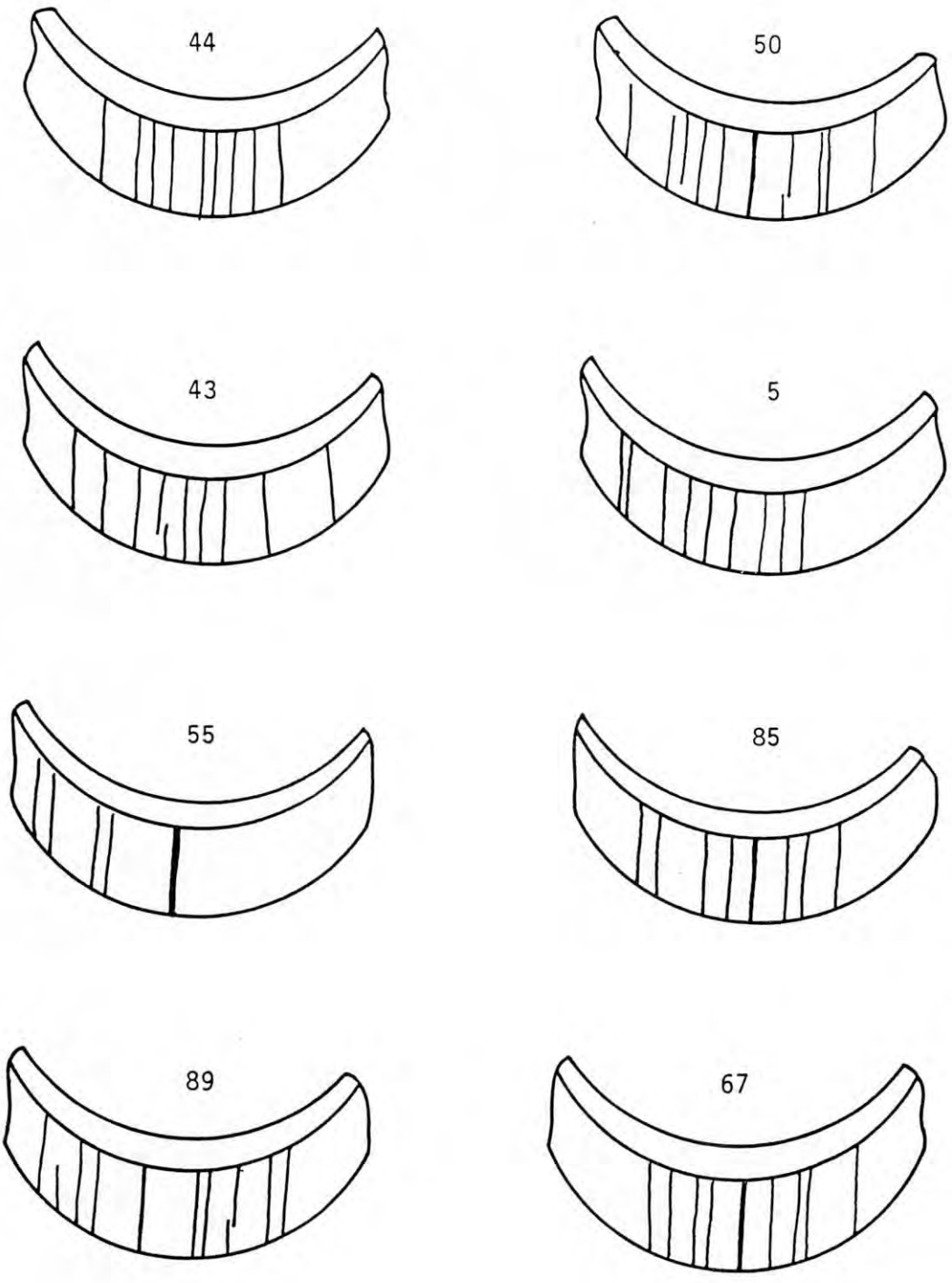

Figure 3.28 Crack patterns in as-prepared Type I Marlex CL-100 HDPE U-bend samples prior to gamma irradiation at 4.4 x 10^5 rad/h. Specimen numbers given above each sketch.

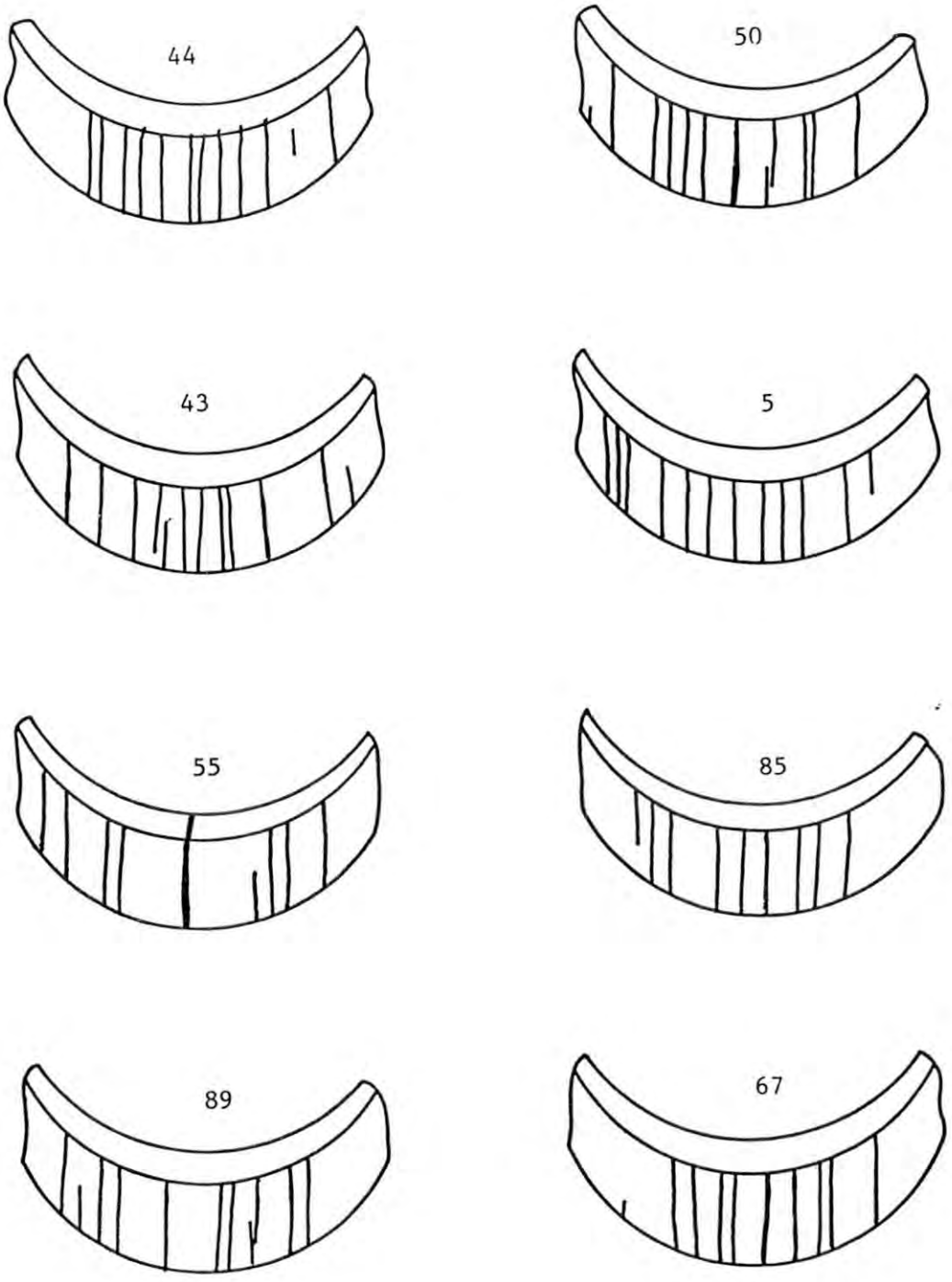

Figure 3.29 Crack patterns in Type I Marlex CL-100 HDPE U-bend samples after irradiation to 1.3×10^9 rad at a dose rate of 4.4×10^5 rad/h. Specimen numbers given above each sketch.

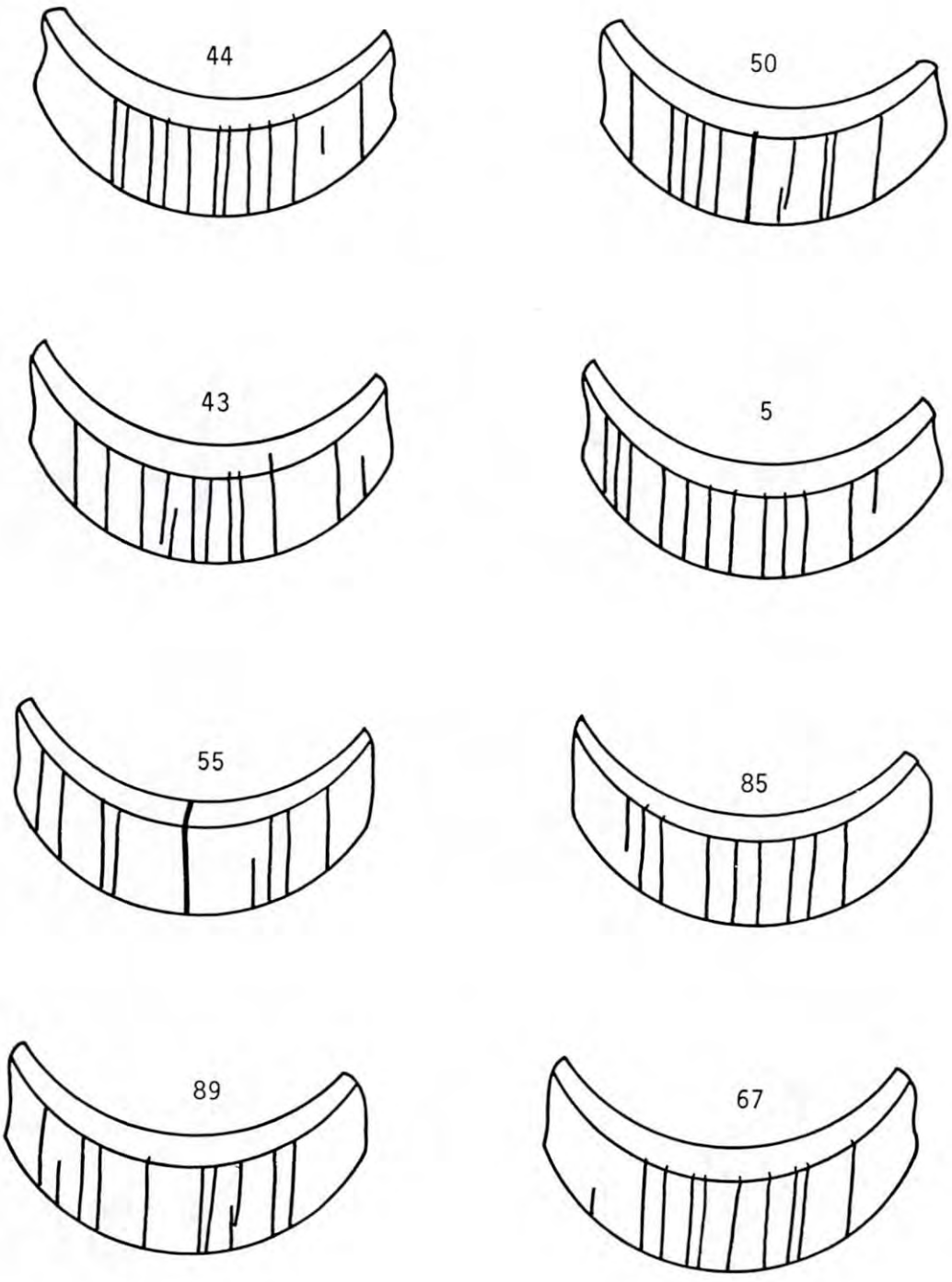

Figure 3.30 Crack patterns in Type I Marlex CL-100 HDPE U-bend samples after irradiation to 3.1×10^9 rad at a dose rate of 4.4×10^5 rad/h. Specimen numbers given above each sketch.

Table 3.5 Crack initiation and propagation in Type I HDPE U-bend specimens after the first gamma irradiation cycle.[1]

Irradiation Dose	Cracks Before Irradiation			Cracks After Irradiation			Percent Change in Numbers of Cracks			Full Penet. Cracks	Near Full Penet. Cracks
	Large	Small	Total	Large	Small	Total	Large	Small	Total		
0	84	11	95	90	13	103	7	18	8	0	0
7.5×10^6 rad (at 1.4×10^3 rad/h)	81	3	84	97	3	100	20	0	19	2	1
6.0×10^7 rad (at 8.4×10^3 rad/h)	78	2	80	95	4	99	22	100	24	2	4
1.3×10^9 rad (at 4.4×10^5 rad/h)	69	3	72	82	4	86	19	33	19	0	1

Note: [1]The numbers of cracks are the totals counted for each batch of eight replicate samples.

Table 3.6 Crack initiation and propagation in Type I HDPE U-bend specimens after the second gamma irradiation cycle.[1]

Irradiation Dose	Cracks Before Irradiation			Cracks After Irradiation			Percent Change in Numbers of Cracks			Full Penet. Cracks	Near Full Penet. Cracks
	Large	Small	Total	Large	Small	Total	Large	Small	Total		
Unirradiated Controls	84	11	95	95	15	110	13	36	16	0	0
1.3×10^7 rad (at 1.4×10^3 rad/h)	81	3	84	97	3	100	20	0	19	7	1
9.5×10^7 rad (at 8.4×10^3 rad/h)	78	2	80	94	8	102	21	300	28	7	1
3.1×10^9 rad (at 4.4×10^5 rad/h)	69	3	72	83	3	86	21	0	19	1	0

Note: [1]The numbers of cracks are the totals counted for each batch of eight replicate samples.

would accelerate crack growth. Since the bulk of the HDPE is already strengthened by crosslinking, relaxation of stresses at the crack tips by plastic deformation is reduced so that crack propagation is still able to take place.

The ability of new cracks to be nucleated in non-irradiated specimens, and their inhibition in irradiated specimens, needs to be discussed more fully. Observations in this work show that the non-irradiated samples retain much flexibility. If the nut and bolt are removed from a U-bend sample after many months, the ends of the specimen spring apart and then slowly creep away from each other. This shows that large stresses are still present. They are the likely reason for the initiation of the large numbers of new cracks in the chemical environment tests described in Section 3.1, above. All of the cracks are easily blunted by plastic flow and they are, consequently, unable to propagate to failure unless an environmental stress cracking mechanism is present. In this case, a crack remains sharp and is able to propagate easily because of a large stress concentration factor.

For irradiated samples, however, chain scission in a statically-stressed specimen will allow reorientation of chain segments to low energy (low stress) configurations. Radiation-induced stress relaxation is, therefore, the probable reason for the very small number of new cracks observed in irradiated Type I specimens (see Table 3.6).

An important implication is that if early cracking can be avoided in a HDPE waste container, so that irradiation-induced stress relaxation can take place, then brittle crack propagation may be greatly retarded, or possibly prevented, even if the container becomes embrittled during its lifetime. The above data on crack initiation and propagation in Types I, II, and III U-bend specimen suggests a practical way to extend container life. It centers on the mechanical removal of the oxidized surface layer formed during container molding. If the oxidized material can be removed by manual or automatic abrasion techniques, then early crack initiation will be avoided and, quite possible, stress relaxation due to gamma irradiation, or long-term viscoelastic deformation, could prevent brittle fracture from occurring.

There exists another effect that may reduce the possibility of radiation-induced brittle fracture of HDPE containers which are emplaced in a burial environment. If limited oxygen is present during burial, then it is expected that the embrittlement effects will be retarded (Section 3.1). Work by Gillen and Clough (1981) has shown that, in the absence of oxygen, the deleterious effects of chain scission are very greatly reduced since oxygen atoms are unable to interact with free radicals generated by the radiation field. Thus, scission processes are likely to self repair, reducing overall degradation effects. Recent relevant work by Adams and Soo (1988) also demonstrates that HDPE U-bend specimens gamma irradiated in the presence of organic ion-exchange resin beads display insignificant crack propagation. Cracks formed during the bending of the specimens do not appear to grow in size despite dose levels in the 10^8 rad range. This is almost certainly connected with stress relaxation and the depletion of oxygen by the resin bed surrounding the HDPE samples. Chain scission effects are able to repair themselves as broken chains recombine with other adjacent chain segments instead of with available oxygen in the environment. Such an oxygen reaction would effectively prevent recombination.

At this time it is not known what level of oxygen is needed to cause a deleterious gamma irradiation effect. It is clear, however, that any procedure to reduce oxygen to very low levels can only be beneficial in terms of reducing degradation.

The effect of stress on crack propagation will now be addressed. From the results given above on crack growth in irradiated Type I U-bends it was shown that cracks which grew faster were seldomly located at the apex of the specimen, where one would normally expect the largest tensile stresses to reside. In nearly all cases the full penetration cracks were in regions on either side of the apex, as shown in Figures 3.17 and 3.18.

To understand this phenomenon more fully it will be necessary to estimate the tensile stresses over the outer surface of the U-bend to see if a correlation can be made between crack growth and stress. Complications occur, however, since bending introduces cracks in Type I specimens which, in turn cause a lowering of the stress. Nevertheless, consider the schematic of a small U-bend specimen used in the irradiation work (See Appendix). By carefully tracing around a typical specimen it is possible to estimate the radii of curvature at the apex and at the "side" of a U-bend. From these values the total deformation at each location may be calculated. The strain at the apex after bending the sample was found to be about 24.3 percent and at the side of the U-bend about 9.1 percent. The value at the apex is, of course, an overestimate for Type I specimens, since cracking occurs and there is less stress and strain than would be calculated on the basis of a non-cracked surface. On the other hand, the estimate of 24.3 percent deformation is in good agreement with creep deformation work, described later, which shows that cracks in the oxidized HDPE surface begins to appear after a deformation of about 20 percent.

When the HDPE is bent to form a U-bend configuration, the stress-strain response on the outer surface is similar to that which would be experienced during a short term tensile test. Figure 3.31 is a schematic of a stress-strain curve for Marlex CL-100 HDPE (Soo, and others, 1986). The yield and break stresses (σ_y and σ_b) are typically 20 MPa (2900 psi) and 15 MPa (2200 psi), respectively, and the elongation at yield and at break (ε_y and ε_b) are typically 18 percent and 230 percent. This shows that at the apex of a U-bend specimen, where the strain is about 24 percent, the material has been strained beyond the yield point and that the associated stress level is much lower than the yield stress. Cracks already present at the apex will inevitably lower the stress even more.

At the side of the U-bend, where the calculated strain is about 9.1 percent, the associated stress level is also less than the yield stress. Since there is no cracking in this region the stress level after bending should be similar to that at the apex. If one now considers the regions between the apex and the sides of the Type I U-bend then these would correspond to a maximum-stress state close to the yield point. This should then be the most favored site for crack initiation and growth in a gamma irradiation field, which is in fact observed.

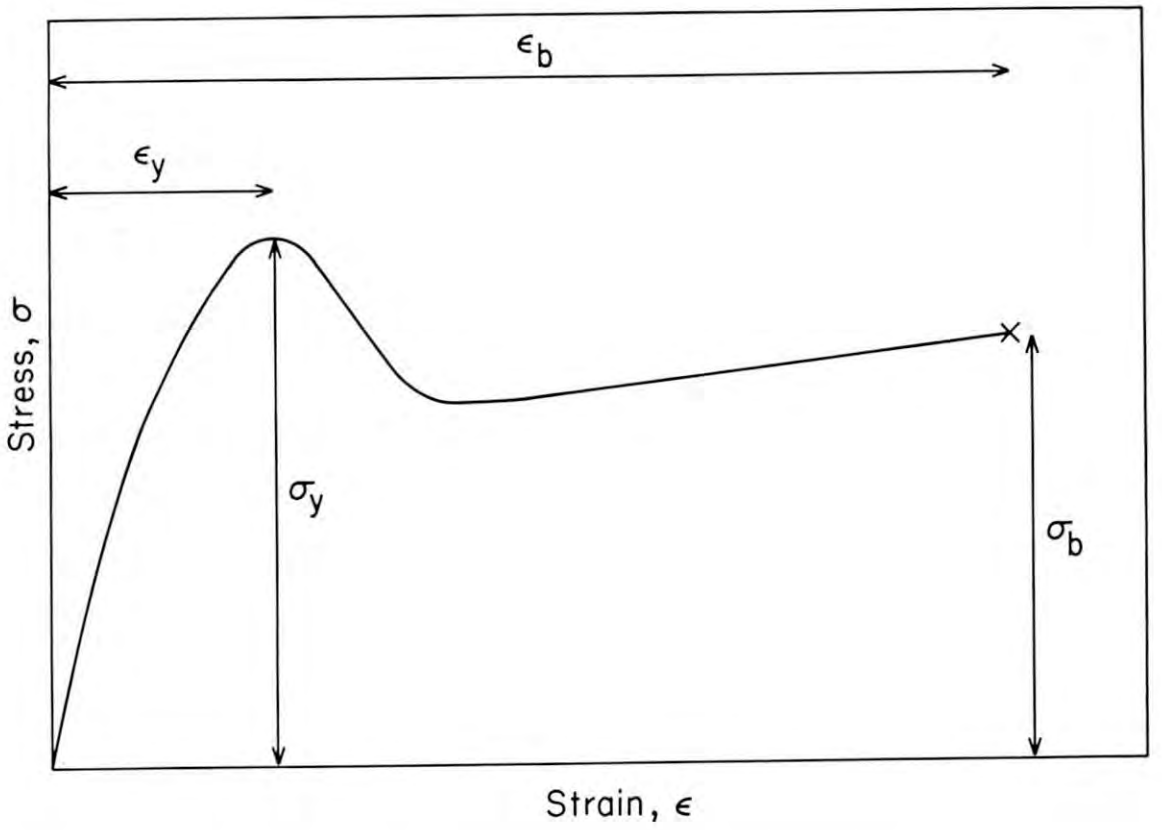

Figure 3.31 Definition of short-term-tensile parameters.

Type II and Type III specimens have a slightly modified behavior since there is no cracking as the U-bends are made and the surface characteristics are also different from Type I samples. This will modify the stress distribution around the U-bend surface and cracking will occur in a different location. From Figures 2.17 and 3.18 it is apparent that the maximum stress region for Type II and Type III specimens is on the sides of the U-bends where the cracks are found to nucleate.

4. UNIAXIAL CREEP IN CHEMICAL ENVIRONMENTS

Creep tests were carried out at 20°C (68°F) using a simple constant load system. Strains were measured continuously using LVDTs (linearly variable differential transducers). Rates of creep, ductility-at-failure, and weight increase in the specimens caused by the absorption of the test liquids during creep were all measured. Usually, the HDPE specimens were in the as-received condition with one surface in the oxidized state. Tests were carried out in the environments specified in Table 2.2.

An additional series of tests was also conducted on specimens which had the oxidized surface removed by emory paper prior to testing. This would allow a quantitative evaluation to be made of the effects of the thin, less-ductile, oxidized material. The various test series are described below. All test data are given in Tables 4.1 and 4.2. Some data on the "old" batch of HDPE are included for comparison purposes.

4.1 Uniaxial Creep of As-Received HDPE in Chemical Environments

4.1.1 Stress-rupture and Ductility Results

Figures 4.1 and 4.2 show stress-rupture and ductility results for the newer batch of HDPE. All of the data plotted are for material in the as-received condition with the oxidized surface intact.

Air and water appear to give similar creep properties. For scintillation fluid, turbine oil, and Igepal, however, there is a significant loss in rupture strength, especially in the low and intermediate stress ranges (Figure 4.1). As the stress level is increased, the curves tend to converge, as expected, since the time to failure becomes primarily stress dependent. This is because failure occurs so quickly that time-dependent environmental effects do not have time to become important. Note, also, in Figure 4.1, that there appear to be stresses below which creep-type failure is unlikely. The "threshold" stress for oil and Igepal is about 8.27 MPa (1200 psi) and for scintillation fluid it is about 6.89 MPa (1000 psi). One might suppose that if the stress levels in a waste container are kept significantly below 6.89 MPa then HDPE should be immune to a creep-type failure mode.

The ductility of HDPE at high stresses is about 60 percent for all test environments (Figure 4.2). This, again, is a result of failure being controlled by the stress rather than the environment. At lower stress levels, in the range 8 to 13 MPa (1150 to 1900 psi), the ductilities for air, water, oil and Igepal are again quite similar. As the stress level decreases, the ductility is significantly reduced. Entrapolation of the curves to stresses of approximately 7 MPa (1015 psi) indicates that a brittle type of failure is likely. The failure time at such low stresses would, of course, be very large, based on the data in Figure 4.1.

Scintillation fluid causes very different behavior compared to the other environments. The results show that failure at low stress levels will not be brittle. In fact, ductilities at 7 MPa (1015 psi) are approximately 100 percent. Observations on deforming samples showed that the oxidized surface

Table 4.1 Creep test data for Marlex CL-100 HDPE tested in air and deionized water at room temperature.

Test Number	Specimen Condition	Test Environment	Stress (MPa)	Stress (psi)	Failure Time (h)	Elong. at Break (%)
381	As rec.	Air	13.79	2000	4.0	56.0
382	As rec.	Air	13.79	2000	0.98	56.6
367	As rec.	Air	13.10	1900	6.8	56.8
369	As rec.	Air	13.10	1900	5.8	46.6
374	As rec.	Air	12.76	1850	5.4	46.2
365	As rec.	Air	12.41	1800	41.0	74.6
359	As rec.	Air	12.41	1800	11.3	50.0
366	As rec.	Air	12.10	1750	52.5	76.0
358	As rec.	Air	11.72	1700	80.3	79.6
362	As rec.	Air	11.65	1690	28.5	56.0
361	As rec.	Air	11.03	1600	457	79.7
360	As rec.	Air	10.86	1575	212	85.4
350(a)	As rec.	Air	10.62	1540	166	72.9
350(b)	As rec.	Air	10.62	1540	502	55.0
300	As rec.	Air	10.34	1500	662	61.6
315	As rec.	Air	10.34	1500	761	58.2
363	As rec.	Air	10.17	1475	4023	60.4
357	As rec.	Air	10.00	1450	3821	55.1
380	As rec.	Air	10.00	1450	2455	66.8
377	As rec.	Air	9.83	1425	5173	53.5
316	As rec.	Air	9.65	1400	5378	36.6
364	As rec.	Air	9.31	1350	1819	71.9
391	As rec.	Air	9.13	1325	2610	38.9
355	As rec.	Air	8.96	1300	3100	37.0
390	As rec.	Air	8.96	1300	2808	33.7
398	As rec.	Air	8.62	1250	6096	13.1
321	As rec.	Air	8.27	1200	7740	16.2
388	As rec.	Air	7.93	1150	>9360	>15.0
409	As rec.	Air	7.58	1100	>2040	>6.0
322	As rec.	Air	7.24	1050	>17500	>8.3
408	As rec.	Air	4.14	600	>1425	>2.3
387	(1)	Air	13.79	2000	>5092	>673
385	(1)	Air	12.41	1800	>5257	>598
338	(1)	Air	11.03	1600	2319	585
323	(1)	Air	10.34	1500	7704	248.9
320	(1)	Air	8.27	1200	>17520	>31.0
337	As rec.	DIW	11.03	1600	112	58.6
347	As rec.	DIW	10.69	1550	57	54.6
301	As rec.	DIW	10.34	1500	2027	95.5
302	As rec.	DIW	9.65	1400	5854	54.5
334	As rec.	DIW	8.27	1200	>14400	>21.0
339	(1)	DIW	11.03	1600	200	221.6
327	(1)	DIW	10.34	1500	452	85.2
326	(1)	DIW	8.27	1200	>17520	>37.0
306	(2)	DIW	10.34	1500	1154	57.5
310	(2)	DIW	9.65	1400	6264	53.5

NOTES:
1. 10 mils removed from oxidized surface of specimen.
2. 10 mils removed from non-oxidized surface of specimen.

Table 4.2 Creep test data for Marlex CL-100 HDPE tested in various environments at room temperature.

Test Number	Specimen Condition	Test Environment	Stress (MPa)	Stress (psi)	Failure Time (h)	Elong. at Break (%)	Weight Change (% per test day)
370	As rec.	Oil	11.03	1600	45.9	92.1	0.19
305	As rec.	Oil	10.34	1500	128	60.3	0.06
345	As rec.	Oil	8.96	1300	102	43.4	0.02
348	As rec.	Oil	8.96	1300	168	51.1	0.04
352	As rec.	Oil	8.62	1250	198	54.5	0.01
325	As rec.	Oil	8.27	1200	1502	36.3	-
396	As rec.	LSF	12.41	1800	7.9	85.0	0.72
379	As rec.	LSF	11.72	1700	9.6	94.8	-
378	As rec.	LSF	11.38	1650	10.5	49.3	1.47
395	As rec.	LSF	11.03	1600	33.1	89.9	0.34
308	As rec.	LSF	10.34	1500	14	83.5	0.25
309	As rec.	LSF	9.65	1400	35	98.0	0.15
341	As rec.	LSF	8.27	1200	50	98.5	1.40
333	As rec.	LSF	7.24	1050	340	95.8	0.02
383	As rec.	LSF	6.89	1000	1602	111.4	-
394	As rec.	LSF	6.72	975	>7340	>39.0	-
407	(1)	LSF	10.34	1500	30.3	366.0	-
330	(1)	LSF	9.65	1400	29	76.0	-
332	(1)	LSF	8.27	1200	85	216.0	-
397	(1)	LSF	7.93	1150	>7020	>77.0	-
331	(1)	LSF	7.24	1050	>15840	>62.0	-
313	(2)	LSF	10.34	1500	12	55.0	0.28
311	(2)	LSF	9.65	1400	31	77.0	0.21
42	Old HDPE	LSF	10.34	1500	12	86.1	-
55	Old HDPE	LSF	9.65	1400	35	37.8	-
62	Old HDPE	LSF	8.27	1200	280	100.7	-
392	As rec.	Igepal	12.41	1800	3.1	52.3	0.27
393	As rec.	Igepal	11.72	1700	17.7	51.8	0.23
401	As rec.	Igepal	11.72	1700	20.7	49.1	-
371	As rec.	Igepal	11.03	1600	45.6	54.7	0.13
303	As rec.	Igepal	10.34	1500	65	49.1	0.06
304	As rec.	Igepal	9.65	1400	106	54.8	0.03
346	As rec.	Igepal	8.96	1300	128	47.3	0.02
324	As rec.	Igepal	8.27	1200	1194	22.0	-
389	As rec.	Igepal	8.10	1175	>8731	>10.9	-
402	(1)	Igepal	11.73	1700	438	89.5	-
340	(1)	Igepal	10.34	1500	312	97.3	0.04
329	(1)	Igepal	9.65	1400	476	59.4	-
328	(1)	Igepal	9.29	1350	12778	31.2	-
314	(2)	Igepal	10.34	1500	56	71.4	0.09
312	(2)	Igepal	9.65	1400	130	50.4	0.03
106	Old HDPE	Igepal	12.41	1800	8	74.8	-
105	Old HDPE	Igepal	12.41	1800	9	69.2	-
107	Old HDPE	Igepal	11.72	1700	50	87.4	-
108	Old HDPE	Igepal	11.72	1700	47	54.6	-
72	Old HDPE	Igepal	10.34	1500	216	68.7	-
113	Old HDPE	Igepal	10.34	1500	366	62.2	-
114	Old HDPE	Igepal	10.34	1500	372	79.2	-
84	Old HDPE	Igepal	10.34	1500	95	115.3	-

Notes:
1. 10 mils removed from oxidized surface of specimen.
2. 10 mils removed from non-oxidized surface of specimen.

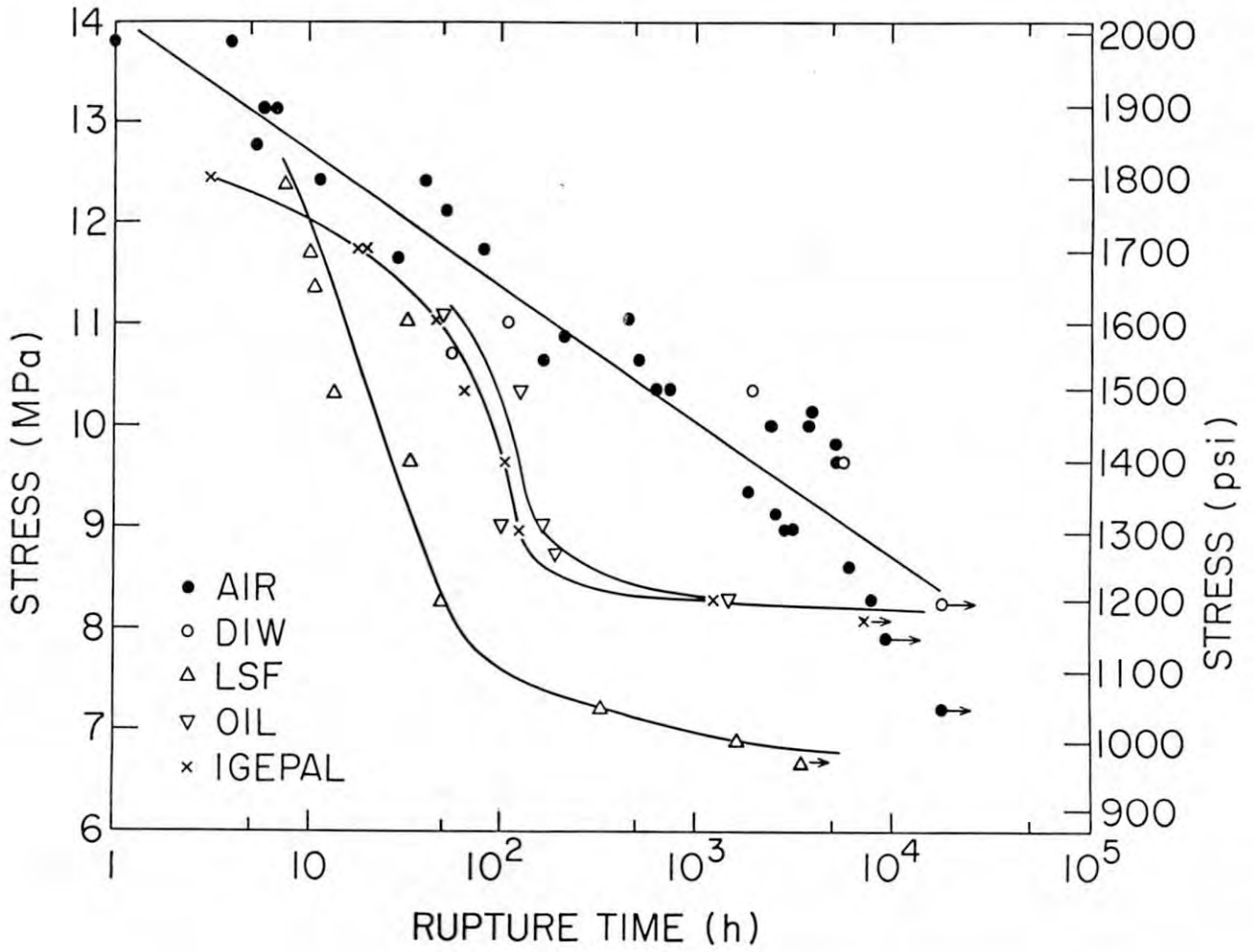

Figure 4.1 Stress-rupture results for Marlex CL-100 HDPE tested at 20°C in various environments.

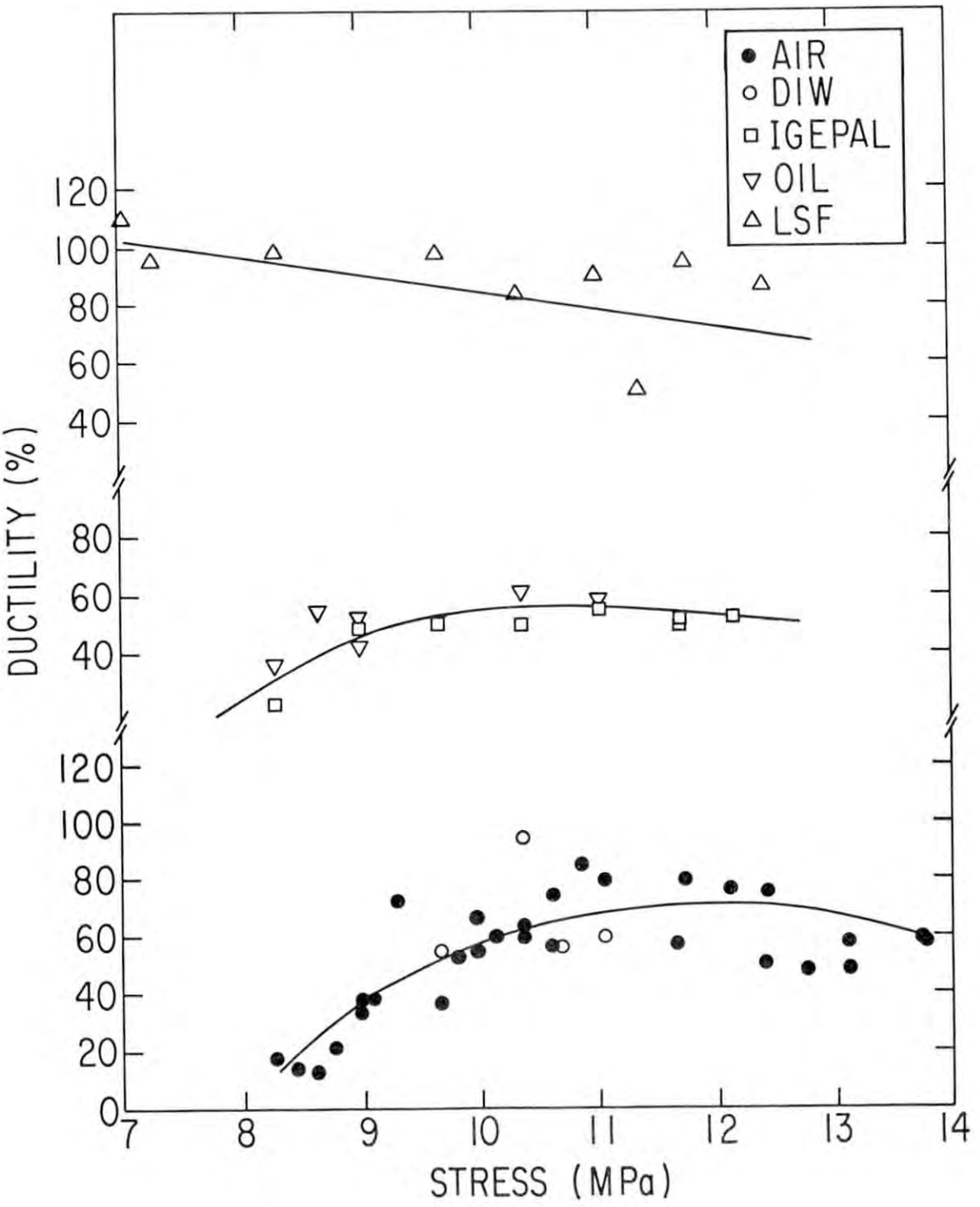

Figure 4.2 Elongations at failure for Marlex CL-100 HDPE tested at 20°C in various environments.

layers on the specimens crack after about 20 percent elongation. Thereafter, much deformation concentrates in the cracked areas with final failure occurring in one of these locations. Scintillation fluid, which typically contains xylene and toluene, probably affects deformation by absorption and/or dissolution effects. It is speculated that during long-term creep the scintillation fluid interacts with the oxidized surface layer making it less prone to cracking. Also, small cracks that are nucleated may be blunted by dissolution of material at the crack tip making crack propagation more difficult. In this way localized deformation in cracked regions is less likely, and large scale uniform deformation in the gagelength occurs giving rise to enhanced elongations. This occurs despite the fact that scintillation fluid gives the fastest failure time for any given stress level (Figure 4.1).

The effect of liquid environments on creep is probably connected with liquid absorption into the HDPE during testing. Table 4.2 gives data on the amounts of liquid absorbed based on weight increase measurements. They are semi-quantitive, however, since the ends of the test specimens were enclosed within grips and not in free contact with the test liquid. Also, samples with extensive creep had a larger surface area for liquid penetration. Despite these inconsistencies there is clearly faster penetration of scintillation fluid into the HDPE compared to the other liquids. Oil and Igepal have similar measureable rates of absorption but little change in weight was noted for test specimens immersed in water. At this time the mechanisms by which creep failure is affected by liquid absorption is speculative.

4.1.2 Creep Curve Results

Figure 4.3 shows a family of creep curves for the older batch of HDPE. The data shown are for the first 190 h of testing in order to illustrate the effect of stress on early creep. There is an initial fast creep rate (Stage I) followed by a linear creep regime (Stage II). For the higher stress levels, Stage II is very short. After Stage II creep, "necking" of the sample starts and failure becomes imminent. The creep rate shows an increase in this period (Stage III).

Figures 4.4 through 4.7 compare the creep curves for the various test environments at four different stress levels. As would be expected from the stress-rupture results in Figure 4.1 air gives by far the slowest rate of creep. Environmental effects are accentuated at low stresses since early failure does not occur. As the stress level is increased there is a noticeable trend for the four creep curves to converge, showing that deformation and failure are increasingly more stress dependent. Oil and Igepal have very similar effects on the creep of HDPE.

4.1.3 Fracture Characteristics

The relationships between applied stress and ductility, shown in Figure 4.2, may be examined in terms of fracture behavior. For samples which can be readily examined during test, such as those exposed to air, it was found that fine cracks in the oxidized surface formed after about 20 percent elongation. Figure 4.8 shows two such brittle cracks formed in HDPE tested in simulated Barnwell, South Carolina, groundwater (Soo, and others, 1986). They formed at the edge of the specimen and grow across the width of the gagelength as deformation proceeds.

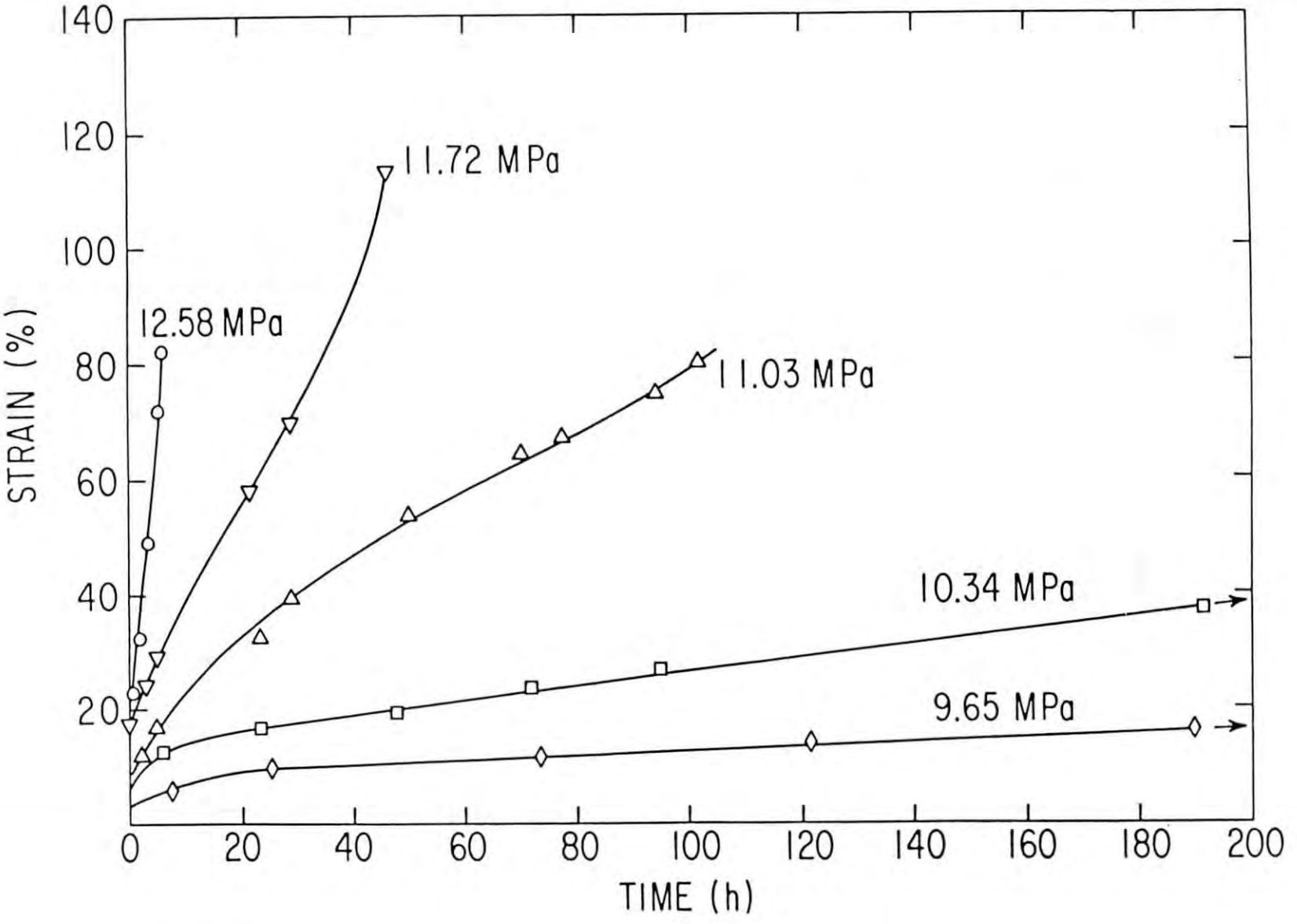

Figure 4.3 Creep deformation in the older batch of Marlex CL-100 HDPE as a function of the applied stress.

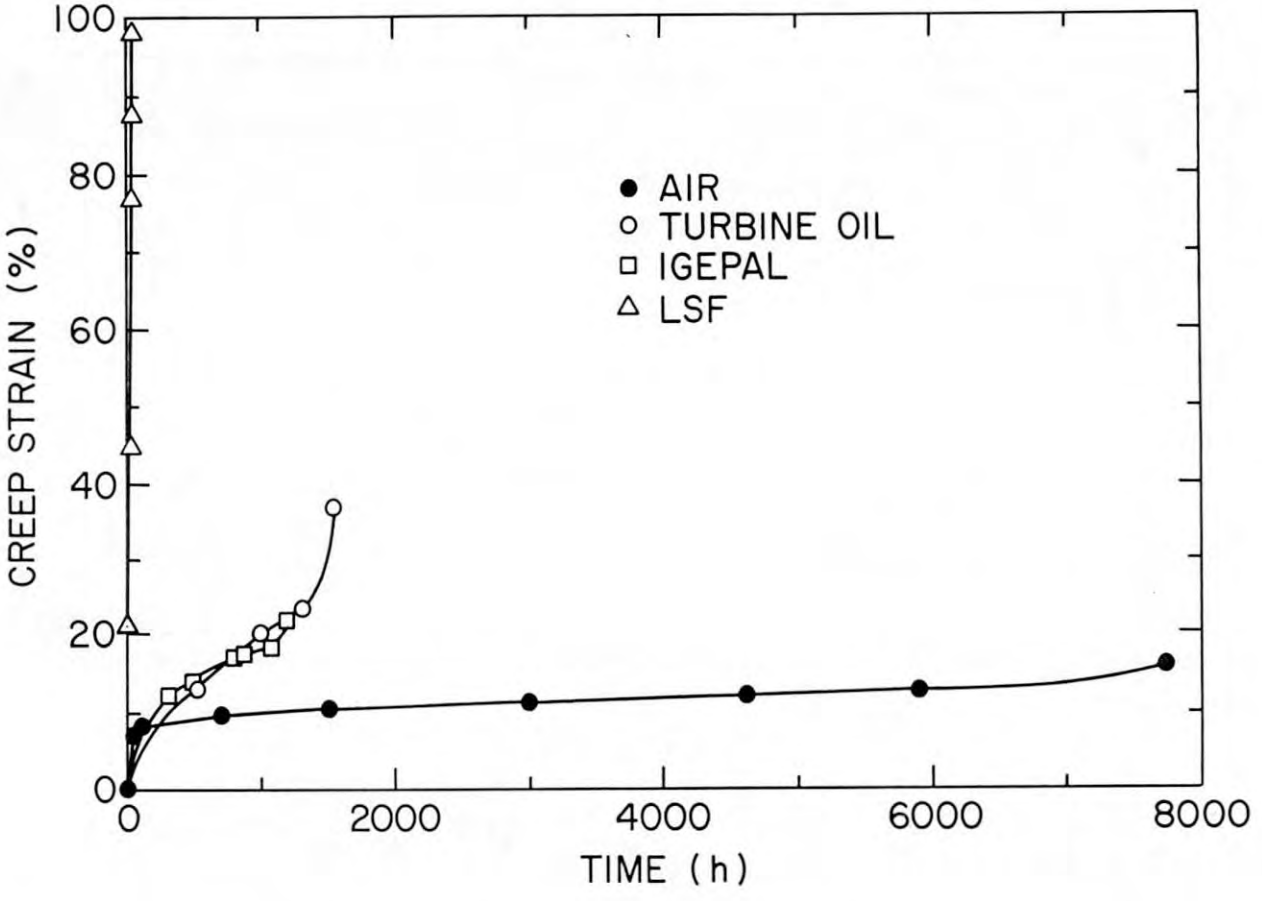

Figure 4.4 Creep of Marlex CL-100 HDPE in various environments at 8.27 MPa (1200psi).

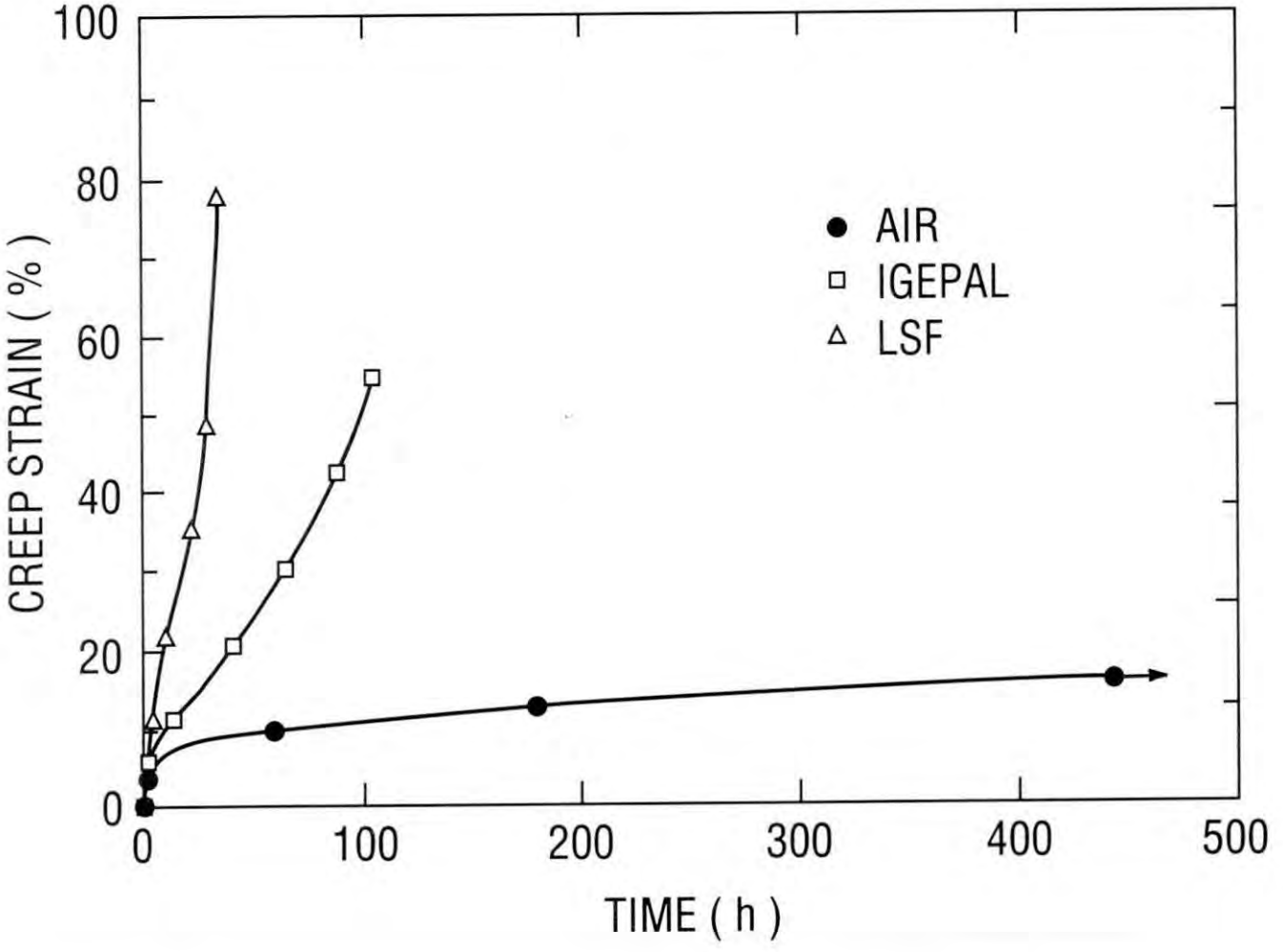

Figure 4.5 Creep of Marlex CL-100 HDPE in various environments at 9.65 MPa (1400psi).

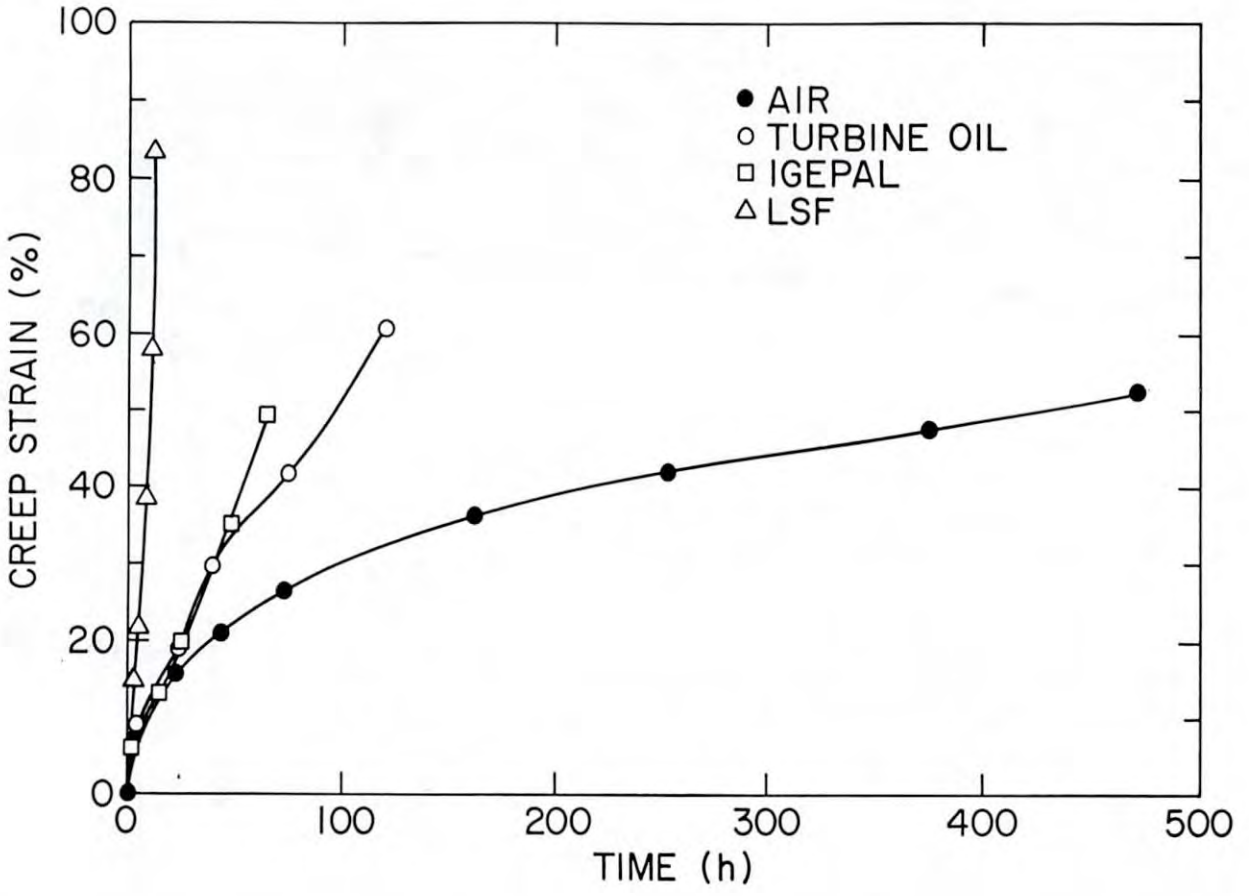

Figure 4.6 Creep of Marlex CL-100 HDPE in various environments at 10.34 MPa (1500psi).

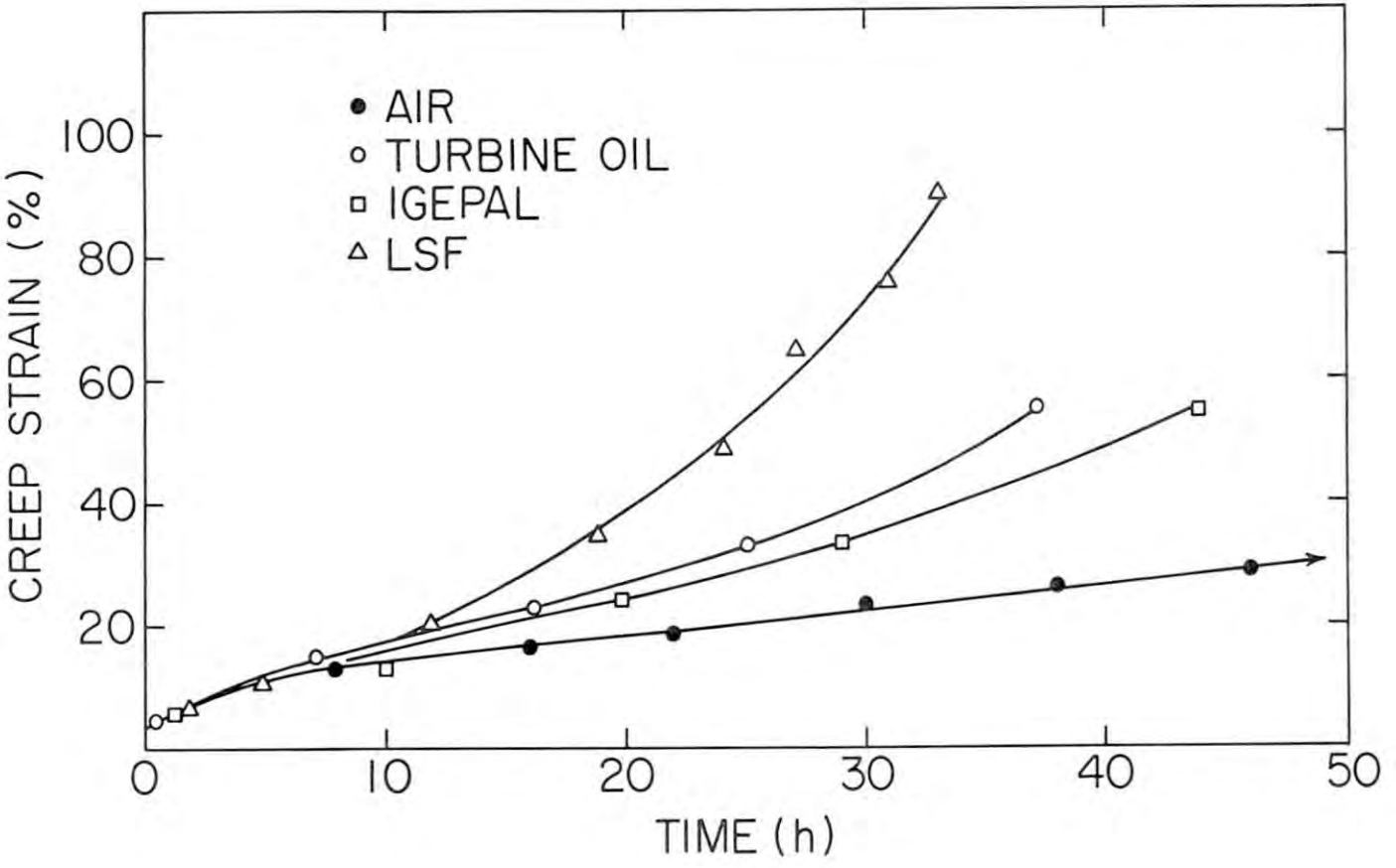

Figure 4.7 Creep of Marlex CL-100 HDPE in various environments at 11.03 MPa (1600 psi).

Another example of brittle cracks is shown in Figure 4.9 from a test in Igepal. At the right of the figure it may be seen that one crack has propagated to failure leaving at the fracture surface a curly tail of material which suffered severe deformation prior to separation.

Figure 4.10 shows a family of HDPE specimens which were tested in air to failure. The sample tested at the lowest stress (8.96 MPa, 1300 psi) has relatively flat fracture surface normal to the stress direction. This shows that a crack propagates through the specimen with only a small amount of plastic deformation associated with it. At the higher stress levels the crack which initially begins to grow in the oxidized surface soon becomes blunted by plastic deformation and a thin "neck" of material forms in the area. Eventually, ductile fracture occurs and each half of the failed specimen displays a small tail in the fracture zone.

The fracture characteristics for the water environment (Figure 4.11) show some subtle differences compared to those for air. At 9.65 MPa (1400 psi) the fracture appears to be more brittle than that for any of specimens failed in air. Also, at 11.03 MPa (1600 psi) a comparison of air and water-tested specimens again shows a distinctive difference. The sample fractured in water shows an essential "clean" fracture with little tailing. On the other hand, the air tested sample (Figure 4.10) shows a large amount of tailing. Water, therefore, encourages crack propagation, leading to a more-brittle type of fracture morphology.

Igepal and oil cause similar fracture behavior (Figures 4.12 and 4.13). In nearly all tests, regardless of the stress level, a clean fracture is observed with little tailing. The two environments, especially Igepal, are more conducive to crack propagation compared to air. Since Igepal is an environmental stress cracking agent, specified in standard ASTM tests (ASTM, 1980a, 1980b), this particular failure mechanism is likely to be the cause of the fast crack growth process observed here.

Finally, for scintillation fluid, the fracture appears to be more stress dependent than for the other liquids. At the two lowest stress levels (Figure 4.14) there is not much plastic deformation associated with the fracture zone. At the intermediate stress (10.34 MPa, 1500 psi) and the highest stress level (12.41 MPa, 1800 psi), however, there is considerable necking in the failure region. In some respects the fracture morphology is similar to that observed for air (compare Figures 4.10 and 4.14).

Figures 4.15 and 4.16 directly compare the fracture morphologies of samples tested in the various environments at specific stress levels. At 8.27 MPa (1200 psi) the stress level is too low to cause extensive plastic deformation and cracks which are formed in the oxidized layer remain sharp. They grow without excessive associated plasticity and "brittle" type fracture morphologies are produced. At 10.34 MPa (1500 psi) failure times are shorter than those for 8.27 MPa so that environmental effects are not able to exert as great an influence. Environmental stress cracking still is important for Igepal and turbine oil as demonstrated by the flat fracture surface but for air, water, and scintillation fluid there is a retardation of the crack propagation rate which allows significant necking and deformation in the fracture zone.

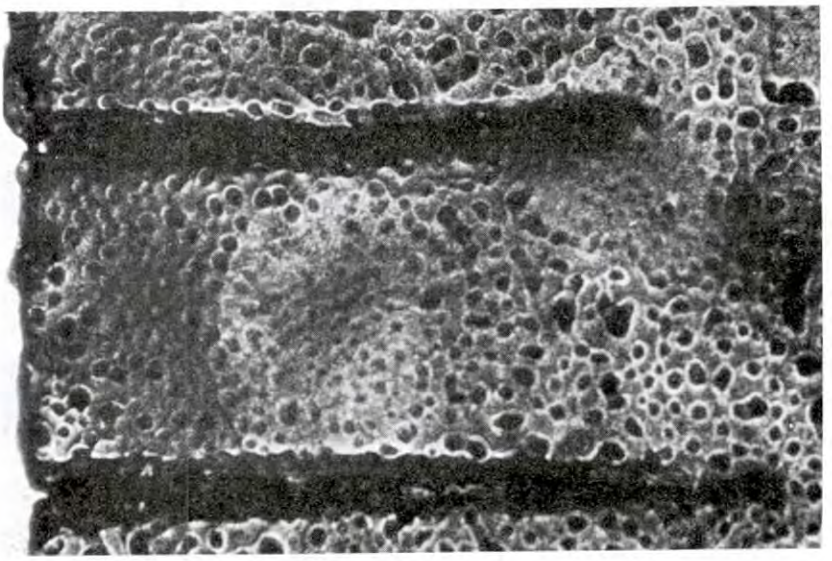

Figure 4.8 Brittle cracks on the edges of the oxidized surface of Marlex CL-100 HDPE creep tested in simulated Barnwell groundwater at 10.34 MPa. The stressing direction is from top to bottom. Magnification 50 X.

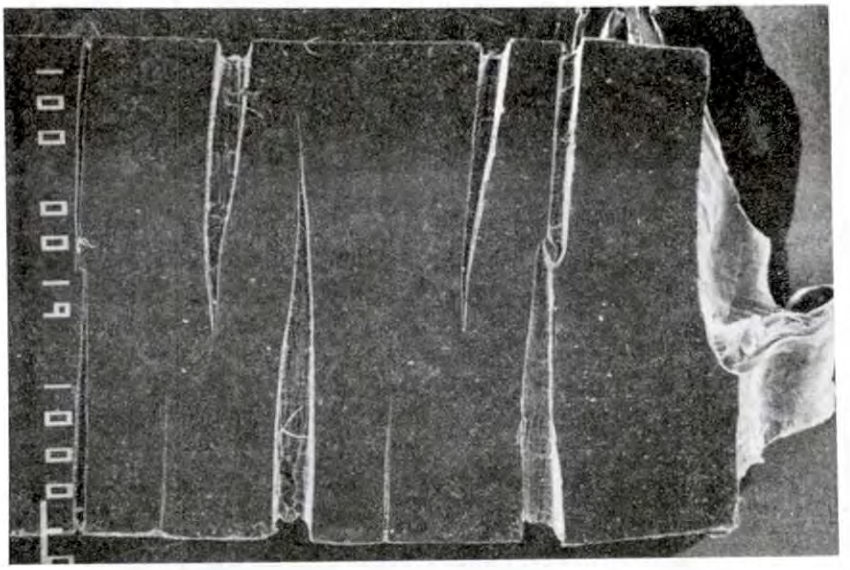

Figure 4.9 Environmental stress cracking in fractured Marlex CL-100 HDPE creep specimen tested at 10.34 MPa in Igepal solution. The surface shown is the oxidized one and displays deep cracks which originated at the edges of the oxidized surface. Magnification 10 X.

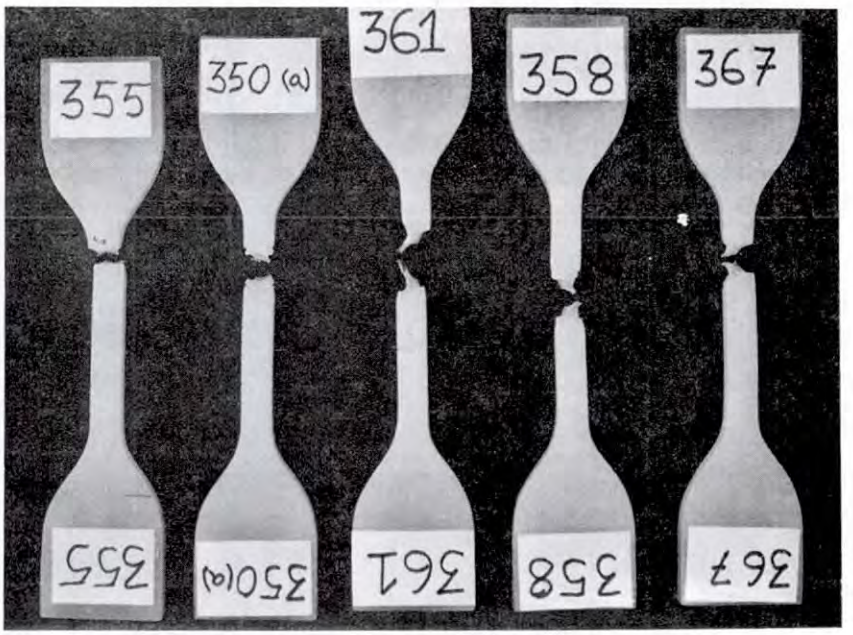

Figure 4.10 Fracture characteristics of Marlex CL-100 HDPE in air. Applied stresses from left to right were 8.96, 10.34, 11.03, 11.72, and 13.10 MPa. Magnification 0.72 X.

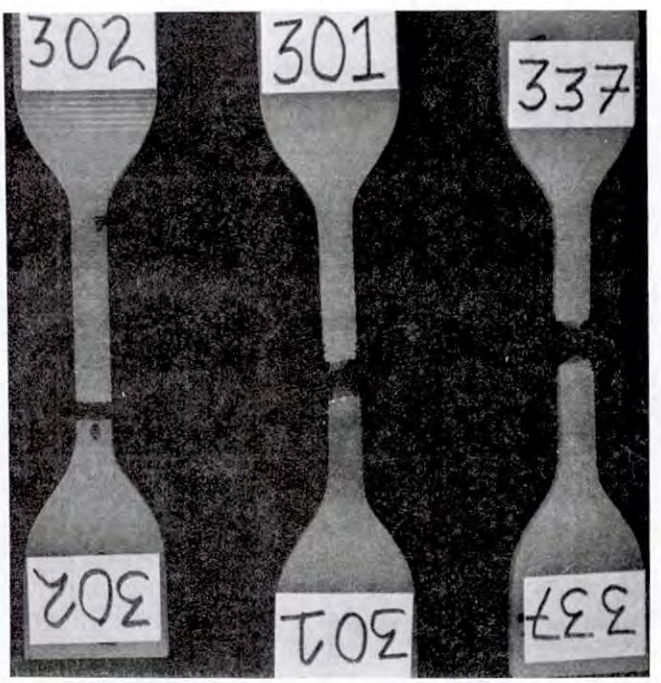

Figure 4.11 Fracture characteristics of Marlex CL-100 HDPE in deionized water. Applied stresses from left to right were 9.65, 10.34, and 11.03 MPa. Magnification 0.72 X.

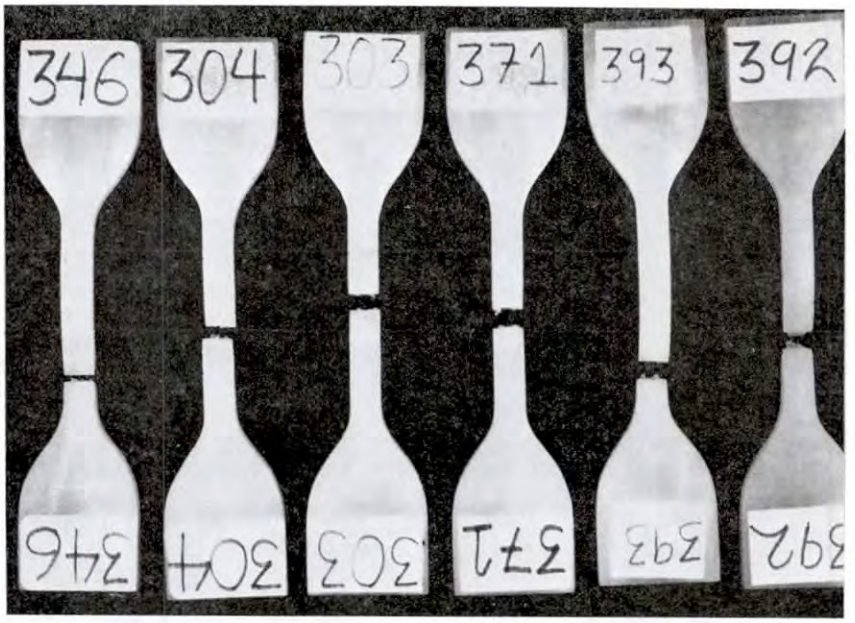

Figure 4.12 Fracture characteristics of Marlex CL-100 HDPE in Igepal CO-630. Applied stresses from left to right were 8.96, 9.65, 10.34, 11.03, 11.72, and 12.41 MPa. Magnification 0.72 X.

Figure 4.13 Fracture characteristics of Marlex CL-100 HDPE in turbine oil. Applied stresses from left to right were 8.27, 8.62, 8.96, 10.34, and 11.03 MPa. Magnification 0.72 X.

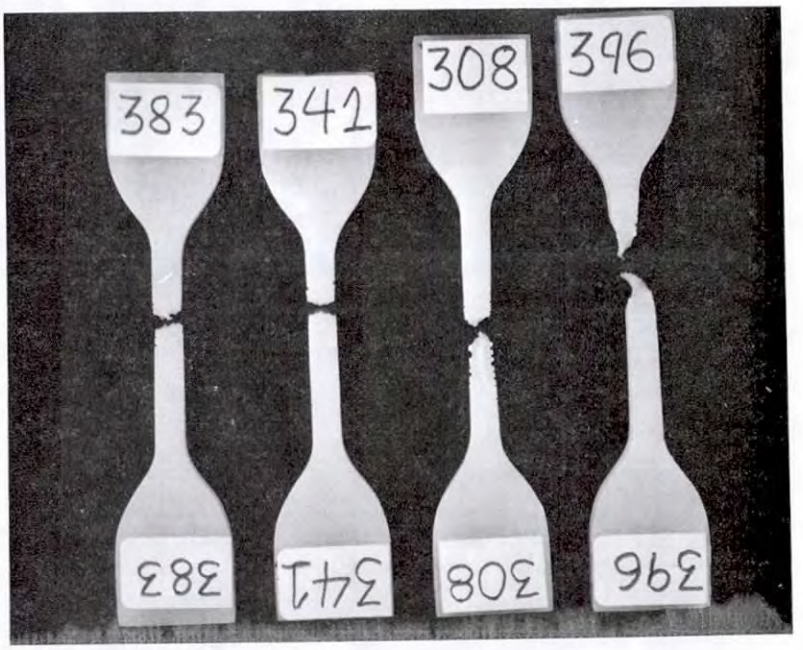

Figure 4.14 Fracture characteristics of Marlex CL-100 HDPE in liquid scintillation fluid. Applied stresses from left to right were 6.89, 8.27, 10.34, and 12.41 MPa. Magnification 0.72 X.

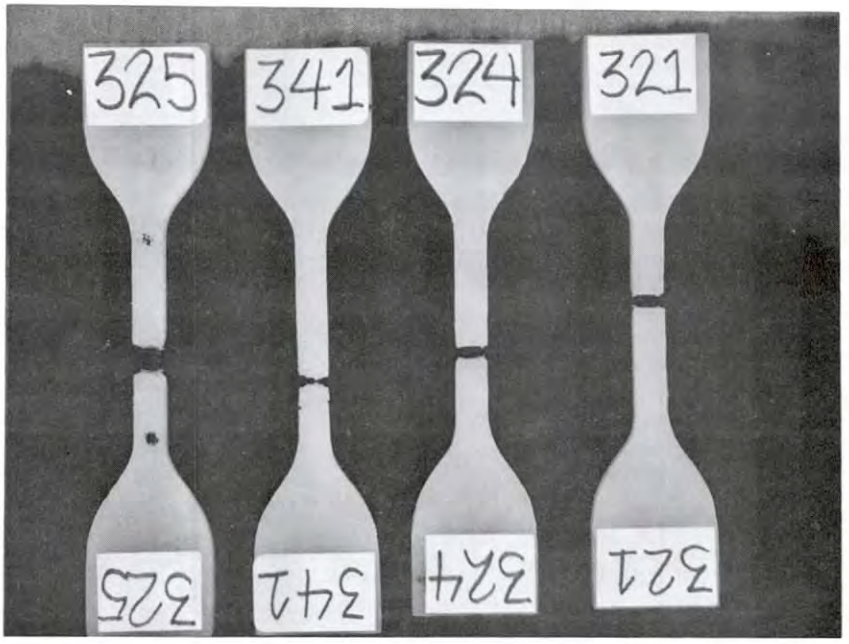

Figure 4.15 Fracture characteristics of Marlex CL-100 HDPE tested in various environments at 8.27 MPa (1200psi). Environments from left to right were turbine oil, scintillation fluid, Igepal CO-630, and air. Magnification 0.72 X.

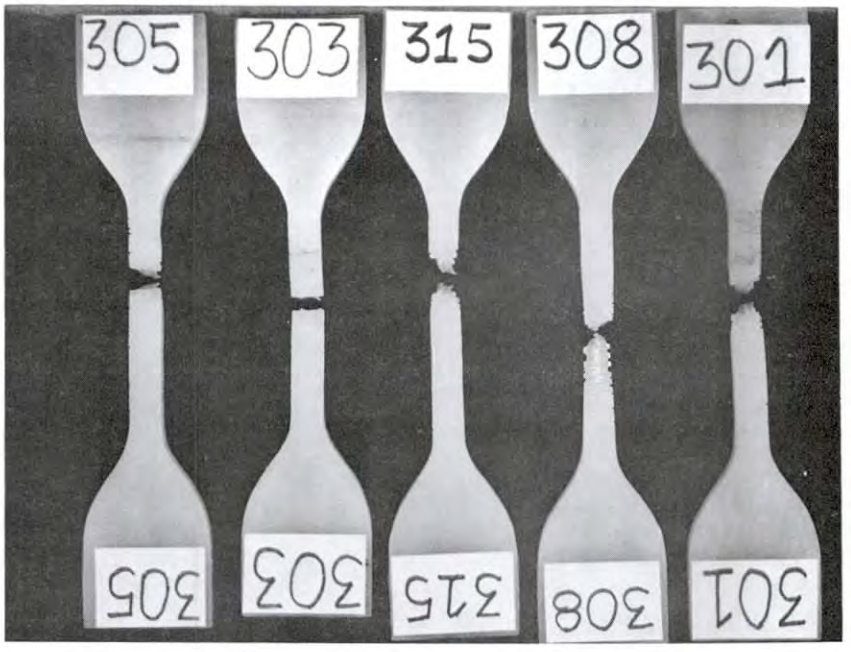

Figure 4.16 Fracture characteristics of Marlex CL-100 HDPE tested in various environments at 10.34 MPa (1500psi). Environments from left to right were turbine oil, Igepal CO-630, air, scintillation fluid, and deionized water. Magnification 0.72 X.

Tables 4.3 through 4.6 schematically summarize the surface cracking and fracture morphologies for the various environments.

4.2 Uniaxial Creep of Non-Oxidized HDPE in Chemical Environments

In Section 4.1 it was shown that the effect of the oxidized surface in promoting early cracking was central to the deformation and failure of HDPE. Work in an earlier BNL program, and elsewhere, supports this conclusion (Terselius, 1982; Soo, 1986). To accurately quantify the effects of the oxidized layer, several series of creep tests were initiated on HDPE specimens from which the oxidized layers were removed by abrasion prior to testing.

4.2.1 Creep in Air

Figures 4.17 through 4.19 compare in-air data for as-received and non-oxidized specimens tested at various stress levels.

At the lowest stress levels, 7.24 to 9.65 MPa (1050 to 1400 psi), creep is initially rapid (Stage I) but eventually slows until a linear rate of deformation is established (Stage II). This is true for as-received material as well as for non-oxidized specimens (Figure 4.17). Although comparisons between the two types of specimens can only be made for the 8.27 MPa (1200 psi) stress level, the creep rates are essentially identical except that the as-received material failed first after 7740 hours. The non-oxidized specimen did not fail. The creep curves in Figure 4.17 also show that just prior to failure, as-received specimens show an acceleration in the creep rate (Stage III) which is associated with "necking" and imminent failure.

At stresses of 10.34 MPa (1500 psi), and higher, major differences in behavior become evident between as-received and non-oxidized HDPE. From Figures 4.18 and 4.19 it may be seen that the initial creep rates for non-oxidized HDPE are usually larger than those for as-received material at any given stress. The difference becomes larger as the applied stress is increased. Stage II creep for non-oxidized specimens tends to be shorter and a very large increase in creep rate (Stage III) occurs. Observation of non-oxidized specimens during testing showed that this large Stage III strain increment did, indeed, involve local necking in the gagelength but it did not lead to fast failure, as is the case for as-received material, but to a remarkable extension of the necked region as it propagated throughout the gagelength. As soon as this was completed, the rate of creep again decreased giving rise to a long "Stage IV" which is not found in as-received HDPE. The important points to note are that, at very high tensile stresses, non-oxidized material will creep faster than as-received HDPE but it will have far superior ductility and rupture life. At stresses of about 8.27 MPa (1200 psi), and probably lower, the creep rates for the two materials are likely to be very similar during Stage I and Stage II creep because of limited cracking in as-received HDPE at low strains. However, after very extended creep, when cracking starts to become important, non-oxidized material should give greatly improved creep performance.

Rupture time data from the in-air tests are given in Figure 4.20. Only two of the five non-oxidized specimens failed. It is very clear from the data, however, that removal of the oxidized surface from HDPE leads to an enormous increase in failure time, compared to that for as-received material.

Table 4.3 Crack patterns in the oxidized surfaces of Marlex CL-100 HDPE creep specimens tested in air and water.

Specimen	Test Envir.	Stress MPa (psi)	Failure Time (h)	Crack Distribution in Oxidized Surface
381	Air	13.79 (2000)	4.0	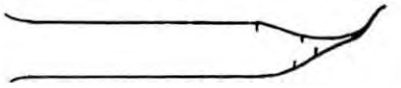
361	Air	11.03 (1600)	457	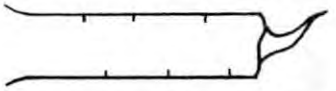
337	DIW	11.03 (1600)	112	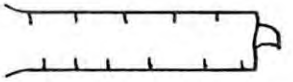
300	Air	10.34 (1500)	662	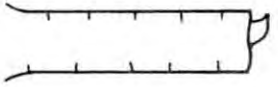
301	DIW	10.34 (1500)	2027	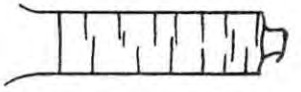
316	Air	9.65 (1400)	5378	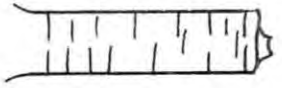
302	DIW	9.65 (1400)	5854	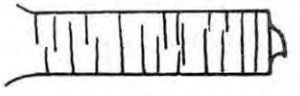
321	Air	8.27 (1200)	7740	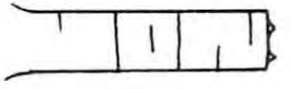

Table 4.4 Crack patterns in the oxidized surfaces of Marlex CL-100 HDPE creep specimens tested in Igepal CO-630.

Specimen	Stress MPa (psi)	Failure Time (h)	Crack Distribution in Oxidized Surface
392	12.41 (1800)	3.1	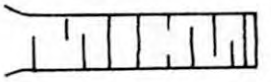
371	11.03 (1600)	45.6	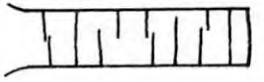
303	10.34 (1500)	65	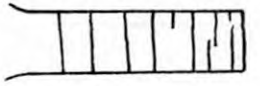
304	9.65 (1400)	106	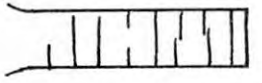
346	8.96 (1300)	128	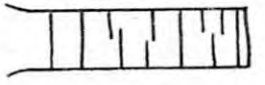
324	8.27 (1200)	1194	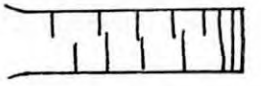

Table 4.5 Crack patterns in the oxidized surfaces of Marlex CL-100 HDPE creep specimens tested in turbine oil.

Specimen	Stress MPa (psi)	Failure Time (h)	Crack Distribution in Oxidized Surface
370	11.03 (1600)	45.9	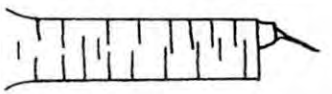
305	10.34 (1500)	128	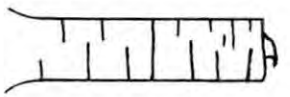
345	8.96 (1300)	102	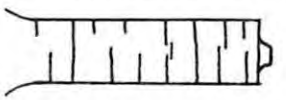
348	8.96 (1300)	168	
325	8.27 (1200)	1502	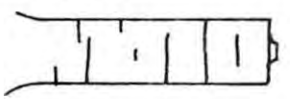

Table 4.6 Crack patterns in the oxidized surfaces of Marlex CL-100 HDPE creep specimens tested in scintillation fluid.

Specimen	Stress MPa (psi)	Failure Time (h)	Crack Distribution in Oxidized Surface
396	12.41 (1800)	7.9	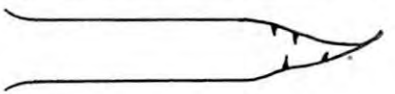
378	11.38 (1650)	10.5	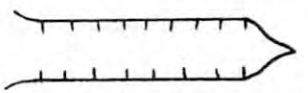
308	10.34 (1500)	14	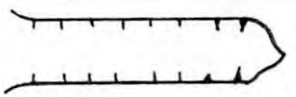
309	9.65 (1400)	35	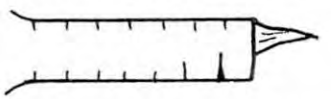
341	8.27 (1200)	50	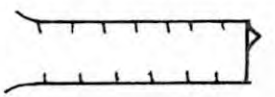
333	7.24 (1050)	340	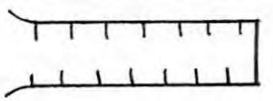
383	6.89 (1000)	1602	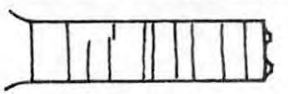

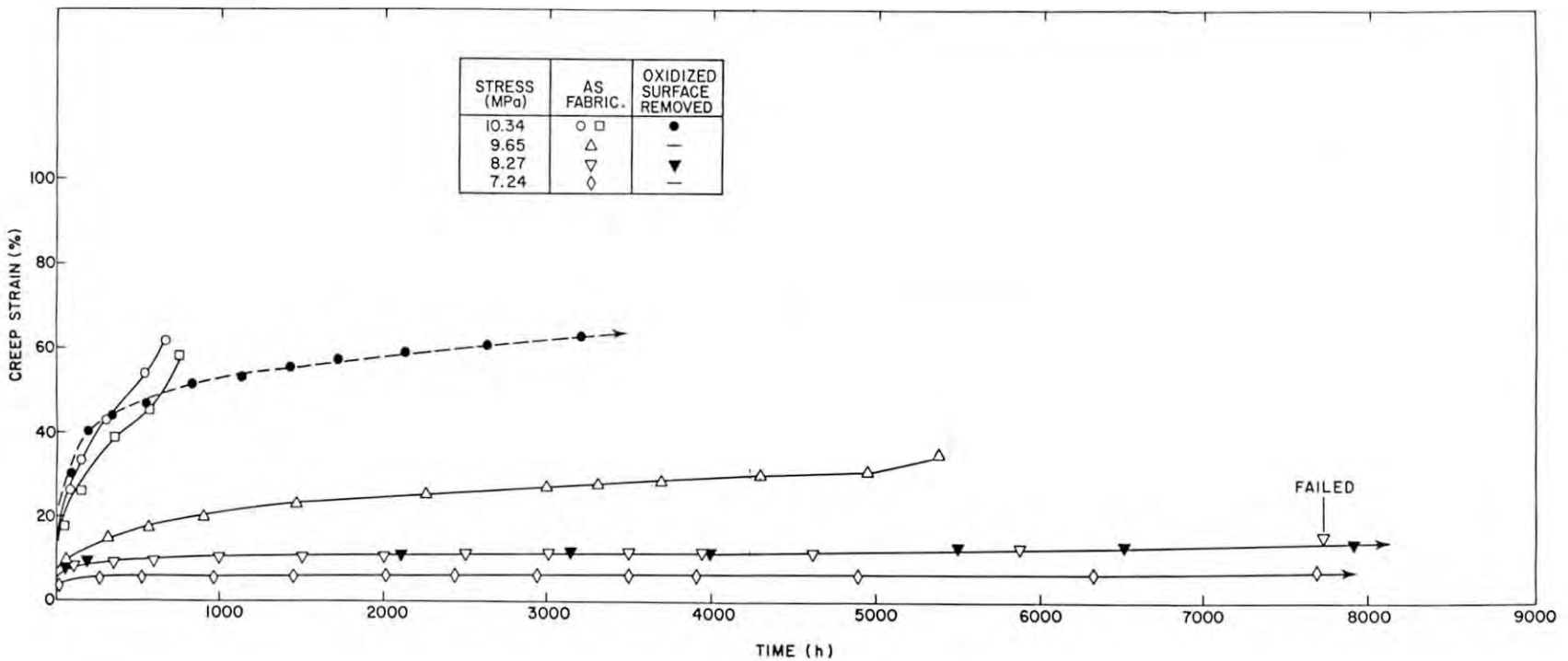

Figure 4.17 Effect of surface oxidation on the creep behavior of Marlex CL-100 HDPE in air at stresses between 7.24 - 10.34 MPa (1050-1500psi), inclusive.

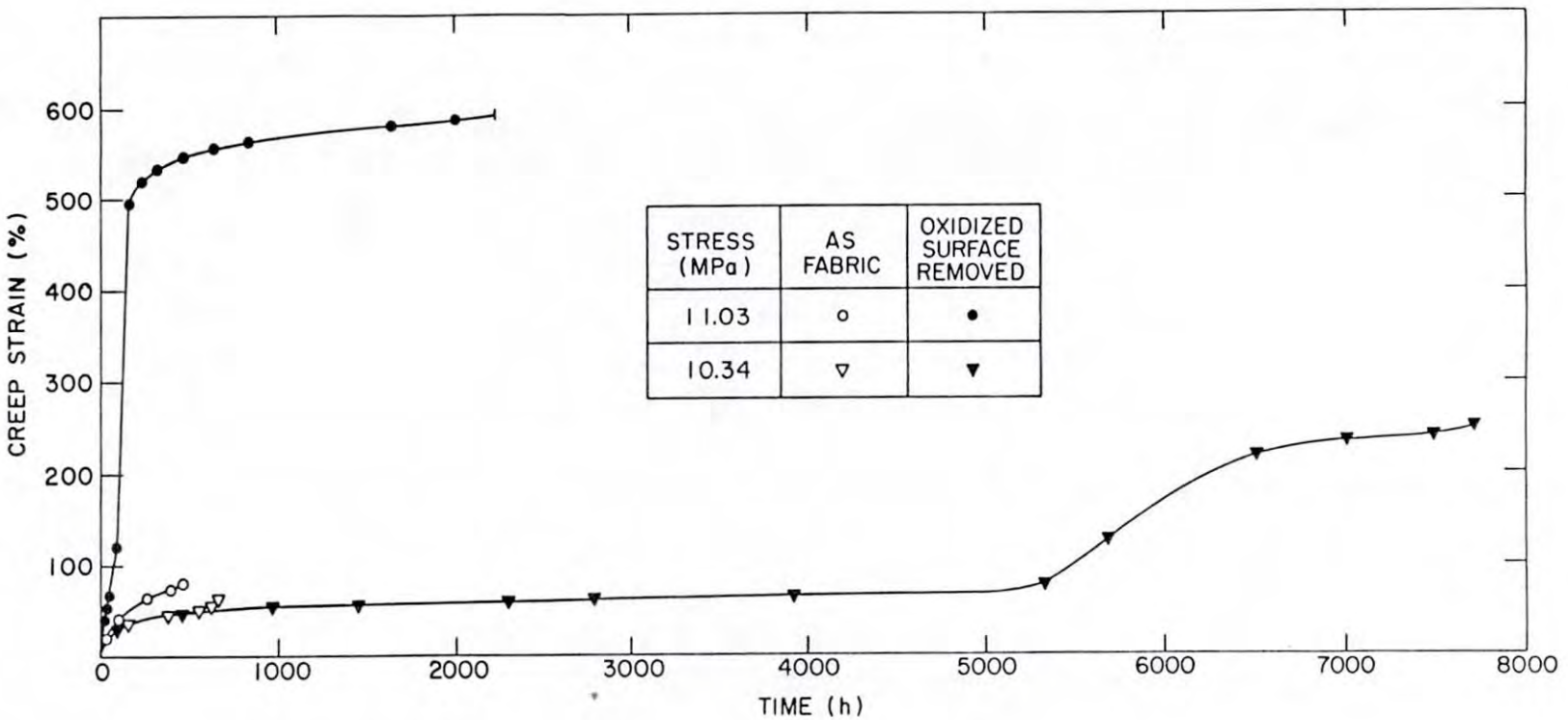

Figure 4.18 Effect of surface oxidation on the creep behavior of Marlex CL-100 HDPE in air at stresses of 10.34 and 11.03 MPa (1500 and 1600psi), inclusive.

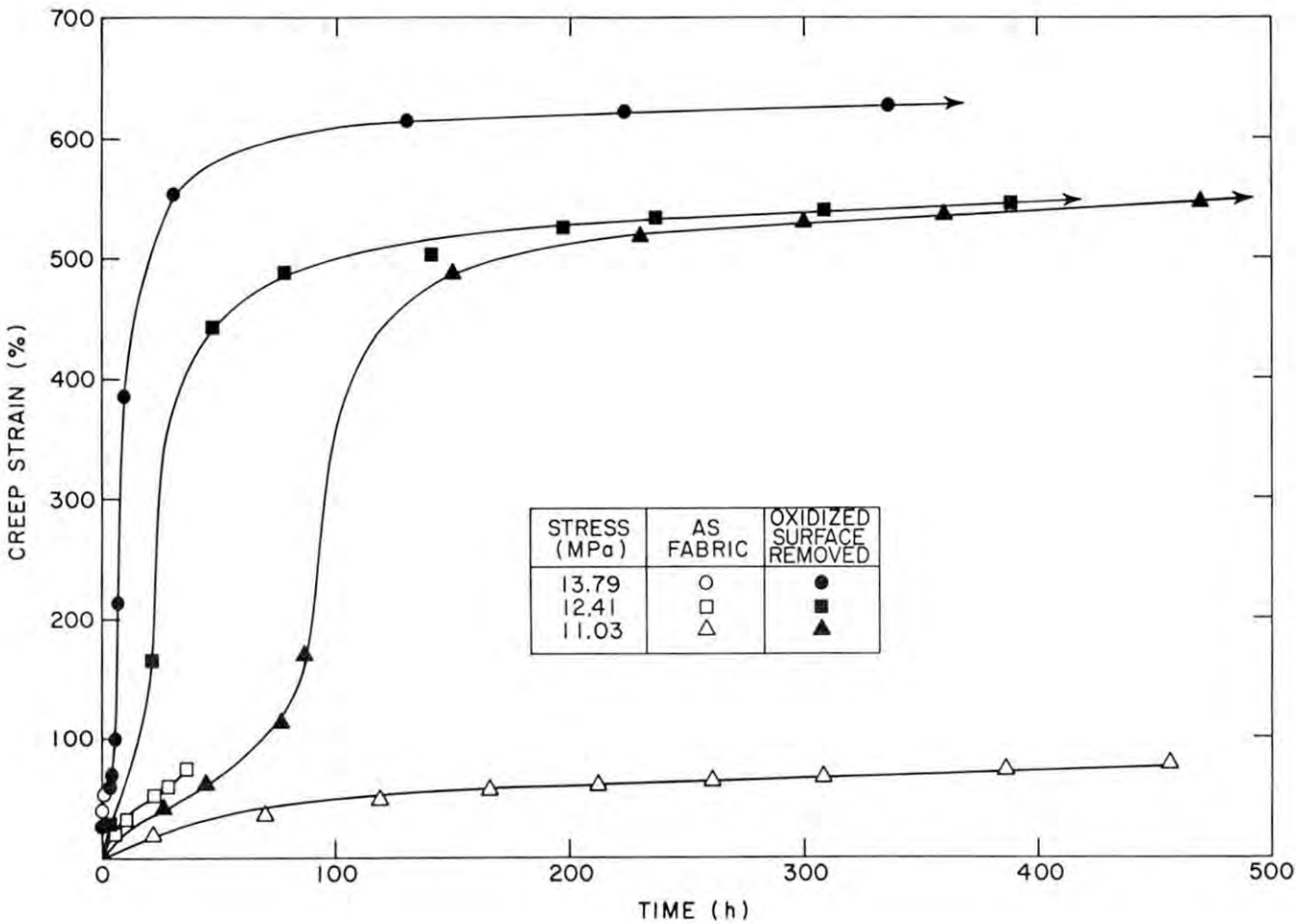

Figure 4.19 Effect of surface oxidation on the creep behavior of Marlex CL-100 HDPE in air at stresses between 11.03 and 13.79 MPa (1100 and 2000psi), inclusive.

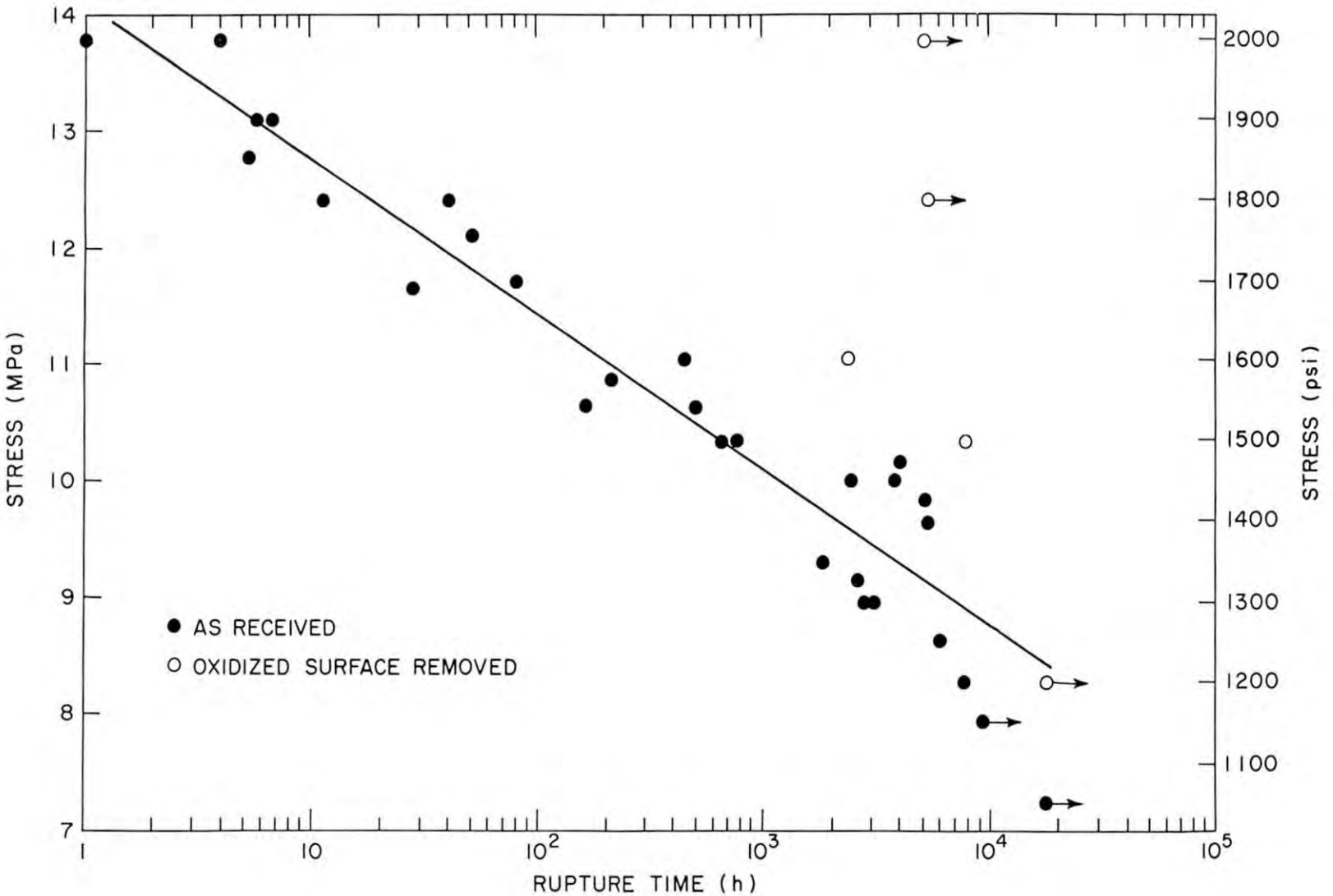

Figure 4.20 Effect of surface oxidation on the stress-rupture behavior of Marlex CL-100 HDPE in air.

4.2.2 Creep in Deionized Water

For deionized water the creep data are more limited than for air and the benefits of removing oxidized material from HDPE are not as clearcut. For example, at the highest creep stress used, 11.03 MPa (1600 psi), the rate of creep is larger for the non-oxidized material as shown in Figure 4.21 and the creep failure time is superior to that for as-received HDPE. At 10.34 MPa (1500 psi), however, the failure time for non-oxidized material is shorter (Figure 4.22). At 8.27 MPa (1200 psi) a non-oxidized specimen appears to display all four stages of creep (I through IV) but since the overall accumulated strain is only 35%, it is obvious that creep is still in the Stage II regime. Failure times for as-received and non-oxidized samples, based on the limited data in Figure 4.23, appear to be similar for a given stress. One clear advantage of removing the oxidized layer, however, is the larger ductility which arises because of the more uniform deformation in the gagelength.

4.2.3 Creep in Igepal CO-630

Creep curves for tests in Igepal are given in Figures 4.24 and 4.25. In Figure 4.24 some data are shown for HDPE specimens from which 0.25 mm (0.010") of material was removed from the non-oxidized surface. This was done to check if oxidation was indeed the main surface effect rather than some other unidentified mechanism. The agreement between the creep curves for these and as-received samples at stresses of 9.65 and 10.34 MPa (1400 and 1500 psi) is quite good.

Removal of the oxidized layer from the samples causes a major improvement in creep behavior. Time-to-failure and ductility are greatly enhanced. The creep rate for the non-oxidized specimens is increased only at the 10.34 MPa (1500 psi) stress level compared to as-received material. The time-to-failure data are compared most clearly in Figure 4.26. Removal of the oxidized layer may increase the rupture time by up to about an order of magnitude, and the "threshold stress" below which failure becomes unlikely (horizontal portions of curves) is increased by about 1 MPa (150 psi).

4.2.4 Creep in Scintillation Fluid

In the case of scintillation fluid, removal of the oxidized layer does not greatly alter the early creep rate compared to oxidized HDPE. However, time-to-failure and ductility are usually increased for non-oxidized material (Figures 4.27, 4.28 and 4.29).

Table 4.7 briefly summarizes the effects which removal of the oxidized layer has on the early creep rate, time-to-failure, and elongation-at-failure for HDPE. There seems to be a clear advantage in removing the oxidized layer after container molding or, perhaps, to stop it from forming by molding in an inert environment, if possible.

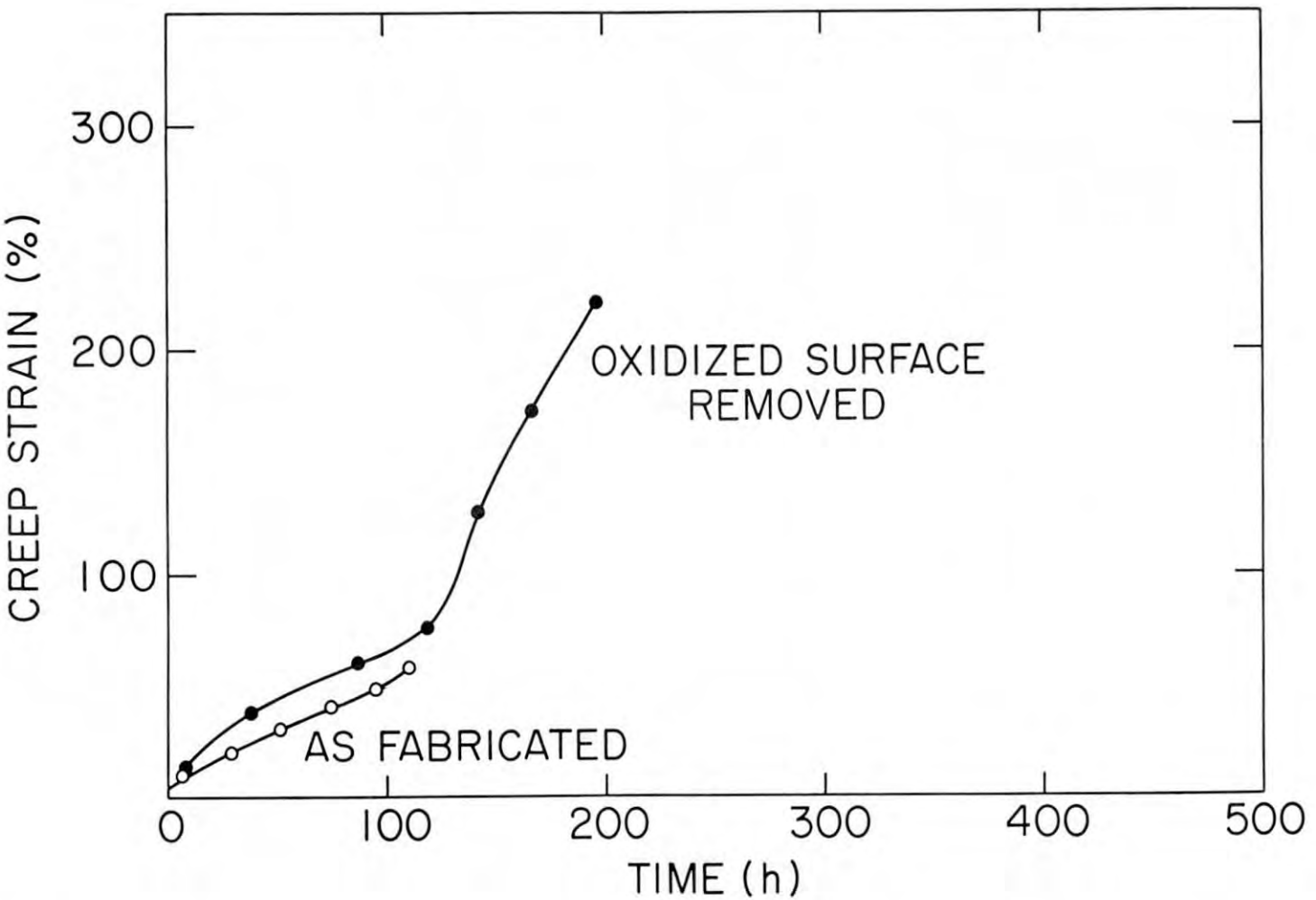

Figure 4.21 Effect of surface oxidation on the creep behavior of Marlex CL-100 HDPE in deionized water at a stress of 11.03 MPa (1600 psi).

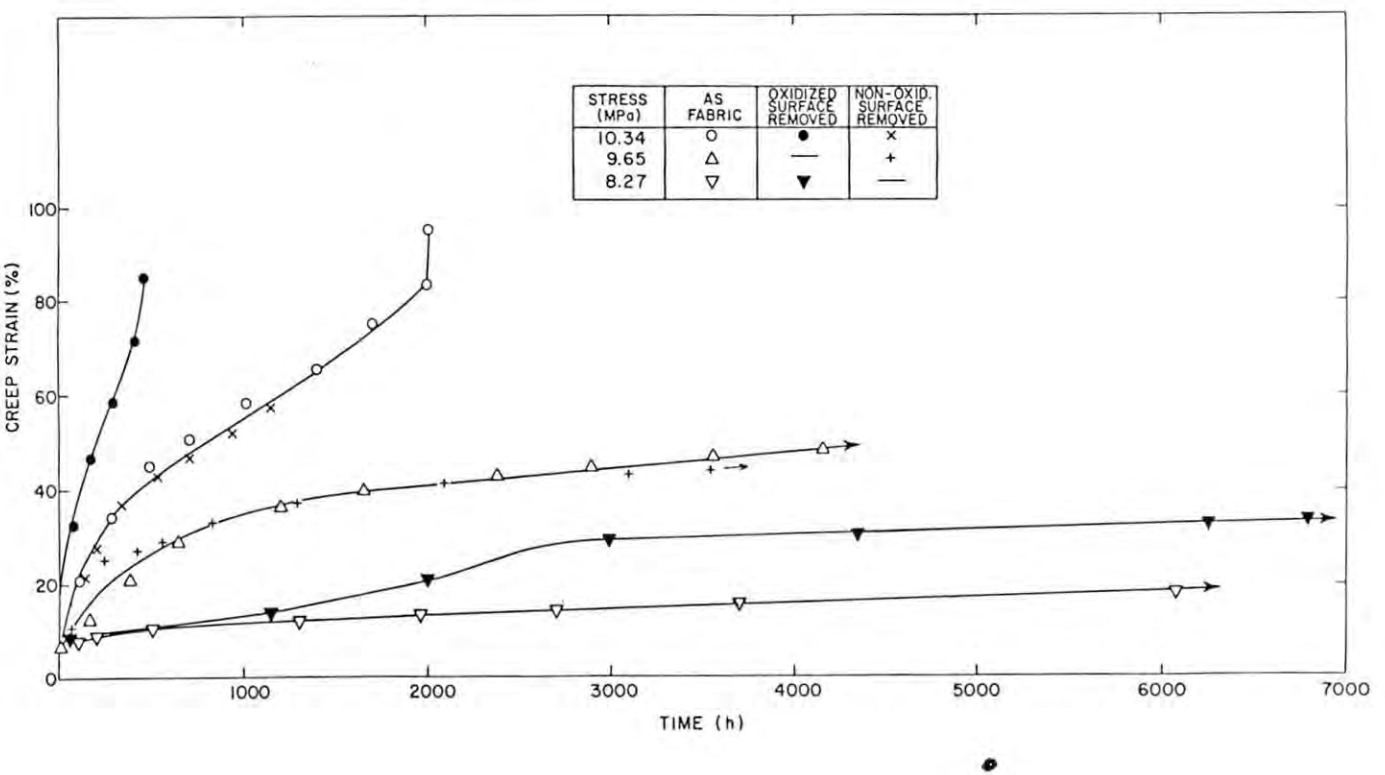

Figure 4.22 Effect of surface oxidation on the creep behavior of Marlex CL-100 HDPE in deionized water at stresses between 8.27 to 10.34 MPa (1200 to 1500psi), inclusive.

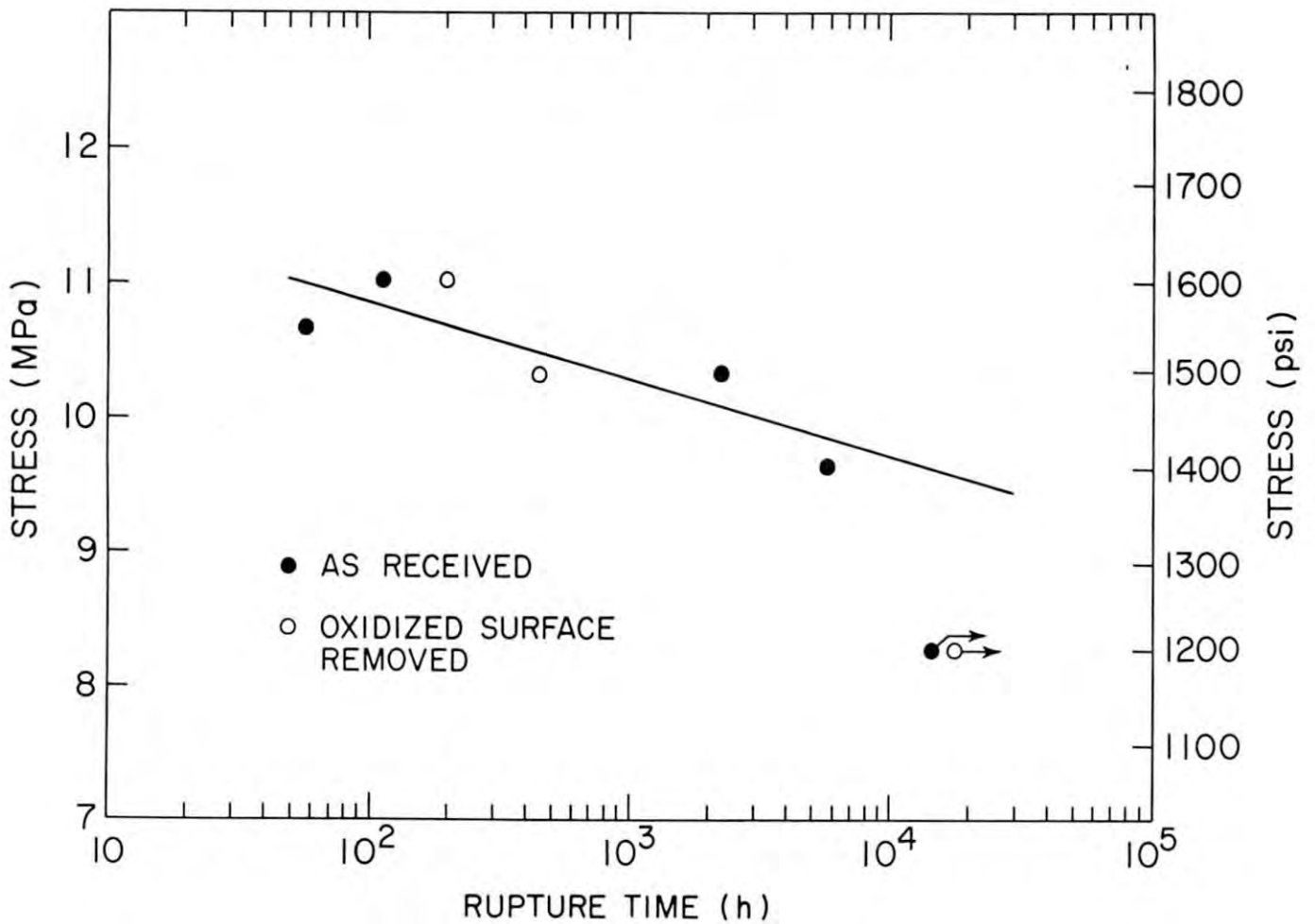

Figure 4.23 Effect of surface oxidation on the stress-rupture behavior of Marlex CL-100 HDPE in deionized water.

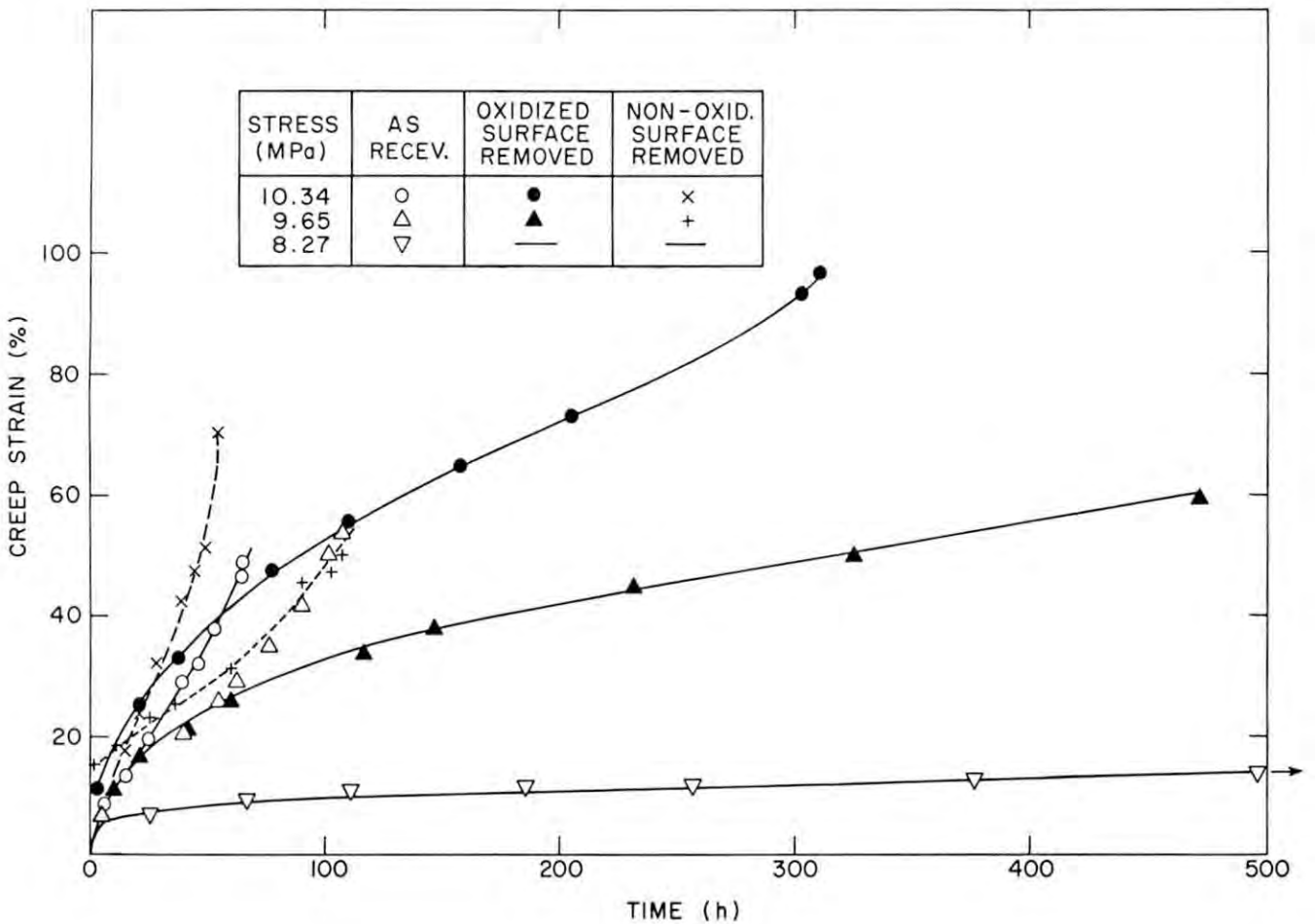

Figure 4.24 Effect of surface preparation on the creep behavior of Marlex CL-100 HDPE in Igepal at stresses between 8.27 and 10.34 MPa (1200 to 1500psi), inclusive.

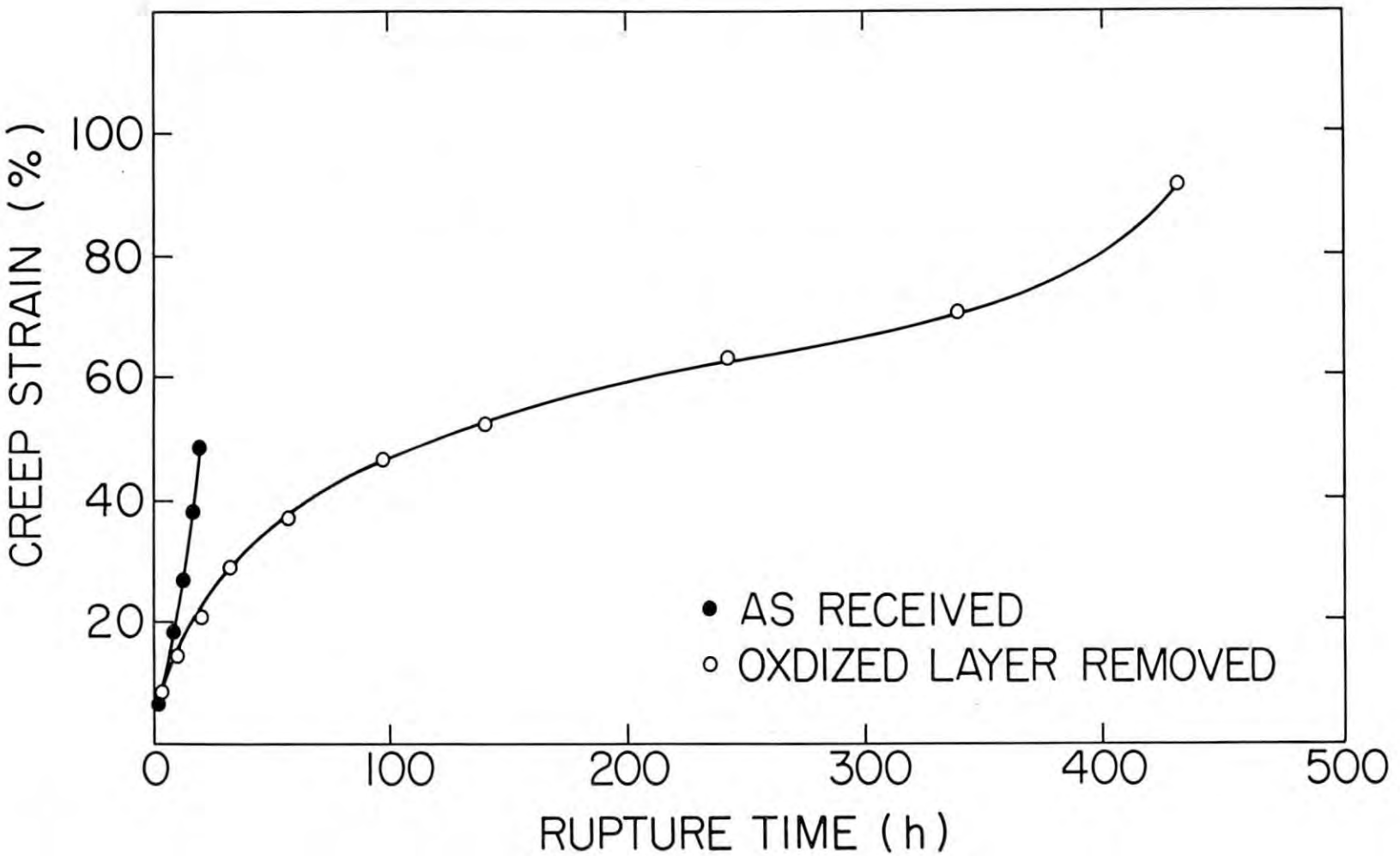

Figure 4.25 Effect of surface oxidation on the creep behavior of Marlex CL-100 HDPE in Igepal at a stress of 11.72 MPa (1700 psi).

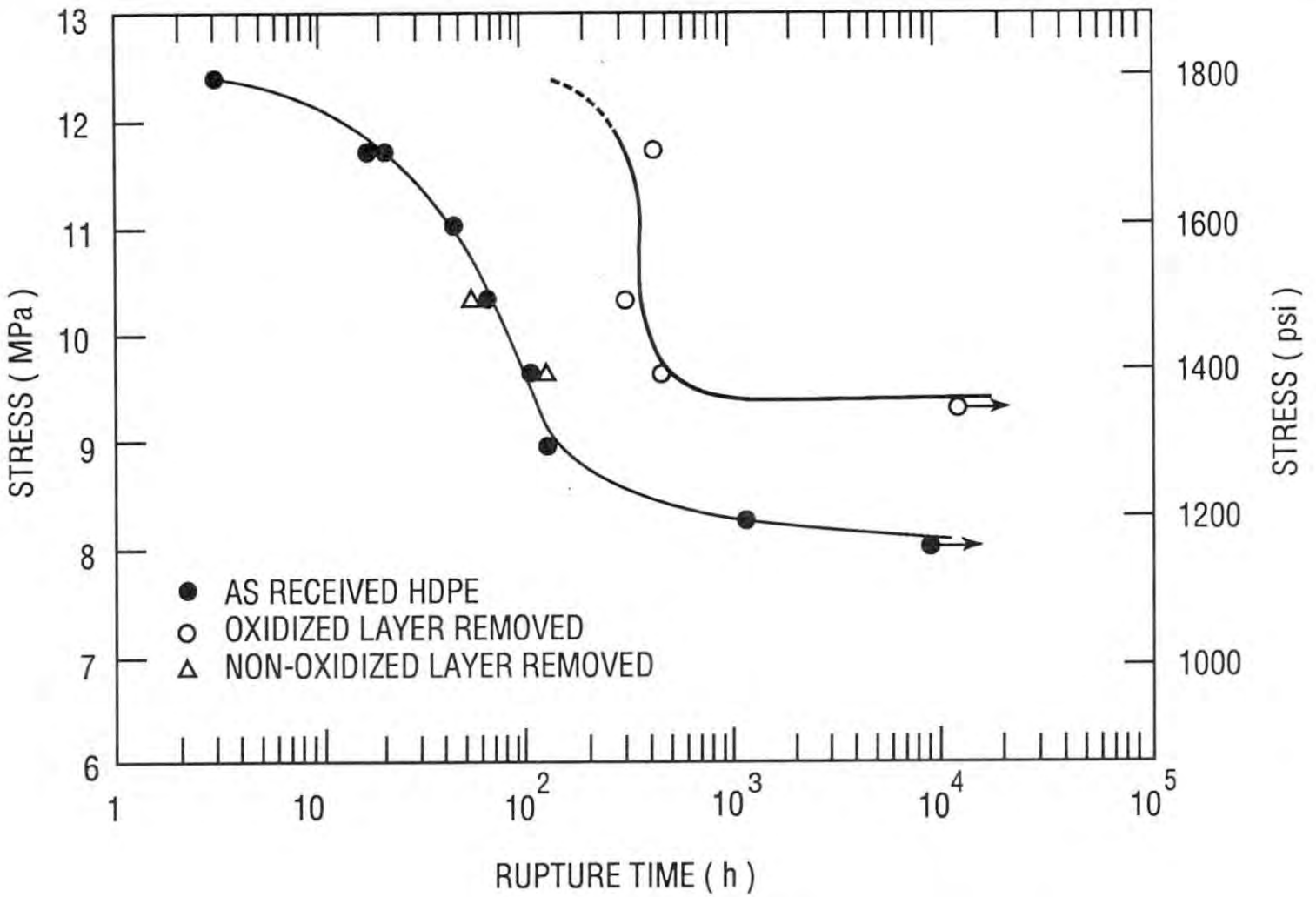

Figure 4.26 Effect of surface preparation on the stress-rupture behavior of Marlex CL-100 HDPE in Igepal CO-630.

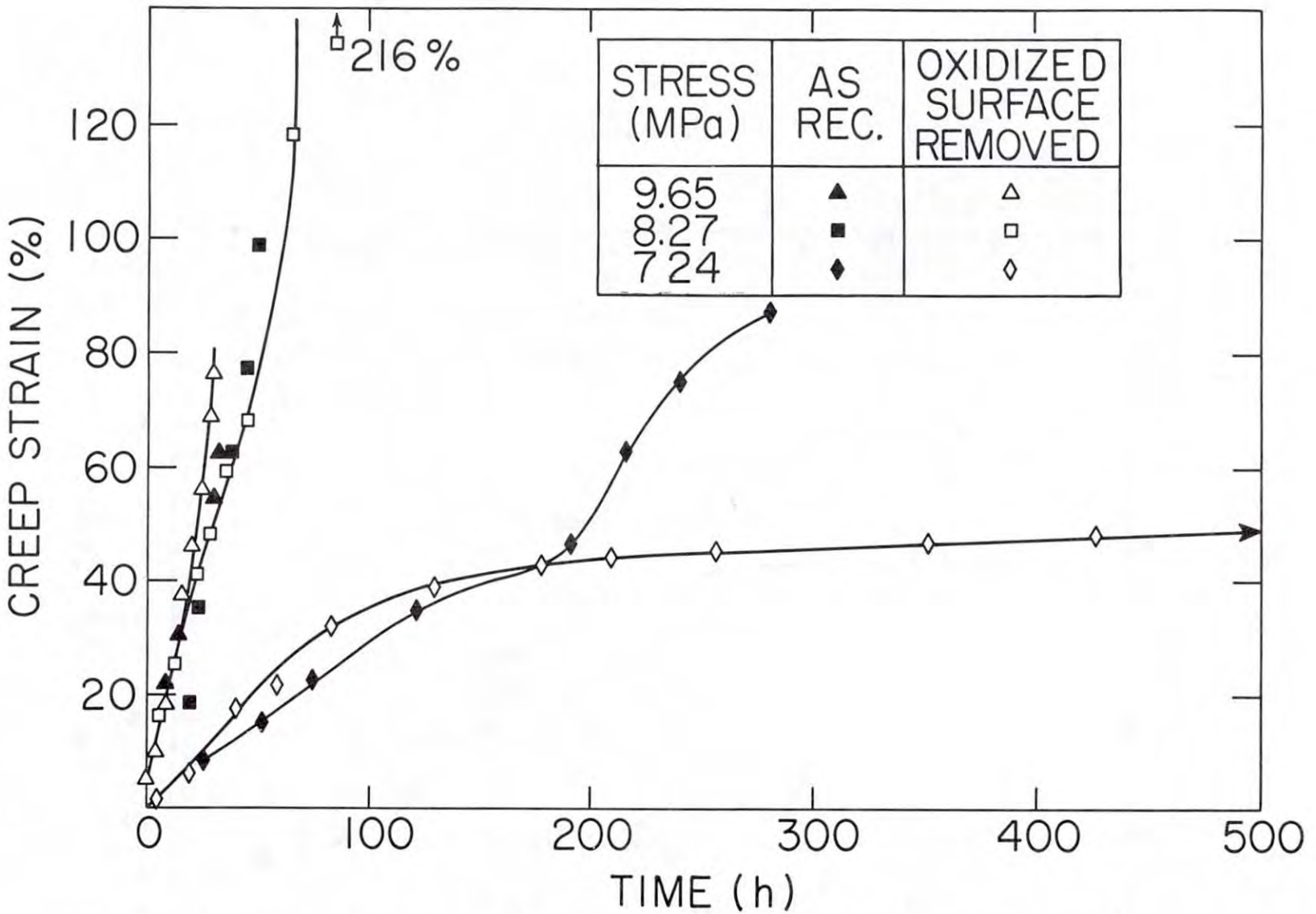

Figure 4.27 Effect of surface oxidation on the creep behavior of Marlex CL-100 HDPE in liquid scintillation fluid at stresses between 7.24 and 9.65 MPa (1050 to 1400psi), inclusive.

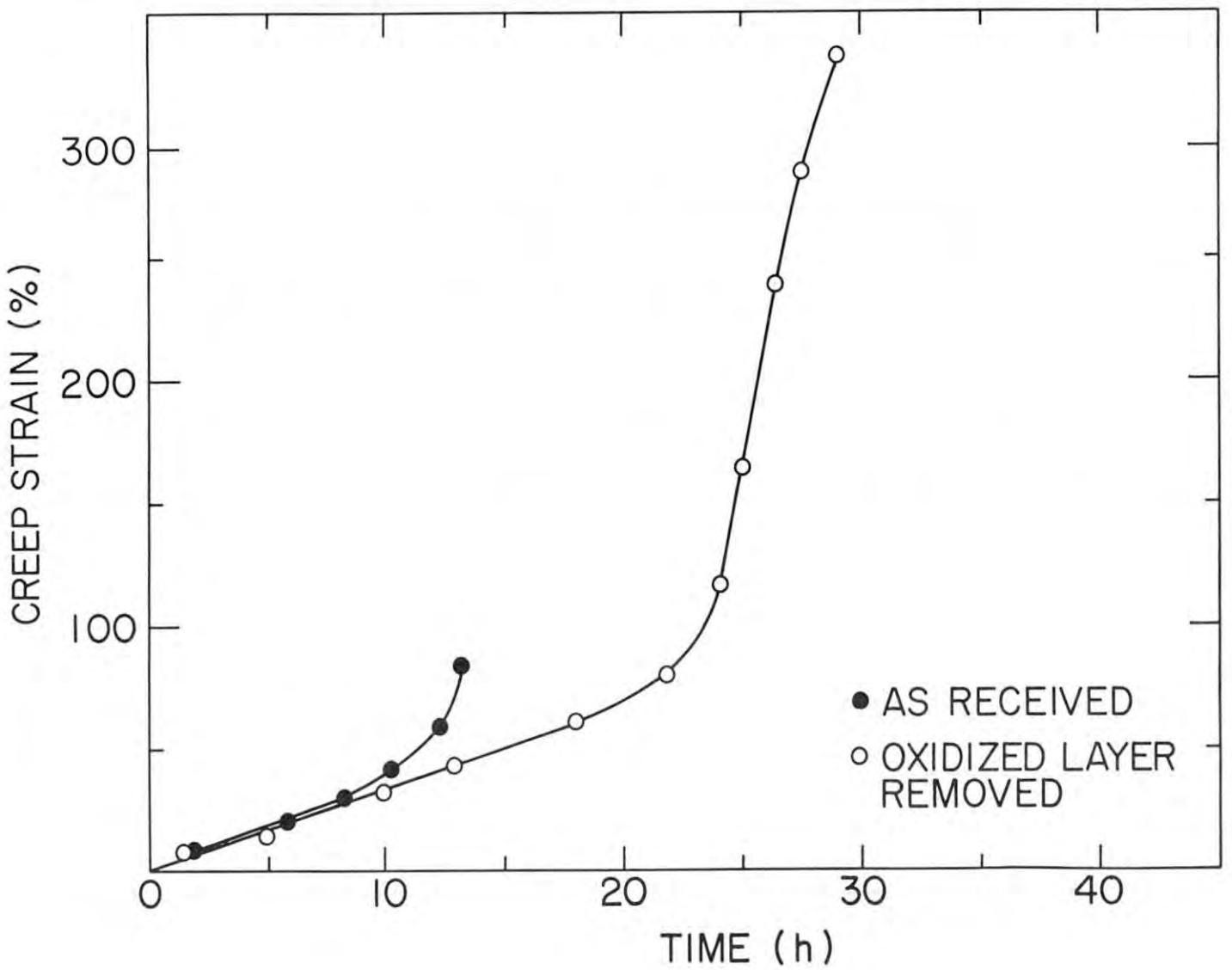

Figure 4.28 Effect of surface oxidation on the creep behavior of Marlex CL-100 HDPE in liquid scintillation fluid at a stress of 10.34 MPa (1500 psi).

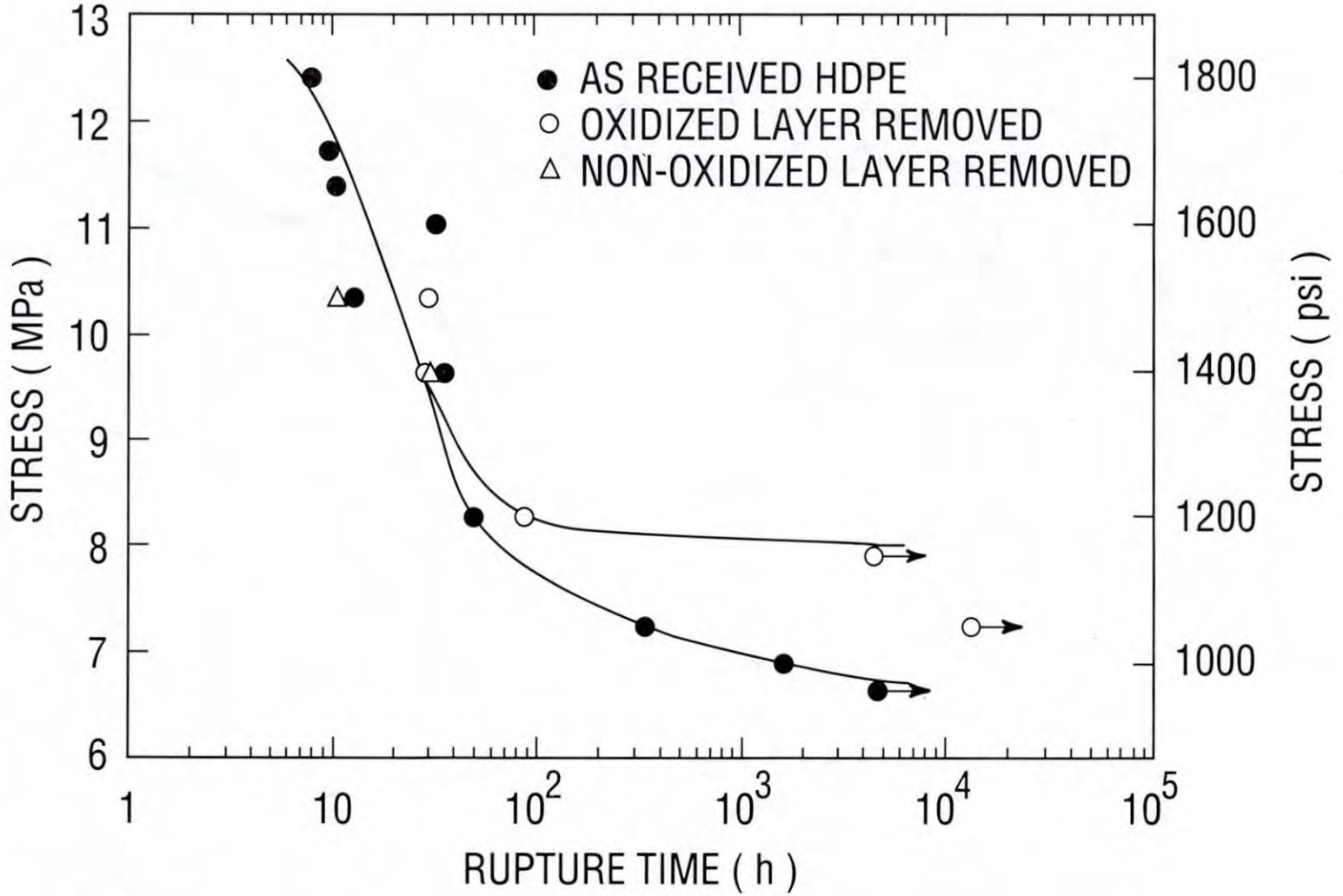

Figure 4.29 Effect of surface preparation on the stress rupture behavior of Marlex CL-100 in liquid scintillation fluid.

Table 4.7 Changes in the creep behavior of Marlex CL-100 HDPE caused by removal of oxidized surface material

Envir.	Stress	Early Creep Rate	Time to Failure	Ductility
Air	13.79	Same	Increase	Increase
	12.41	Increase	Increase	Increase
	11.03	Increase	Increase	Increase
	10.34	Increase	Increase	Increase
	8.27	Same	Increase	Increase
DIW	11.03	Increase	Increase	Increase
	10.34	Increase	Decrease	Same
	8.27	Increase	(1)	(1)
Igepal	11.72	Same	Increase	Increase
	10.34	Increase	Increase	Increase
	9.65	Same	Increase	Same
LSF	10.34	Same	Increase	Increase
	8.27	Same	Increase	Increase
	7.24	Same	Increase	Same

Note:

(1) Not known; specimen did not fail.

4.3 Discussion of Creep in Chemical Environments

From the data described in Sections 4.1 and 4.2 the effects of stress, test environment and surface oxidation have been generally quantified and a basic understanding of the underlying creep process has been obtained from this study. In particular, the role of the surface oxidized layer in causing early cracking and localized deformation, necking and failure in crosslinked HDPE is clear. Removal of the layer often results in faster creep rates but it usually leads to higher ductility and longer failure times for a given stress level. Close examination of the creep curves for as-received and non-oxidized HDPE shows that the differences usually appear after about 20 percent elongation. This is almost certainly associated with the first appearance of cracks in the oxidized layer. Until the cracks are nucleated, deformation in both types of specimen occurs uniformly throughout the gagelength in a similar fashion. When cracks appear then localized deformation occurs in the cracked regions because of stress concentration effects. This will lead to several types of failure in as-received HDPE depending on the environment:

a) "Environmental stress-cracking" in which the cracks grow quickly in a "brittle" manner causing early failure. Igepal and turbine oil cause such failure over a range of low stresses.

b) "Ductile failure" which is common for environments such as air, water, turbine oil and Igepal at intermediate and high stresses.

c) "Superplastic failure" in which the cracks formed in the oxidized layer become blunted by easy plastic deformation so that they grow very slowly, if at all. Deformation then occurs more evenly throughout the gagelength giving higher ductility and failure times compared to those for stress-cracking conditions. Such failure is promoted by high stress levels and, more importantly, by the removal of oxidized surface material.

d) "Low stress creep embrittlement" which occurs when the stress level is too low to give large scale plasticity. Failure, if it occurs, takes a long time and results from "brittle" crack growth.

Removal of the oxidized layer often accelerates the rate of creep during early deformation, compared to as-received material (Table 4.7). Scintillation fluid, however, is the environment which is the exception and no change in the early creep rate is observed. A possible explanation for the enhanced creep rate in non-oxidized HDPE is that the more brittle oxidized surface material is also stronger than the bulk HDPE. Therefore, removal of the oxidized layer, and its associated strengthening effect, would allow the specimen to creep faster compared to as-received material.

5. IRRADIATION - CREEP IN AIR

It is generally recognized that prior gamma irradiation of unstressed HDPE, and many other plastics, leads to an increase in strength and decreases in elongation-at-yield and elongation-at-break (Dougherty, and others, 1984; Clough, and others, 1984; Soo, and others, 1986; Philips Chem. Co., 1975; Schoenbacher, 1985). Such effects, however, became noticeable only after some critical dose. The results are usually attributable to radiation-induced crosslinking of polymer chains, which eventually causes embrittlement.

5.1 Irradiation-Creep Results

Some very interesting effects on creep are found, however, if gamma irradiation is carried out during creep rather than before creep. A previous BNL study by Dougherty, and others, (1984) showed that Marlex CL-100 displays an increase in creep rate during in-test irradiation. They found that the effect is significant at high stress levels and becomes less important at lower stresses. On the other hand, other BNL work on the same batch of Marlex CL-100 shows contrary behavior and the rate of creep was found to be greatly reduced by in-test irradiation compared to unirradiated HDPE tested at the same stress (Soo, and others, 1986). Careful examination of the data from the two BNL studies reveals internally-consistent behavior (Soo, and others, 1986).

Some support for the irradiation-induced acceleration of creep may be found in the literature. For example, Bell, and others, (1967) electron-irradiated three glassy polymers (88 percent polyvinyl chloride/12 percent polyvinyl-acetate; polymethymethacrylate ; and polystyrene) and found significant increases in the creep rate when the electron current was applied. They postulated that gas formation within these materials is responsible for the effect. However, no other irradiation-creep data appear to be available for HDPE under conditions similar to those used in the two BNL studies.

In order to rationalize the apparently conflicting effect of in-test irradiation in the two BNL studies it is necessary to first specify any differences in test conditions. The only significant differences lie in the applied creep stresses and the gamma dose rates. These are summarized in Table 5.1. Dougherty, and others, discovered an irradiation effect at higher stresses and lower dose rates compared to tests in the study by Soo, and others. Thus, no definitive comparison can be made between the two studies.

To check under what conditions in-test irradiation can accelerate or retard creep a new set of irradiation-creep experiments was initiated. Stress levels and gamma dose rates were selected so that those for the two earlier studies were encompassed within the new test conditions. Table 5.2 gives the test matrix used. The HDPE samples were stamped from the "old" batch of material since this was used in the two earlier studies. In addition, most of the unirradiated control tests were already completed so that only a few additional spot check tests were needed.

Table 5.3 shows all irradiation-creep data attained in this effort. Many tests were not completed because of program termination and unanticipated long failure times. However, they still provide invaluable results because irradiation and stress effects were observed early in the creep tests.

Table 5.1 Comparison of test conditions during irradiation-creep of Marlex CL-100

Study	Dose Rate (Rad/h)	Stress (MPa)	Effect of In-Test Irradiation
Dougherty et al. (1984)	5×10^3 (Co-60)	12.41 (1800 psi)	Irradiation greatly increases creep rate
Dougherty et al.	5×10^3 (Co-60)	11.07 (1600 psi)	Irradiation slightly increases creep rate
Soo et al. (1986)	3×10^4 (Cs-137)	10.34 (1500 psi)	Irradiation greatly decreases creep rate

Table 5.2 Irradiation-creep test matrix for HDPE

Test Environment	Stress (MPa)	Stress (psi)	Gamma Dose Rate (rad/h)
Air	12.58	1825	0
Air	12.58	1825	5×10^3
Air	12.58	1825	2×10^4
Air	11.72	1700	0
Air	11.72	1700	5×10^3
Air	11.72	1700	2×10^4
Air	11.07	1600	0
Air	11.07	1600	5×10^3
Air	11.07	1600	2×10^4
Air	10.34	1500	0
Air	10.34	1500	5×10^3
Air	10.34	1500	2×10^4

Table 5.3 Irradiation-creep data for Marlex CL-100 HDPE

Test	Material Cond.	Temp. (°C)	Dose Rate(rad/h)	Stress (psi)	Stress (MPa)	Failure Time(h)	Elong. (%)
405	As rec.	20	5×10^3	1825	12.58	27.5	206.1
403	As rec.	20	5×10^3	1700	11.72	209.7	326.2
406	As rec.	23	5×10^3	1600	11.03	1198	80.7
404	As rec.	20	5×10^3	1500	10.34	1783	51.4
417	As rec.	20	2×10^4	1825	12.58	50.4	140.6
418	As rec.	20	2×10^4	1700	11.72	>337	>73.5
416	As rec.	20	2×10^4	1600	11.03	>811	>33.0
415	As rec.	20	2×10^4	1500	10.34	>210	>15.3
414	As rec.	26	2×10^4	1825	12.58	6.6	195.0
413	As rec.	26	2×10^4	1700	11.72	>501	>567
384	As rec.	20	0	2000	13.79	1.8	67.6
368	As rec.	20	0	1900	13.10	5.3	46.6
375	As rec.	20	0	1850	12.76	18.6	(1)
351	As rec.	20	0	1825	12.58	5.8	82
344	As rec.	20	0	1700	11.72	47	113.6
343	As rec.	20	0	1600	11.03	127	92.0
342	As rec.	20	0	1500	10.34	2544	96.3
317	As rec.	20	0	1500	10.34	7514	93.4
318	As rec.	20	0	1400	9.65	>18100	>43.3
386	As rec.	20	0	1200	8.27	>8300	>7.5

Note:

(1) LVDT failure; elongation not known.

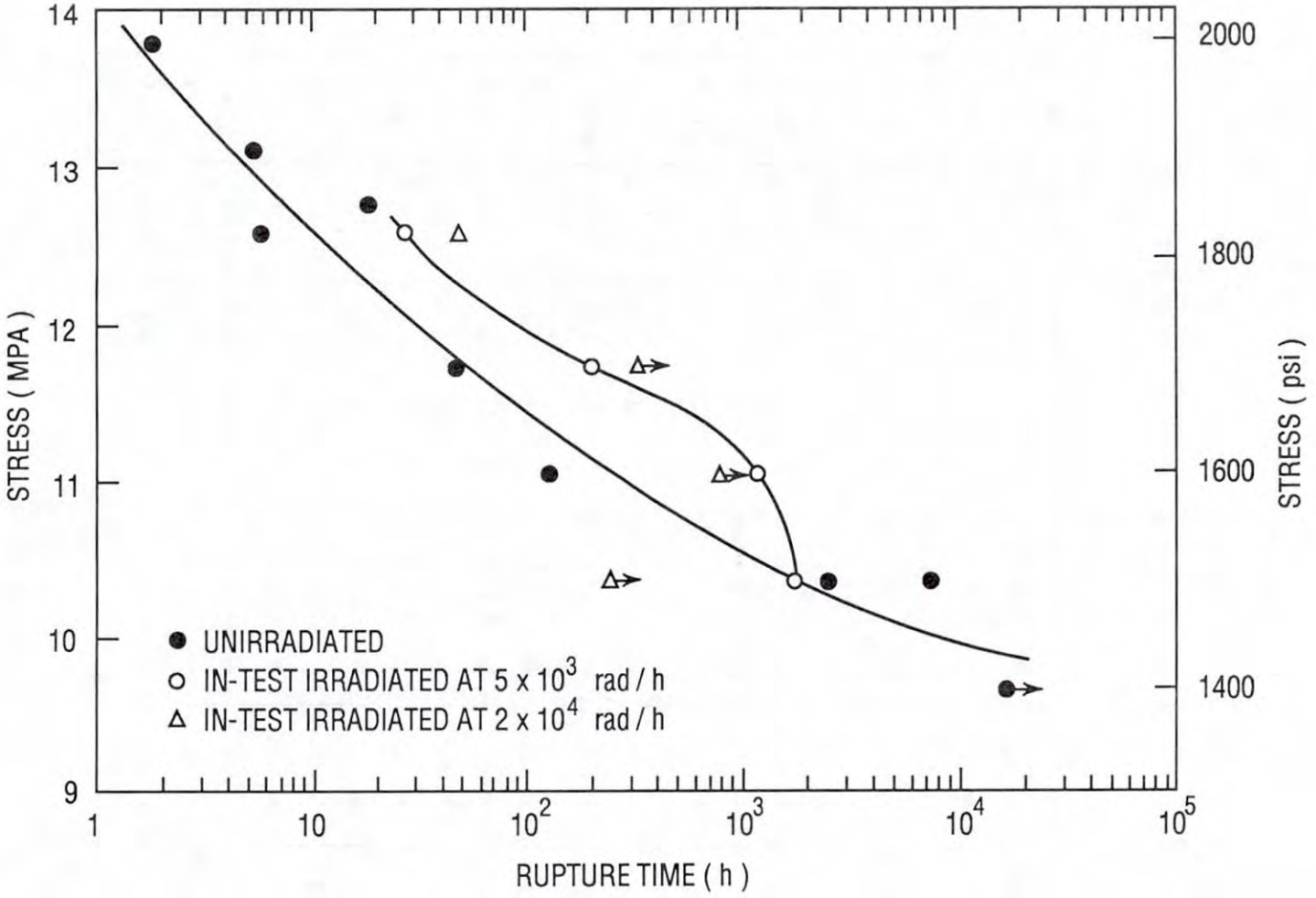

Figure 5.1 Effect of in-test gamma irradiation at 5 x 10^3 rad/h on the stress-rupture behavior of Marlex CL-100 HDPE.

Note that two tests were run at 26°C since they were run in mid summer and the temperature-control system in the laboratory was temporarily not operating.

The stress-rupture data in Figure 5.1 show that in-test irradiation normally increases the failure time compared to non-irradiated controls. However, the single test carried out at 10.34 MPa (1500 psi) seems to indicate that at this stress, and lower, irradiation reduces the failure time. This conclusion is based mainly on the tests conducted at the 5×10^3 rad/h dose rate, since most of the tests at 2×10^4 rad had to be terminated prior to failure. Nevertheless, the "early" failure at low stresses under irradiation conditions is consistent with the previously-described crack-propagation phenomena observed in U-bend specimens exposed to radiation (Section 3.3). Such U-bend tests are similar to those for low-stress irradiation-creep.

Examination of the creep curves in Figures 5.2 through 5.5 shows a strong irradiation strengthening effect. Irradiation reduces the creep rate, with the degree of reduction increasing with increasing dose rate. For the 10.34 and 11.03 MPa (1500 and 1600 psi) tests the shapes of the creep curves are classical with the normal Stage I, II and III regimes. At the higher stress levels, however (Figures 5.4 and 5.5) irradiation at the 5×10^3 rad/h rate leads to a very prominant Stage III and high elongation. Towards the end of Stage III the creep rate decreases and deformation enters a Stage IV period. Comparison of the irradiation-creep curves with those for unirradiated, unoxidized HDPE (Figures 4.19 and 4.20) show close similarities. The main difference lies in the shorter Stage IV for the irradiated specimens.

The long Stage III in both series of tests is associated with rapid extension of necked region throughout most of the gagelength. Once this is achieved the rate of deformation slows and Stage IV begins. For the irradiated HDPE, embrittlement occurs resulting in a very short Stage IV compared to non-oxidized, unirradiated material.

Only the 10.34 MPa (1500 psi) specimen showed normal cracking during irradiation creep. At this low stress level, cracks which are nucleated remain sharp and are able to grow in a brittle manner. At higher stresses the cracks become blunted by plastic deformation and do not grow. Therefore, more even deformation occurs in the specimen giving rise to high elongation.

For the 2×10^4 rad/h irradiation-creep tests, only the highest-stress specimen failed. A long, necked region was present which was similar to, but shorter than, that for the specimens tested at the lower dose rate.

In general, gamma irradiation during the creep of Marlex CL-100 HDPE is beneficial. It decreases the creep rate, enhances the ductility, and lengthens the time to failure.

5.2 Discussion of Irradiation-Creep Behavior

Marlex CL-100 is a crosslinked HDPE which has been shown here to be strengthened by gamma irradiation during creep. Prior irradiation is also known to strengthen its creep and tensile strengths (Soo, and others, 1986). Most types of polyethylene undergo crosslinking as a result of ionizing

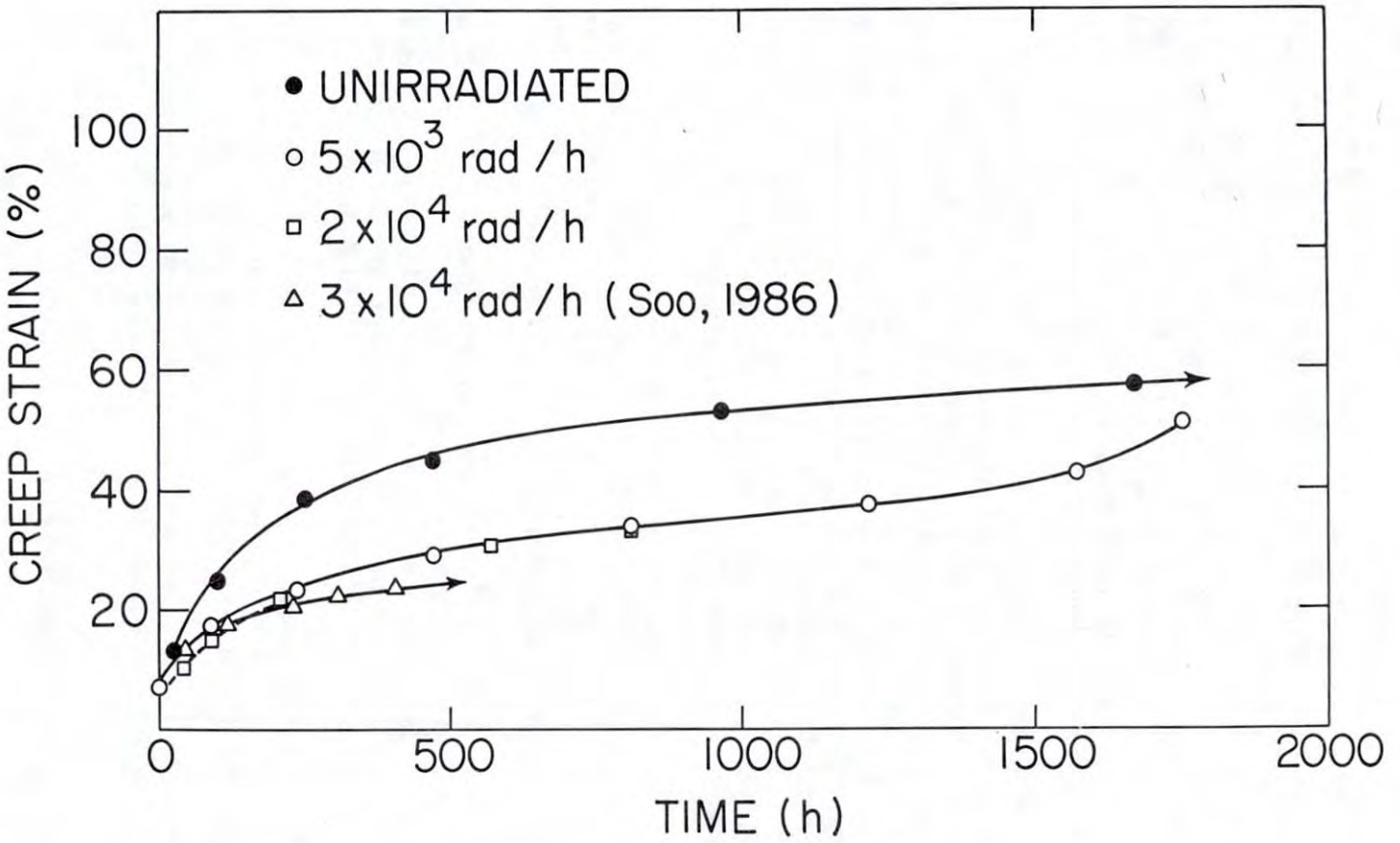

Figure 5.2 Effect of in-test gamma irradiation on the creep behavior of Marlex CL-100 HDPE at a stress of 10.34 MPa (1500 psi).

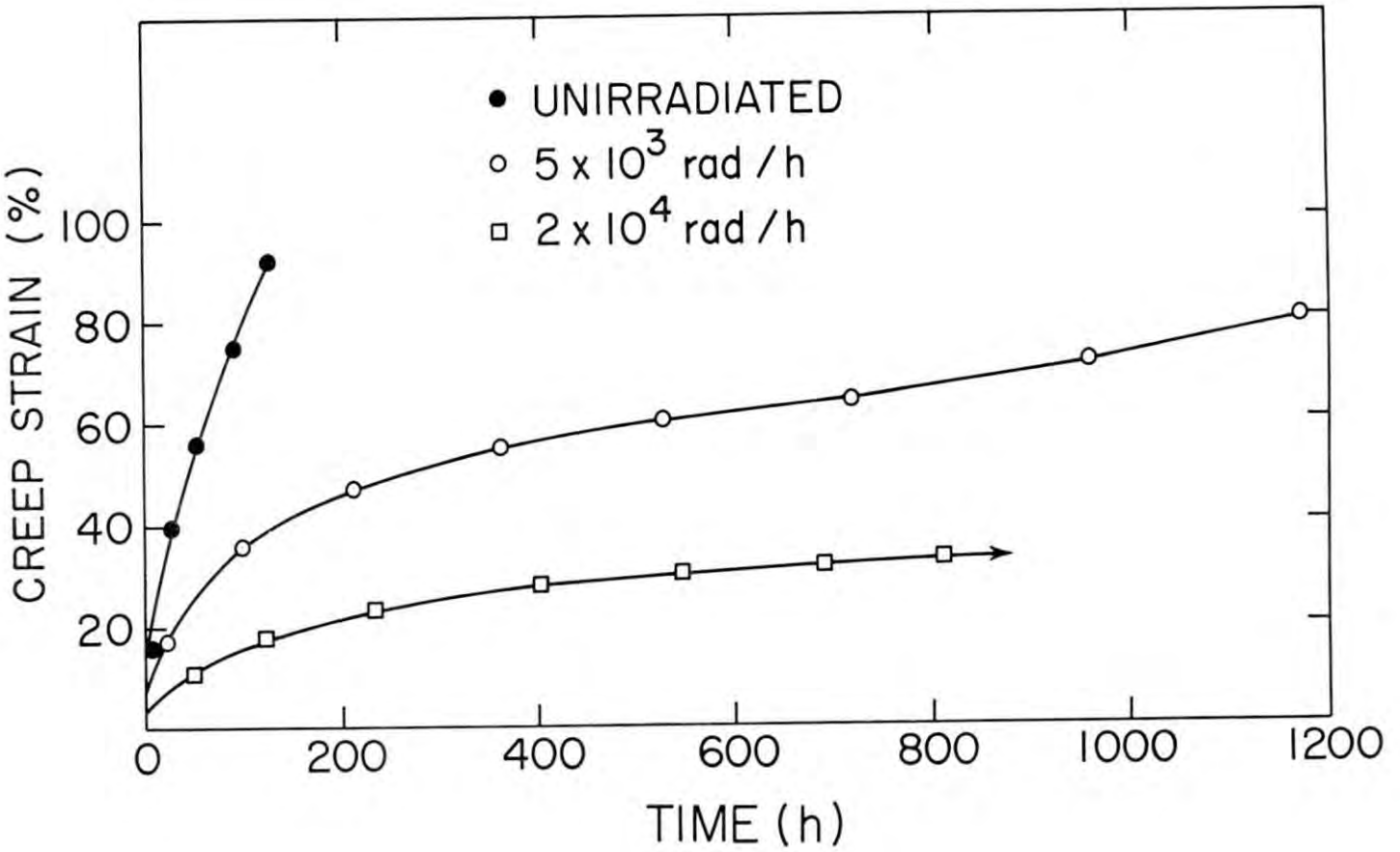

Figure 5.3 Effect of in-test gamma irradiation on the creep behavior of Marlex CL-100 HDPE at a stress of 11.03 MPa (1600 psi).

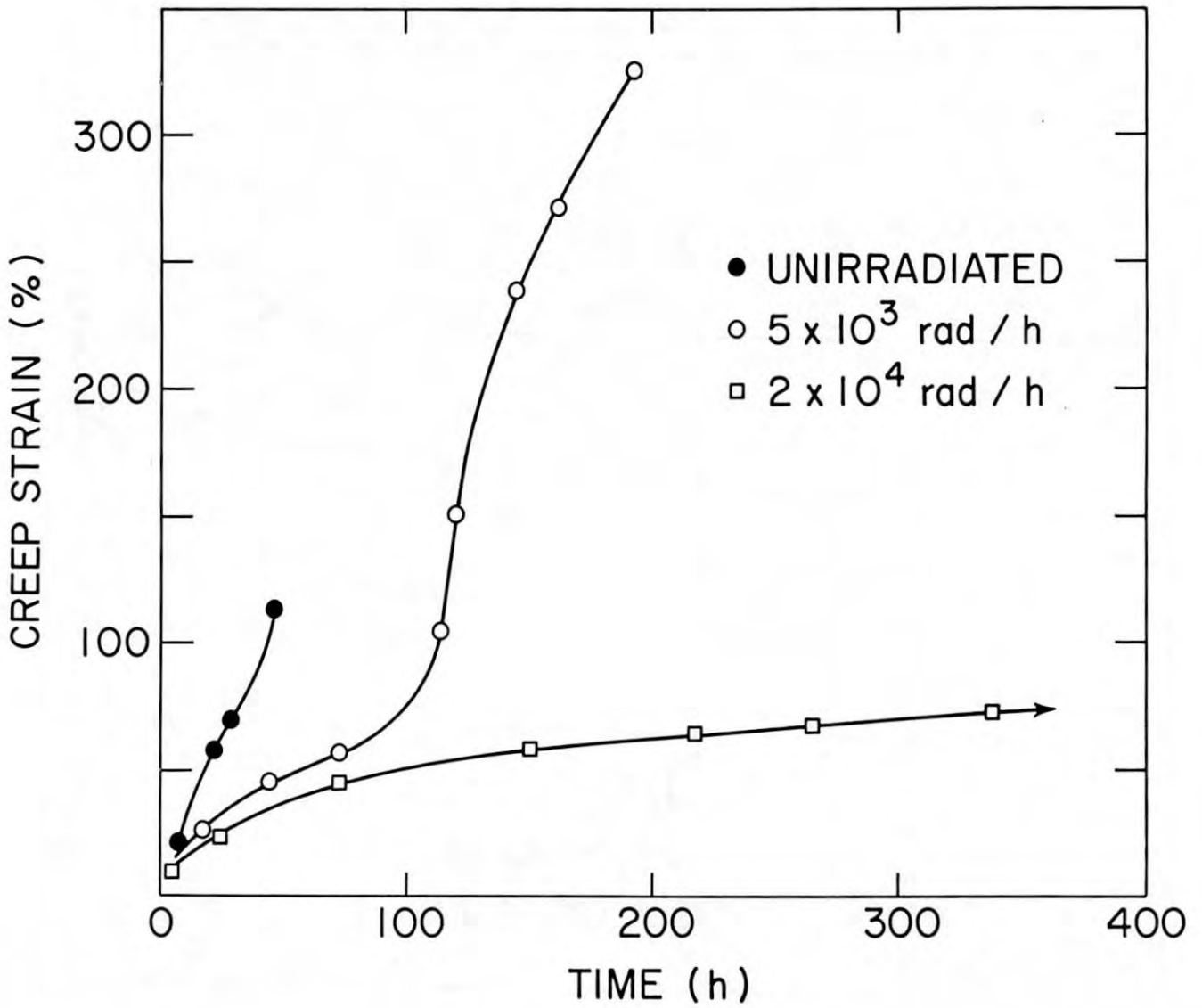

Figure 5.4 Effect of in-test gamma irradiation on the creep behavior of Marlex CL-100 HDPE at a stress of 11.72 MPa (1700 psi).

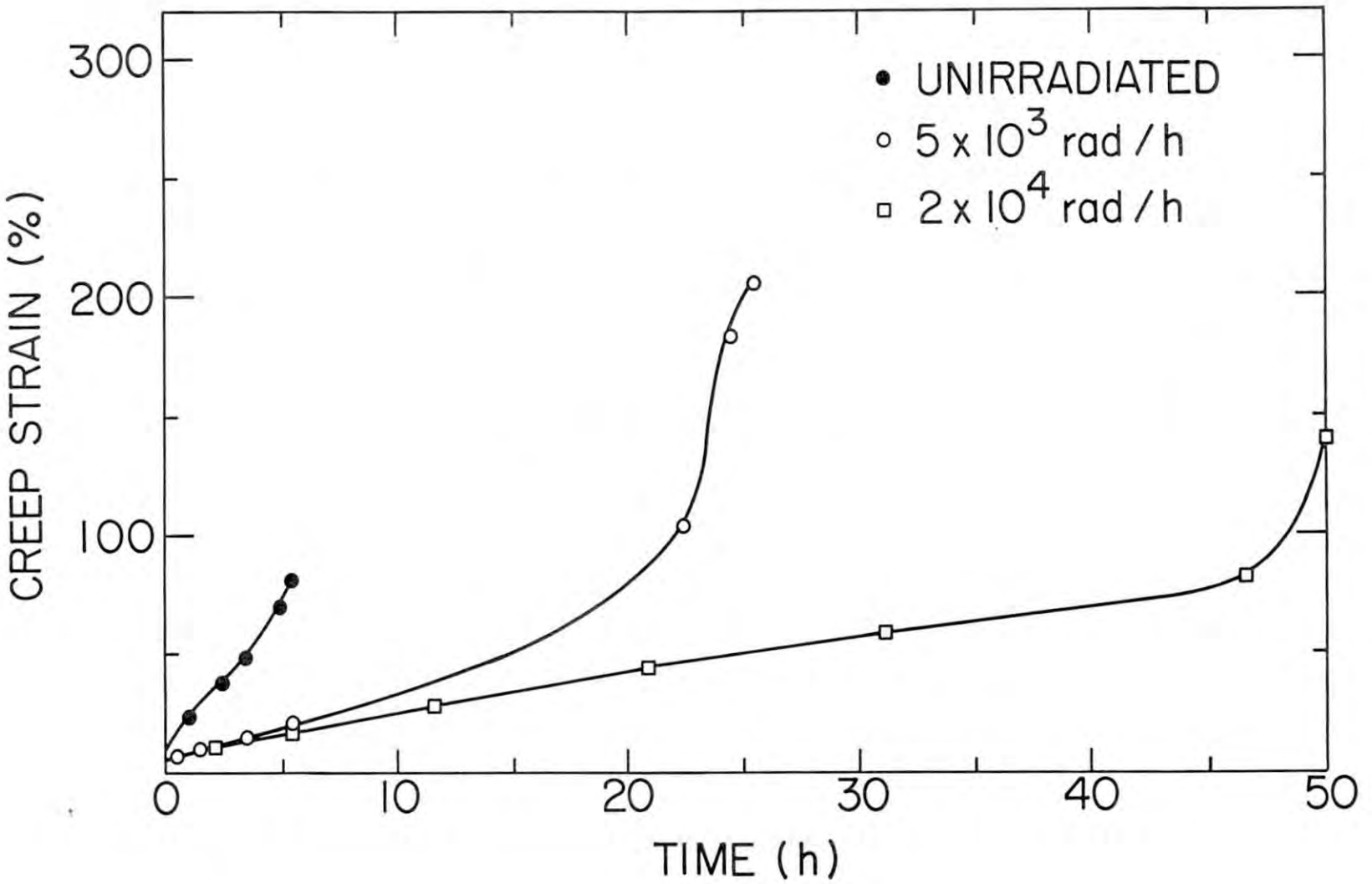

Figure 5.5 Effect of in-test gamma irradiation on the creep behavior of Marlex CL-100 HDPE at a stress of 12.58 MPa (1825 psi).

radiation (Schnabel, 1981) and it is very probable that additional crosslinking occurs in Marlex CL-100 irradiation-creep, giving rise to the slower rate of creep because of the strengthening it causes.

It should be appreciated that the effects of gamma irradiation become important very early during irradiation-creep. For example, at a stress of 12.58 MPa (1825 psi) the greatly reduced creep rate caused by irradiation at 5×10^3 and 2×10^4 rad/h is noticeable after about 1 h, or less (Figure 5.5). The accumulated doses would be 5×10^4 and 2×10^5 rad, respectively, which are quite low dose levels. Obviously, stress and irradiation together provide a strong interactive effect.

One might have expected that main chain scission would become very important in stressed and irradiated HDPE since both stress and radiation can cause chains to rupture. Together they would be expected to cause an increased scission rate. This would also be encouraged by the presence of oxygen during testing, since it is well known that scission rates in many polymers are increased when oxygen interacts with broken chains, thereby preventing their recombination (King and others, 1964; Sisman, and others, 1963). However, the strong reduction in the creep rate caused by irradiation suggests that although scission must be occuring, its effects are outweighed by the crosslinking process, at least during stages I and II of creep.

The greatly enhanced rupture times and ductilities of in-test irradiated HDPE needs to be addressed since it has been shown previously that prior irradiation causes a decrease in failure time and ductility upon subsequent testing (Soo, and others, 1986). Quite likely, the enhanced plasticity is associated with chain scission which could become important in Stage III creep. At this period of creep one might expect that the chain segments have become more aligned along the tensile stress direction and scission rates should increase. Scission in poly (vinyl chloride acetate) was shown to cause a reduction in molecular weight, an increase in crystallinity, and a large increase in viscous flow (Sisman and others, 1963). It is postulated that this mechanism is also responsible for the enhanced rupture times and ductilities observed in the current Marlex CL-100 HDPE irradiation-creep specimens. Work by Akay and Tincer (1981) and Seguchi and others (1982) is in accord with the above specimens on the effects of gamma irradiation on the creep of HDPE. Akay and Tincer showed that radiation induces crosslinking in drawn HDPE during the early irradiation period and prevents microcracking. Seguchi and others found that scission would be important at a later time and cause degradation of the crosslinked structure.

Finally, with respect to the controversy regarding the acceleration in creep during irradiation of highly stressed HDPE, observed by Dougherty and others (1984), no confirmation could be made of this effect. Irradiation-creep tests conducted in the current work at a dose rate of 5×10^3 rad/h and stresses of 12.58 and 11.72 MPa (1825 and 1700 psi which are similar to conditions used by Dougherty) show that irradiation initially retards creep and causes a large increase in the creep rate only when failure begins to commence in Stage III. High ductility is associated with the failure.

At this time the early acceleration of creep observed by Doughery during gamma irradiation is still in question. Data from the present effort consistently shows that creep enhancement only occurs after some lengthy slower period of creep. The reasons for the continued discrepancy between the current irradiation-creep results and those of Dougherty and others remains unclear.

6. TESTING PROTOCOL FOR HDPE

The useful lifetime for a HDPE waste container will normally depend on many variables, including the level of stress, the irradiation dose rate, the internal chemical and irradiation environment determined by the waste composition, and the external environment determined by the burial conditions. These conditions may change with time so the estimation of the failure time for a container is extremely difficult.

To develop an approach to determining container performance requires consideration of several factors, which include the following:

a) A specification of all possible material degradation modes which could lead to eventual failure in the service environment. Lack of identification of a failure or degradation mode will preclude the development of a strategy to eliminate its occurence, or reduce its impact, within the design lifetime.

b) Performance of experiments to characterize the individual failure modes under prototypic and accelerating conditions. Accelerating conditions are useful in that they often allow a degradation/failure mode to be observed and quantified within practical testing periods. Through a knowledge of the fundamental mechanism responsible it may be possible to fit the data from accelerated tests to a theoretical expression which may then be used to predict long-term performance under service conditions. In the absence of a sound description of the mechanism, an empirical expression could be used. This, also, could be used to estimate failure times for prototypic environments despite the greater uncertainty in the prediction.

   An example of a useful empirical equation to predict lifetime may be found in studies of carbon steel corrosion in soils (Kempf, and others, 1987). Using pitting corrosion data from Romanoff (1957) it was shown that the maximum pit depth could be given by:

$$d_m = 29\ t^{0.39}$$

   in which d_m is the depth in mils and t is the corrosion time in years. Such an expression will allow an estimation to be made of the maximum depth of attack so that the thickness of the steel component being designed for in-soil service can be sized to avoid penetration during the design lifetime.

c) The use of experiments specified in (b), above, may identify conditions for which a particular failure mode ceases to exist. For example, there are instances for which the stress on a material becomes too low for stress-assisted cracking to occur. With this in mind, stress-corrosion and fatigue are often avoided by ensuring that the maximum service stress in the component being designed is significantly lower than the threshold stress required to cause failure. An important goal in designing a HDPE waste container should, then, be the adjust-

ment of the design paramenters and environmental conditions in such ways that the container becomes immune to as many potential failure modes as possible. The remaining failure modes must then be addressed by obtaining data from accelerated tests, as described above, or, if available, from long-term prototypic in-service evaluations on the material of interest.

The work described below will address all of the three items listed above. Specifically, failure/degradation modes for HDPE will be identified for conditions which may exist during the pre- and post- disposal periods. Testing protocols will be defined to supplement those that currently exist in the literature. The test data that are obtainable from such tests will be discussed with respect to their use in container design, and suggestions will be made on ways to minimize, or eliminate, the occurrence of specific failure or degradation modes in HDPE.

6.1 Failure/Degradation Modes for HDPE

At the present time the following degradation/failure modes have been identified either from the literature or from research carried out in the current program.

a) Environmental Stress-Cracking

This involves the conjoint action of a tensile stress and a susceptible environment. The environment may provide a chemical (corrosive) effect or it may simply involve a non-reactive surface wetting phenomenon which accelerates crack propagation and failure (Shanahan; 1979, 1980). Igepal CO-630, is an ASTM-specified liquid for evaluating the susceptibility of HDPE to environmental stress-crack (see ASTM Standard D-2552). It is stated to be non-reactive and probably it acts as a simple surface wetting agent. On the other hand, BNL creep tests in scintillation fluid (see Table 4.2) show that the specimens have a relatively rapid rate of absorption of this fluid during test, which could indicate the presence of a chemical reaction with the HDPE. Therefore, a distinction should be made between non-reactive and reactive environments in the evaluation of environmental stress-cracking. Failure times as well as weight changes during test should be carried out to distinguish between the various environmental effects, if possible.

In the specific case of scintillation fluid the results in Table 4.6 show that failure occurs with relatively little cracking. Significant plasticity is often associated with failure. For such cases, it may be appropriate to classify failure as ductile failure rather than environmental stress-cracking which, by definition, is a cracking type mechanism.

b) Ductile Failure

The usual type of ductile failure involves deformation at relatively high stress levels, such as those encountered during short-term tensile testing at a constant strain rate (e.g., ASTM D-638, Test for Tensile Properties of Plastics) or high stress creep behavior under a constant load (e.g., ASTM D-2990, Tensile, Compressive, and Flexural Creep and Creep-Rupture of Plastics). In many cases the HDPE test material is prepared by the melting of polyethylene resin which is molded or fabricated to a specific shape (sheet, drum, pipe, etc.). Normally, the fabrication process is carried out in air, and this results in the formation of an oxidized surface layer which has inferior ductility compared to underlying bulk material (Terselius, 1982).

In BNL tests this surface-oxidized material cracks after about 20 percent elongation, and subsequent deformation tends to concentrate in the cracked areas, eventually giving rise to failure in one of these regions. If the oxidized layer is mechanicaly removed prior to creep testing then deformation occurs more uniformly throughout the gagelength of the specimen and "superplastic" type behavior often occurs.

c) Superplastic Failure

Superplastic failure is defined here as tensile failure involving extremely large elongations at rupture, viz. >200 percent strain. Note that this is an arbitrary definition and other workers may regard such high elongations as being normal rather than superplastic. Nevertheless, the distinction between regular ductile failure described in (b) needs to be made since there are mechanistic differences in the two types of failure. From the results described in earlier sections of this report, superplastic failure occurs in HDPE from which the oxidized layer has been removed and, also, in irradiation-creep specimens tested at high stress levels.

d) Low-Stress Embrittlement

The data in Figure 4.2 show ductilities at failure for creep tests carried out in air, deionized water, Igepal CO-630, turbine oil and scintillation fluid, as a function of stress. For air, water, oil, and Igepal it is seen the ductilities are tending to low values as the stress is decreased below 8.27 MPa (1100 psi). Liquid scintillation fluid does not show a drop in ductility in the low stress range. Clearly, at low stresses, embrittlement usually occurs under creep conditions. Failure, based on work in this program, is caused by the propagation of cracks which are nucleated in the oxidized surface material. Since deformation occurs most easily in these cracked region it

results in failure at low ductility. Other work by Graube (1976) on internally-pressurized HDPE pipes shows similar brittle failure at low pressures. Note that such failure in Igepal and turbine oil is often classified as environmental stress-cracking. Although these environments give creep ductilities that are similar to those for air and water, the latter two environments have far greater times to failure. However, the distinction between environmental stress-cracking and low-stress embrittlement is not very clear.

e) Impact Embrittlement

Low-temperature impact testing on a material measures the resistance to failure from a high velocity impact. Calibrated machines are used to measure the energy absorbed by a stationary sample as a heavy load falls under gravity to impact and fracture it. This type of failure mode is not likely to be of great importance with respect to container service conditions unless, for example, a HDPE container is embrittled by irradiation and fast loading from earth movement is encountered. Also, a container subjected to very low temperatures during the pre-burial period could suffer impact failure if accidently dropped onto an unyielding surface. The failure mechanism is mainly specified here because of its importance as a measure of the quality of polyethylene manufactured by industry (Philips Chem. Co., 1982). Such testing warrants serious consideration as a quality control test for HDPE container materials.

f) Irradiation Embrittlement

The U-bend tests in gamma-radiation environments show that crack initiation and fast propagation may occur if oxygen is present. Intermediate dose rates and intermediate stress levels are more likely to cause failure (Soo, and others, 1988). The mechanism is associated with bond cleavage which produces free radicals, which react with oxygen by a chain mechanism to form oxidation products that include hydroperoxides (Clough, 1981). As a consequence of these gamma-induced reactions, polymer chain scission and crosslinking occur. Tests to characterize cracking may include static U-bend tests, such as those used in the current study. More sophisticated low-load creep tests could be used in which the failure ductility and rupture time are measured and compared to non-irradiated HDPE. Note that, at high stresses, irradiation increases ductility (Section 5) so that irradiation embrittlement is not a consideration. However, embrittlement is possible at low stresses although no data are available in this program to show this. Stress-relaxation tests may also be used to study gamma-induced embrittlement. They are different from the standard creep test in which a constant load is used in

that stress-relaxation is studied under a constant strain. The drop in stress with time is measured with an appropriate load cell. Fracture mechanics techniques can also be used to investigate cracking as a function of stress intensity level and dose rate.

g) Buckling

Buckling failure in a container may occur as a result of the action of soil overburden loads at a burial site. It is characterized by unstable deformation as a result of compressive stresses. Buckling is a complex process and may involve components of other failure processes such as creep and irradiation effects which could lead to a condition of unstable deformation and collapse. Because of the NRC requirement for long term waste/container stability after disposal, container buckling, and the factors controlling it, are of great concern.

6.2 Standard Tests for Evaluating HDPE Behavior

Table 6.1 lists standard ASTM tests which are available for testing HDPE properties. Many of the failure/degradation modes, described in the sections above, may be quantified through their use. The BNL U-bend test is also included because of its demonstrated versatility for crack initiation/propagation studies in chemical and radiation environments.

6.3 Development of a Testing Protocol

In qualifying HDPE for use in a high-integrity container that meets NRC performance criteria, several specific procedural steps should be recognized. These include the following:

a) Preliminary literature surveys and testing to show that the material does not have any failure mode that would unacceptably compromise its integrity,

b) Specification of container design criteria which, together with NRC or State performance criterion, need to be met if the container is to be successfully licensed, and

c) Performance of "final" materials testing to obtain data which would be needed to quantify the various failure modes. This information will be needed to finalize the container design such that all design criteria and performance objectives are likely to be met during service.

These are discussed below.

6.3.1 Preliminary and Final Materials Testing

In the selection of a particular type of HDPE it should be a goal to specify a material with as few documented failure/degradation modes as possible. Since superior materials are usually more expensive, a compromise

Table 6.1 Available tests for evaluating failure/degradation modes in HDPE

Failure/Degradation Mode	Test Methods	Scope of Test Method
Environmental Stress-Cracking	ASTM D 1693	General scoping test to determine susceptibility of material to cracking under the action of a local multiaxial stress and a surface-active liquid (Igepal CO-630).
	ASTM D 2552	More quantitative test than D 1693 to determine failure time of material under a given stress and a surface-active agent (Igepal CO-630)
	BNL U-bend Test	General scoping test, similar to ASTM D 1693, but designed to quantify crack initiation and propagation under a tensile stress. Various test environments may be used.
	Fracture Mechanics	Tests using precracked specimens to measure crack propagation rates as a function of the stress-intensity factor. See reference by Ward (1979).
Ductile Failure, Superplastic Failure	ASTM D 638	Standard tensile test to measure strength and ductility. May be used to test in various environments.
	ASTM D 2990	Standard test for creep under tensile, compressive, or flexural conditions. May be used to test in various environments.

Table 6.1 Available tests for evaluating failure/degradation modes in HDPE (Continued)

Failure/Degradation Mode	Test Methods	Scope of Test Method
Low-Stress Creep Embrittlement	ASTM D 2990	Standard test that can be used to evaluate low-ductility creep failure under tensile and flexural conditions for various environments. Depending on test conditions, very long-term testing may be required. Higher temperatures may possibly be used to accelerate time for failure, so that failure times and ductilies may be extrapolated to service conditions.
	ASTM D 2991	Standard test for stress relaxation at constant strain level. This test is useful to evaluate crack initiation/propagation under low stress conditions. In particular, it will show how temperature and environment influence the rate of change in residual stresses in a plastic.
Impact Embrittlement	ASTM D 3029	Standard test to determine energy to fracture plastic by high speed falling weight. It is also a valuable procedure when used to measure low-temperature impact energy since it is a good indication of the degree of crosslinking.

Table 6.1 Available tests for evaluating failure/degradation modes in HDPE (Continued)

Failure/Degradation Mode	Test Methods	Scope of Test Method
Irradiation Embrittlement	BNL U-bend Test	General scoping test to determine crack initiation and propagation in material under a tensile stress.
	ASTM D 638	Standard tensile test to measure tensile strength (at yield or break), elongation (at yield or break), and the modulus of elasticity. Comparison of properties for non-irradiated and pre-irradiated material will quantify degree of embrittlement.
	ASTM D 790	Standard test to measure flexural (bending) properties of bar specimens. Test continued until fracture or until 5% maximum fiber strain is reached.
	ASTM D 2990	Standard tensile, compressive, and flexural creep test to quantify creep rates and ductilities. Effects of irradiation may be quantified by comparing properties of non-irradiated and pre-irradiated material or, more preferably, comparing properties of in-test irradiated material and corresponding non-irradiated methods.
	ASTM D 2991	Standard stress-relaxation test which may be used to quantitative measure crack propagation in irradiation environments. Complements the BNL U-bend test.

Table 6.1 Available tests for evaluating failure/degradation modes in HDPE (Continued)

Failure/Degradation Mode	Test Methods	Scope of Test Method
Irradiation Embrittlement (Cont.)	Fracture Mechanics	Tests using precracked specimens to measure crack propagation rates as a function of the stress-intensity factor.
Liquid Absorpsion	ASTM D 570	Test specifically developed to measure amount of water absorbed by plastic in a given time at a given temperature. It should be very useful for a range of liquids pertinent to HDPE usage since these may influence mechanical properties.

must be reached on a cost/benefit basis. A material with a large number of failure modes will only be qualified for use after lengthy testing for each failure mode. Once each failure mode is quantified, steps may then be taken to finalize the container design such that the failure mode does not cause failure during the design lifetime. Two approaches are possible. One is to "design out" the failure mode. For example, it is possible that the testing program will identify a threshold stress level below which environmental stress-cracking will not occur. By reducing the service stresses in the container to a value below the threshold one could argue that such a failure mode will not occur during service. Hence, it does not need to be considered further in the container design process. The second approach is often more difficult since it must consider how fast a failure/degradation mode is progressing. An example would be the velocity of a crack in a stressed container in the presence of a gamma irradiation field. If the crack can be shown to travel a distance less than the wall thickness of the container over the design lifetime then, again, it could be argued that such a failure mode will not prevent the container from meeting performance requirements. Much testing would need to be done for such a case since accelerated tests would need to be conducted over wide ranges of stress intensity and gamma dose rate. Uncertainties in the data would need to be addressed and certified procedures for extrapolating the data to prototypic service conditions must, also, be developed.

6.3.2 Specification of Container Design Criteria

Of great importance to the development of a successful container is the specification of design criteria which need to be met if NRC performance objectives are to be complied with. In many cases the design criteria used are arbitrary and reflect the degree of conservatism the designer chooses. For example, a design criterion to prevent failure by tensile creep could be one of the following:

a) Specification of a design stress limit in the container which would insure that creep never enters the Stage III creep region where failure begins.

b) Specification of a maximum allowable design strain (elongation) so that failure could not occur.

Alternate design criteria could also be defined but once one has been selected it would be used to demonstrate compliance with an NRC (or State) requirement. Below is summarized a sequence of events which would lead to demonstration of compliance.

Step 1

Identify from literature surveys and preliminary testing all possible failure/degradation modes for HDPE containers. Rank them in order of importance with respect to early failure.

Step 2

Initiate comprehensive testing to quantify the failure modes concentrating, first, on the most important ones.

Step 3

Try to specify container service conditions which would render the container immune to as many failure modes as possible.

Step 4

Specify container design criteria which, if met, will prevent failure during service.

Step 5

Use materials test data to show that the design criteria are likely to be met, and, therefore, that regulatory requirements are similarly met.

6.3.3 A Recommended Testing Protocol

Any testing protocol must eventually produce quantitative information that can lead to certified procedures that will demonstrate compliance with numerical performance objectives. Some ASTM tests are qualitative insofar as they will indicate a material's susceptibility to failure or degradation under specific, often accelerating, conditions. Such tests are of use in identifying potential failure processes but they do not usually allow a material to be qualified for long term service. The tests may, for example, not detect the existence of a failure mode that has a very long incubation time. Also, the conditions of test may be such that the material is immune to a particular failure process although it could occur under supposedly more benign prototypic service conditions. Such a situation was observed in the irradiated U-bend tests (Section 3.3) where it was found that cracking was most pronounced at lower, more prototypic, gamma dose rates. Therefore, a combination of preliminary and final test methods should be carried out to obtain a sufficiently accurate understanding of the material's long term behavior.

A general engineering rule-of-thumb regarding the maximum duration of tests is that they should last for periods up to one-tenth of the design life of the component being evaluated. Thus, creep behavior in a component with a design life of 20 years should be analyzed using creep data from tests lasting up to at least 2 years. This approach is impractical for a container with a 300 y design life, since few manufacturers would commit resources to 30 y creep tests. Therefore, a satisfactory creep analysis would probably entail comprehensive accelerated testing (at higher stresses and temperatures) to provide parametric procedures for extrapolating to service conditions. There would also be a need to employ larger design safety margins to offset the greater uncertainty in very long term creep properties.

Table 6.2 is a recommended testing protocol to provide preliminary data to support a material's basic suitability for use as a container material and final tests that will provide a quantitative basis to show that predetermined design criteria can be met. This will lead to a demonstration of compliance with regulatory performance objectives.

Table 6.2 Suggested testing protocol for HDPE

Failure Mode	Qualification Tests	Rationale for Tests
Environmental Stress-Cracking	Preliminary Tests ASTM D-1693. Accelerated qualitative test in Igepal. Final Tests a) ASTM D-2552. Constant load tests in Igepal and other selected service environments. b) Static-load fracture mechanics tests in Igepal and selected service environments.	Preliminary tests will determine if the HDPE is sufficiently resistant to ESC to proceed with the final long-term tests. If so the latter tests should be carried out in Igepal and selected environments at 20°C per ASTM D-2552 and at 20°C using fracture mechanics specimens to determine crack propagation rates in selected service environments as a function of the stress-intensity factor. The low stress tests should last for periods up to 3 years to quantify behavior more comprehensively.
Impact Failure	Preliminary Test Quality control test useful to show that the material is able to withstand low-temperature impact during storage or transportation. Also will show that the HDPE is satisfactorily cross-linked. Final Test None required	Tests will determine the basic integrity of the HDPE during the preburial phase and also serve as a quality control test for the container molding/curing process.

Table 6.2 Suggested testing protocol for HDPE
(Cont'd.)

Failure Mode	Qualification Tests	Rationale for Tests
Ductile/Super-Plastic Failure	Preliminary Tests None recommended Final Tests ASTM D-638 (tensile test) ASTM D-2990 (creep test)	The tensile tests establish basic strength and ductility data for design purposes. Creep data will be used to establish deformation rates, ductilities, and failure times for specific tensile loads. Estimation of very slow creep failure may be made as recommended below in "Low-stress creep embrittlement." Tests for creep should last up to about 3 years.
Irradiation Embrittlement	Preliminary Tests BNL U-bend test in gamma field Final Tests a) Static-load fracture mechanics tests in gamma field. b) ASTM D-2990 (creep test) in gamma field.	U-bend tests in gamma environment will establish semi-quantitatively the rates of crack initiation and propagation and allow a determination to be made if the anticipated embrittlement is mild enough to justify additional testing. If so, the fracture mechanics specimens will quantify the rates of crack propagation as a function of the stress-intensity factor. The creep tests will establish for container design purposes the modified creep properties brought about by in-situ gamma irradiation. Tests should last up to about 3 years.

Table 6.2 Suggested testing protocol for HDPE
(Cont'd.)

Failure Mode	Qualification Tests	Rationale for Tests
Low-Stress Creep Embrittlement (Without Irradiation)	Preliminary Tests None recommended	The creep tests should be conducted over a range of temperatures so that the existence of a ductile to brittle transition can be studied. The high temperature creep rupture curves will allow the transition time to be quantified as a function of stress. Parametric equations may then be developed to extrapolate to anticipated stresses and times (Gloor, W.G., 1958). Low stress irradiation-creep failure is needed only if in-test irradiation testing, outlined above, is found to adversely affect creep properties. Tests should last up to about 3 years.
Buckling	Preliminary Analyses Structural analyses based on prototype container design and available HDPE property data. Final Tests/Analyses a) Structural analyses based on final container design, and latest data on mechanical properties in chemical and irradiation environments. b) Full scale buckling tests on production container.	Preliminary analyses used to size the container and establish design criteria. Final tests/analyses will confirm that container meets design buckling criteria.

It must be stated that the testing protocol is necessarily subjective, being based on the authors' experience with Marlex CL-100 HDPE. Alternate protocols may be equally valid. The tests are listed in order of estimated importance and should be initiated in the approximate sequence shown. If, for example, environmental stress cracking is shown to be a serious problem based on preliminary ASTM tests, then consideration may be given to the selection of a new type of HDPE, or to a modification of the molding and curing parameters in order to improve the behavior to an acceptable level.

Buckling is included as a failure mode, although it is really a combination of slow creep and subsequent fast deformation processes. These are quantified in other tests. However, it is an important failure process which has gained much publicity in recent times with respect to the ability of HDPE containers to withstand soil overburden stresses at burial sites (Jur and Poplin, 1986).

As mentioned above, it would be extremely desirable if the container could be designed to specifications (molding/cure conditions, stress level, gamma dose rate, temperature, etc.) such that particular failure modes are not able to occur, i.e., the material becomes immune. Such immunity allows these failure modes, and any additional long term testing associated with them, to be removed from further consideration.

Finally, in any testing protocol the importance of batch-to-batch variations in materials properties must be addressed. There is always the likelihood that information from one batch of HDPE could reflect superior behavior because of some lucky combination of processing variables that took place during manufacture. The likely variation in a measured property may be best estimated by conducting tests on several batches of material. Appropriate data from the literature may also be used, if they are available.

7. REFERENCES

ASTM, "Test for Environmental Stress Cracking of Ethylene Plastics," Standard ASTM D1693-7, 1980a.

ASTM, "Test for Environmental Stress Rupture of Type III Polyethylene Under Constant Tensile Load," Standard ASTM D2552-69, 1980b.

Bell, J. B. and others, "Transient Acceleration of Creep Rates of Polymers During High Intensity Irradiation," in Irradiation of Polymers, R. F. Gould (Edit.), Amer. Chem. Soc., p. 79, 1967.

Clough, R. L. and K. T. Gillen, "Combined Environmental Aging Effects: Radiation-Thermal Degradation of Polyvinylchloride and Polyethylene," J. Polymer Sci.: Polymer Chemistry Edit., Vol. 19, pp. 2041-2051, 1981.

Clough, R. L. and others, "Accelerated Aging Tests for Predicting Radiation Degradation of Organic Materials," Nuc. Safety, 25, p. 238, 1984.

Dougherty, D. R., J. W. Adams, and R. E. Barletta, "An Evaluation of the Effects of Gamma Irradiation on the Mechanical Properties of High Density Polyethylene," NUREG/CR-3898, 1984.

Gillen, K. T. and R. L. Clough, "Occurrence and Implications of Radiation Dose-Rate Effects for Material Aging Studies," Radiat. Phys. Chem., 18, p. 679, 1981.

Gloor, W. L., "Application of Larson-Miller Correlation to Service Test Data on High-Density Polyethylene," Modern Plastics, 36, p. 144, 1958.

Graube and others, "Thermoplastic Pipes: Experience of 20 years of Creep Rupture Testing," Kunstoffe, 66, 2, 1976.

Jur, T. A. and W. Poplin, "A Critical Review of Materials Selected for High Integrity Containers," in Waste Management '86, R. G. Post (Edit.), Univ. of Arizona, pp. 531-537, 1986.

King, R. W. and others, "Polymers," in Effects of Radiation on Materials and Components, J. F. Kircher and R. E. Bowman (Edit.), Reinhold Pub. Corp., New York, p. 89, 1963.

Phillips Petroleum Co., "Rotational Molding of Polyethylenes," Technical Information Bulletin, Undated.

Philips Chemical Co., "Engineering Properties of Marlex Resins," Tech. Service Memo #TSM-243, 1975.

Philips Chemical Co., "Quality Control Tests for Crosslinking of Marlex CL-100 and CL-50," Philips Chemical Co., Bartlesville, OK 74004, Tech. Service Memorandum TSM-291, 1982.

Schnabel, W., Polymer Degradation, Hansen International, p. 139, 1981.

Schoenbacher, H., "How Plastics Perform Under Nuclear Radiation," Mod. Plastics, 62, p. 64, 1985.

Seguchi, T. and others, "Radiation Induced Oxidative Degradation of Polymers - II," Rad. Phys. and Chem., 19, p. 321, 1982.

Shanahan, M. E. R. and J. Schultz, "Environmental Stress Cracking of Polyethylene: Criteria for Liquid Efficiency," J. Polymer Sci., 17, p. 705, 1979.

Shanahan, M. E. R. and J. Schultz, "Correlation Between Environmental Stress Cracking and Liquid Sorption for Low-Swelling Liquids," J. Polymer Sci., 18, p. 19, 1980.

Sisman, O. and others, "Polymers," in Radiation Effects on Organic Materials, R. O. Bolt and J. G. Carroll (Edit.), Academic Press, New York, Chapter 5, 1963.

Soo, P., K. J. Swyler, M. Arora, W. Becker, and E. Sobel, "The Effects of Environment and Gamma Irradiation on the Mechanical Properties of High Density Polyethylene," NUREG/CR-4607, Brookhaven National Laboratory, 1986.

Soo, P., "Effects of Chemical and Gamma Irradiation Environments on the Mechanical Properties of High-Density Polyethylene (HDPE)," in Waste Management '88, R. G. Post (Edit.), Univ. of Arizona, pp. 619-626, 1988.

Terselius, B., V. W. Gedde, and J. F. Jansson, "Structure and Morphology of Thermally Oxidized High Density Polyethylene Pipe," Polymer Eng. and Sci., 22, p. 422, 1982.

Ward, I. M., Mechanical Properties of Solid Polymers, Second Edition, J. Wiley, Chichester, Chap. 12, 1979.

APPENDIX

Estimation of Strain Levels on the Surface of a U-Bend Specimen.

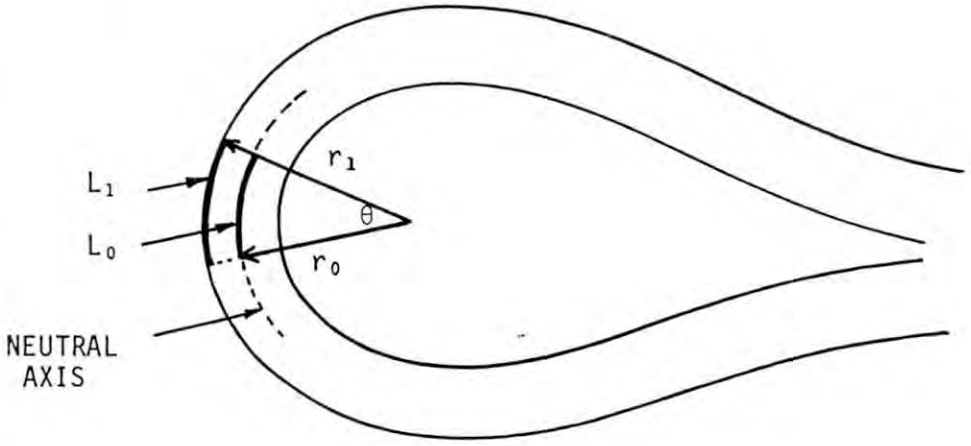

Consider a segment of a circle at the apex of a U-bend subtending an angle θ at the center of curvatures. It is obvious that:

$$\frac{L_1}{L_0} = \frac{r_1}{r_0} \qquad (1)$$

where r_1 is the radius of curvature of the outer surface and r_2 is the radius of curvature of the neutral (stress free) axis which is assumed to lie midway between the inner and outer bend surfaces.

r_1 was measured to be 0.32"

Since the thickness of the U-bend is 0.125", then r_0 is equal to 0.32" - 0.5 x 0.125" = 0.258"

From equation 1,

$$\frac{L_1}{L_0} = \frac{L_0 + \Delta L}{L_0} = 1 + \frac{\Delta L}{L_0} = \frac{0.32}{0.2575} = 1.243$$

where ΔL is the increase in length at the outer surface caused by bending. By definition, $\Delta L/L_0$ is the "strain," therefore:

$$\text{strain} \quad \Delta L/L_0 = 0.243 \quad \text{or} \quad \underline{24.3 \text{ percent}}$$

At a location P on the side of a U-bend, the radius of curvature r_1 is typically 0.75". Using Equation (1) the calculated strain is 9.1 percent.

DISTRIBUTION LIST

External Distribuition

Office of Nuclear Regulatory Research
U.S. Nuclear Regulatory Commission
Mail Stop 1130 SS
Washington, DC 20555

Attention: F. A. Costanzi
W. R. Ott
J. Philip (5)
M. Silberberg

Office of Nuclear Materials Safety and Safeguards
U.S. Nuclear Regulatory Commission
Mail Stop 623 SS
Washington, DC 20555

Attention: M. J. Bell
J. T. Greeves
T. C. Johnson
R. J. Starmer
M. Tokar
E. A. Wick

Chem-Nuclear Systems, Inc.
220 Stoneridge Drive
Columbia, SC 29210

Attention: L. Poppe

Engineering Design and Testing Corp.
Columbia, SC 29201

Attention: T. A. Jur
W. M. Poplin

LN Technologies
1501 Key Road
Columbia, SC 29201

Attention: R. Voit

NUS Process Services
1501 Key Road
Columbia, SC 29201

Attention: G. Mott

Philips 66 Inc.
Plastics Technical Center
Bartlesville, OK 74004

Attention: W. C. Dillard

Poly Processing Co.
P. O. Box 4150
Monroe, LA 71211

Attention: G. E. Carrow

DISTRIBUTION LIST
(Cont'd.)

Ralph M. Parson Co.
100 West Walnut Street
Pasedena, CA 91124

Attention: R. Duda

Sandia National Laboratories
P. O. Box 5800
Albuquerque, NM 87185

Attention: R. L. Clough
K. T. Gillen

TFC Nuclear Associates
425 Bridgeboro Road
Moorestown, NJ 08057

Attention: J. Chando

U. S. DOE
Germantown, MD 20874

Attention: T. C. Chee

Westinghouse Hittman Nuclear Inc.
9151 Rumsey Road
Columbia, MD 21045

Attention: R. Leduc

BNL Distribution

R. Bari, Bldg. 197C
B. Bowerman, Bldg. 830
P. Columbo, Bldg. 703
M. G. Cowgill, Bldg. 830
M. Fuhrmann, Bldg. 703
W. Y. Kato, Bldg. 197C
D. R. MacKenzie, Bldg. 830
B. Siskind, Bldg. 830
P. Soo, Bldg. 830 (50)
T. M. Sullivan, Bldg. 830

NRC FORM 335 (8-87) NRCM 1102, 3201, 3202

U.S. NUCLEAR REGULATORY COMMISSION

BIBLIOGRAPHIC DATA SHEET

SEE INSTRUCTIONS ON THE REVERSE

1. REPORT NUMBER (Assigned by PPMB: DPS, add Vol. No., if any)
NUREG/CR-5363
BNL-NUREG-52196

2. TITLE AND SUBTITLE
A Study of the Use of Crosslinked High-Density Polyethylene For Low-Level, Radioactive Waste Containers

3. LEAVE BLANK

4. DATE REPORT COMPLETED
MONTH: March YEAR: 1989

5. AUTHOR(S)
P. Soo, C. I. Anderson, J. H. Clinton

6. DATE REPORT ISSUED
MONTH: June YEAR: 1989

7. PERFORMING ORGANIZATION NAME AND MAILING ADDRESS (Include Zip Code)
Brookhaven National Laboratory
Upton, NY 11973

8. PROJECT/TASK/WORK UNIT NUMBER

9. FIN OR GRANT NUMBER
FIN A-3291

10. SPONSORING ORGANIZATION NAME AND MAILING ADDRESS (Include Zip Code)
Division of Engineering
Office of Nuclear Regulatory Research
U.S. Nuclear Regulatory Commission
Washington, DC 20555

11a. TYPE OF REPORT
FORMAL

b. PERIOD COVERED (Inclusive dates)

12 SUPPLEMENTARY NOTES

13. ABSTRACT (200 words or less)

A comprehensive research program has been completed to evaluate the effects of chemical and gamma-irradiation environments on the mechanical properties of crosslinked high-density polyethylene. The studies included uniaxial creep tests and crack initiation and crack propagation studies in statically-stressed U-bend samples. From the results obtained standard testing protocols were recommended for quantifying the various failure modes which could be present in this material during service as a low-level waste container.

14. DOCUMENT ANALYSIS - a. KEYWORDS/DESCRIPTORS
Low-level radioactive waste, high-density polyethylene, container, mechanical properties, test environment, gamma irradiation effects, microscopy.

b. IDENTIFIERS/OPEN-ENDED TERMS

15. AVAILABILITY STATEMENT
Unlimited

16. SECURITY CLASSIFICATION
(This page) Unclassified
(This report) Unclassified

17. NUMBER OF PAGES

18. PRICE

☆U.S. GOVERNMENT PRINTING OFFICE:1989-241-590:00126